NASA Technical Memorandum 85806

Langley Aeronautics and Space Test Highlights 1983

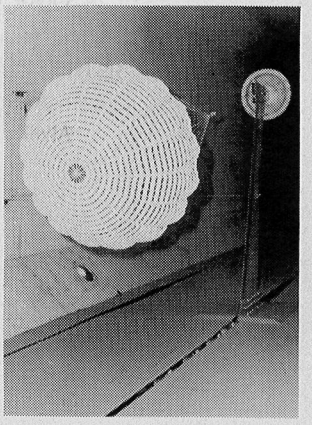

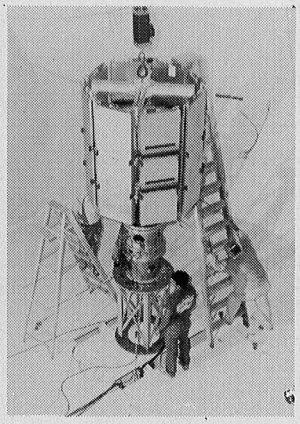

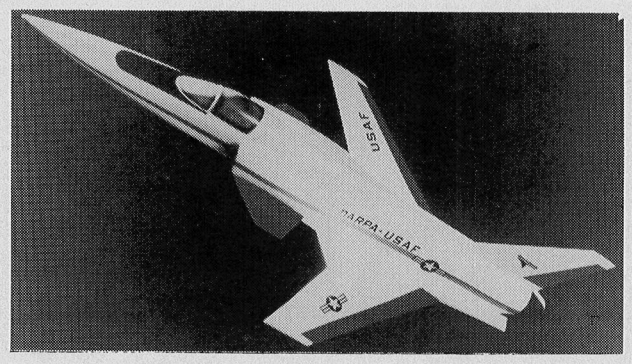

NASA
National Aeronautics and Space Administration

NASA Technical Memorandum 85806

Langley Aeronautics and Space Test Highlights 1983

NASA
National Aeronautics and
Space Administration

Langley Research Center
Hampton, Virginia 23665

1984

Foreword

The role of the Langley Research Center is to perform basic and applied research necessary for the advancement of aeronautics and space flight, to generate new and advanced concepts for the accomplishment of related national goals, and to provide research advice, technological support, and assistance to other NASA installations, other government agencies, and industry. This report highlights some of the significant tests which were performed during calendar year 1983 in Langley test facilities, a number of which are unique in the world. The report illustrates both the broad range of the research and technology activities at the Langley Research Center and the contributions of this work toward maintaining United States leadership in aeronautics and space research. Other highlights of Langley research and technology for 1983 are described in "Research and Technology—1983 Annual Report of the Langley Research Center." Further information about both reports is available from the Office of the Chief Scientist, Mail Stop 103, Langley Research Center, Hampton, Virginia 23665 (804-865-3316).

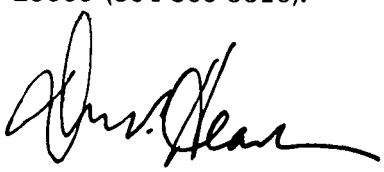

Donald P. Hearth
Director

Availability Information

For additional information on any highlight, contact the individual identified with the highlight. This individual is generally either a member or a leader of the research group. Commercial telephone users may dial the listed extension preceded by (804) 865. Telephone users with access to the Federal Telecommunications System (FTS) may dial the extension preceded by 928.

Contents

30- by 60-Foot Tunnel

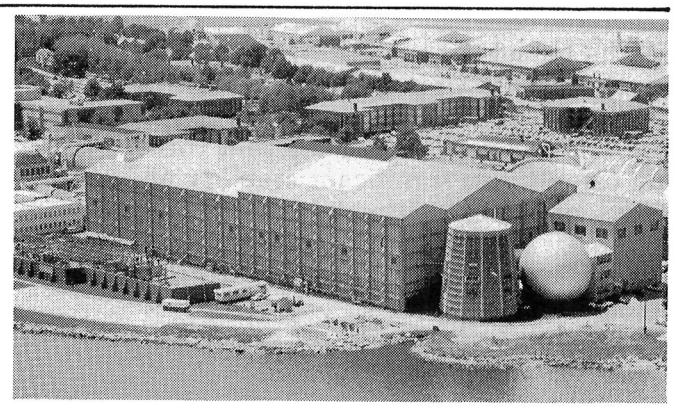

The 30- by 60-Foot Tunnel is a continuous-flow open-throat double-return tunnel powered by two 4000-horsepower electric motors, each driving a 4-blade 35.5-foot-diameter fan. The tunnel test section is 30 feet high and 60 feet wide and is capable of speeds up to 100 mph. The tunnel was first put into operation in 1931 and has been used continuously since then to study the low-speed aerodynamics of commercial and military aircraft. The large open-throat test section lends itself readily to tests of large-scale models and to unique test methods using small-scale models.

Large-scale and full-scale aircraft tests are conducted using the strut mounting system. This test method can handle airplanes up to the size of present-day light twin-engine airplanes. Such tests provide static aerodynamic performance and stability and control data, including the measurement of power effects, wing pressure distributions, and flow visualization.

Small-scale models can be tested to determine both static and dynamic aerodynamics. For all captive tests, the models are sting mounted using internal strain gauge balances. The captive test methods include conventional static tests for performance and stability and control, forced-oscillation tests for aerodynamic damping, and rotary tests for spin aerodynamics. Dynamically scaled subscale models, properly instrumented, are also freely flown in the large test section using a simple tether, to study their dynamic stability characteristics at low speed and at high angles of attack. A small computer is used in this free-flight test technique to represent the important characteristics of the airplane flight control system.

Thrust Vectoring Free-Flight Tests

As part of a research program to investigate advanced control concepts for fighter aircraft, free-flight tests of a 0.16-scale model of the F-18 airplane configured with pitch and yaw thrust vectoring were conducted in the 30- by 60-Foot Tunnel. The primary objectives of the tests were to assess the viability of the thrust vectoring concept for stability and control augmentation at high angles of attack and to investigate control system requirements associated with the concept.

For the tests, the model was flown unconstrained in the test section of the tunnel and was controlled remotely by pilots situated at appropriate positions around the test section. Inputs from the pilots and motion sensor signals from the model were fed into a digital computer, which

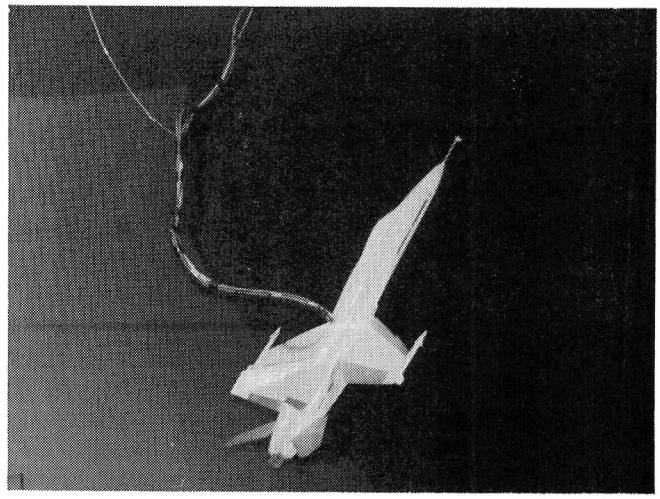

Free-flight tests of F-18 model with thrust vectoring.

generated commands to drive the control surfaces on the model. Using this system, the effects of control law variations could be assessed easily and efficiently.

The test results indicate that thrust vectoring can provide significant stability and control augmentation at high-angle-of-attack flight conditions, which can result in dramatically improved maneuverability and resistance to loss of control during air combat.

Luat Nguyen, 2184

Free-Flight Tests of Fighter With Spanwise Blowing

As part of a cooperative NASA/Air Force research program, a free-flight model investigation was conducted in the 30- by 60-Foot Tunnel to determine the effects of spanwise blowing on the low-speed dynamic stability and control characteristics of a 13-percent scale model of the F-4C airplane. Spanwise blowing was applied to enhance the wing leading-edge vortex and provide improved maneuvering aerodynamics. The objective of the present research effort is to further mature the technology by actually taking the spanwise blowing concept into flight on the F-4C at NASA Ames/Dryden. Tests conducted in the 30- by 60-Foot Tunnel included static, forced-oscillation-in-roll, and free-flight model tests.

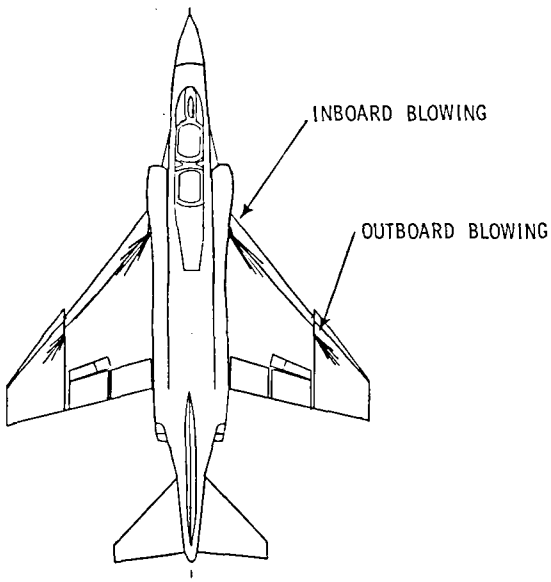

Blowing arrangement on F-4C model.

Results of these stability studies showed that applying realistic levels of blowing (obtainable from engine bleed air) substantially changed low-speed static and dynamic stability characteristics of the model at and above angles of attack that produced significant separated flow on the wings. In particular, the proper distribution of blowing was found to provide improved static lateral and directional stability and improved roll damping in the maneuvering angle-of-attack range below maximum lift. Improved dynamic stability characteristics predicted from the captive force tests correlated well with the flight dynamics exhibited by the model during the tethered free-flight tests. Results of this and other Langley wind tunnel studies are now being used by NASA in planning the flight test program to be conducted at the NASA Ames/Dryden Flight Research Facility.

David Hahne, 2184

Low-Turbulence Pressure Tunnel

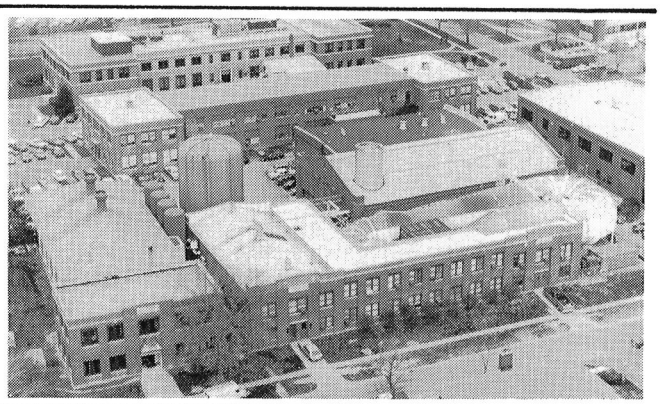

The Langley Low-Turbulence Pressure Tunnel (LTPT) is a single-return closed-circuit tunnel which can be operated at pressures from near-vacuum to 10 atmospheres. The test section is rectangular in shape (3 feet wide and 7.5 feet in height and length) and the contraction ratio is 17.6:1. The LTPT is capable of testing at Mach numbers from 0.05 to 0.50 and unit Reynolds numbers from 0.1 $\times 10^6$ to 15 $\times 10^6$ per foot. The tunnel has provisions for removal of the sidewall boundary layer by means of a closed-loop suction system mounted inside the pressure chamber. This system utilizes slotted vertical sidewalls just ahead of the model test section, and the removed air is reinjected through an annular slot downstream of the test section. A flow control system allows the flow and pressure requirements to be varied as dictated by tunnel operation. This system can be used to provide boundary layer control (BLC) for low-drag airfoil research.

A BLC system for high-lift airfoil testing is also available. This system utilizes compressed dry air and involves tangential blowing from slots located on the sidewall mounting endplates. Flowmeters can be used to monitor the amount of air blown into the tunnel. An automatically controlled vent valve is utilized to remove the air injected into the tunnel by this system. A high-lift model support and force balance system is provided to handle both single-element and multiple-element airfoils.

The measured turbulence level of the LTPT is very low due to the large contraction ratio and the many fine-mesh antiturbulence screens. This excellent flow quality facility is particularly suitable for testing low-drag airfoils. Recent flow quality measurements in the LTPT indicate that the velocity fluctuations in the test section range from 0.025 percent at Mach 0.05 to 0.30 percent at Mach 0.20 at the highest unit Reynolds number.

The drive system is a 2000-horsepower direct-current motor with power supplied from a motor-generator set. The tunnel stagnation temperature is controlled by a heat exchanger which provides both heating and cooling using steam injectors and modulated valves that control the flow volume of water through a set of coils.

Juncture Flow Tests

Fluid flow prediction methods in the juncture region on airplanes are presently unavailable. For example, there are no known and accepted design tools to design the junctures between the fuselage and wing or fuselage and tail surfaces. When the mean flow velocity (U) is parallel to the juncture, secondary flow velocities (V and W) can be generated by Reynolds stresses within the boundary layers of the two adjacent surfaces. Because these secondary flows are within the boundary layers of the surfaces, detailed experimental data are difficult to obtain using intrusive conventional probe techniques, especially in the near-wall region.

Initial basic tests were conducted in the LTPT using a nonintrusive laser Doppler velocimeter (LDV) specifically designed to measure the three mean components of velocity and six Reynolds stresses along the juncture region for several locations. The LDV system measures the velocity of very small particles that are inserted into the flow stream near the juncture. A technique for inserting the small particles into the flow stream was developed especially for the LPTP and proved to be quite adequate.

The basic juncture was formed by a spanwise-mounted wing and a sidewall splitter plate, providing a 90° corner. The juncture was adaptable for a sharp corner, a 0.5-in.-radius fillet, or a 1.0-in.-radius fillet. The wing could be either a flat surface or a circular arc in the streamwise direction, to provide a juncture with or without the influence of the pressure gradient. Tests were conducted at 1 atmosphere and Mach 0.1.

The LDV results obtained will provide a basis for comparison with results from future planned fluctuating-velocity and mean flow measurements using conventional probe techniques (*i.e.,* hot wires, pitot and Preston tubes) as well as with current surface static pressure data. The LDV data obtained should be helpful to the further development of theoretical computational aerodynamics. The LDV test results indicated that the large-radius fillet exerted less influence than the sharp corner on the interaction of the boundary layers of each surface (as might have been expected) as well as less subsequent effects on the secondary flow field.

Jim Scheiman, 4514

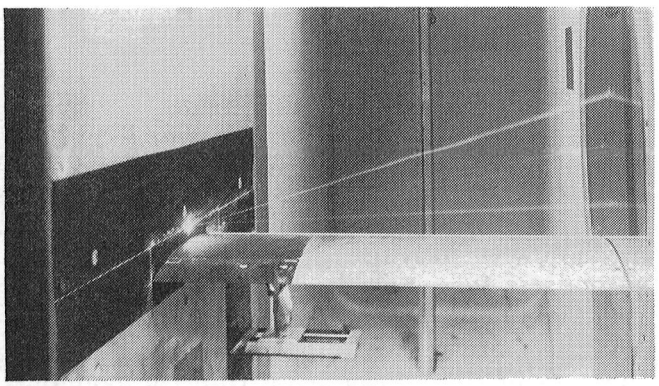

LDV beams used to test juncture flow in LTPT.

Airfoils for Long-Endurance Applications

One means of achieving long range for a given aircraft is to significantly reduce drag through extensive laminarization. Tests were conducted in the Langley Low-Turbulence Pressure Tunnel in cooperation with the Boeing Company to determine the aerodynamic performance of an airfoil designed to achieve long runs of natural laminar flow for long-endurance application. The airfoil was designed and provided by Boeing and had a medium thickness/chord ratio and a relatively high lift coefficient. In order to obtain low drag, the airfoil was shaped to provide a pressure profile suitable for maintaining laminar flow back to 30 percent chord on the upper surface and 70 percent chord on the lower surface at a Reynolds number of 14 million.

Test results indicated that extensive laminar flow and low drag were achieved up to chord Reynolds numbers of 18 million at design conditions exceeding original expectations.

Bob McGhee, 4514

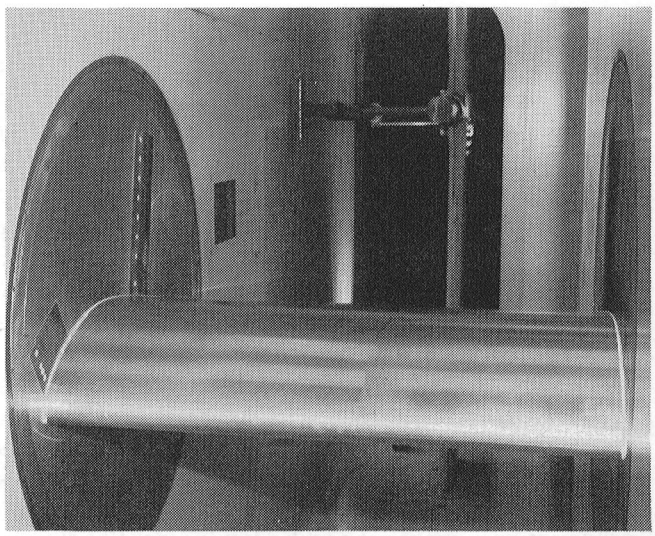

Long-endurance airfoil in LTPT.

20-Foot Vertical Spin Tunnel

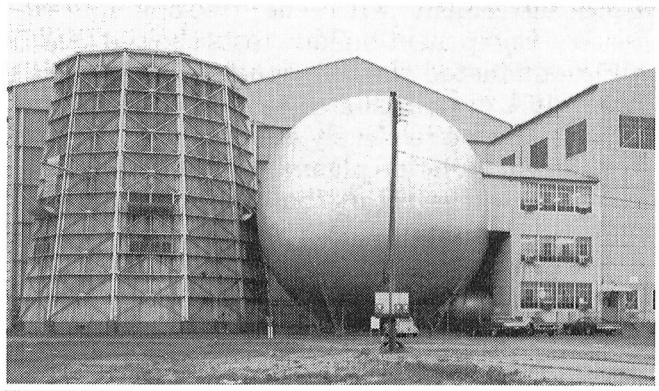

The Langley 20-Foot Vertical Spin Tunnel is the only operational spin tunnel in the United States and one of only two in the free world. The tunnel, which is used to investigate spin characteristics of dynamically scaled aircraft models, is a vertical tunnel with a closed-circuit annular return passage. The vertical test section has 12 sides and is 20 feet wide and 25 feet high. The test medium is air. Tunnel speed can be varied from 0 to 90 feet per second with accelerations to 15 feet per second squared. This facility is powered by a 1300-horsepower main drive.

Spin recovery characteristics are studied by remotely actuating the aerodynamic controls of models to predetermined positions. Force and moment testing is performed using a gooseneck rotary-arm model support, which permits angles of attack from 0° to ±90° and sideslip angles from 0° to ±20°. Motion picture and video records are used to record the spinning and recovery characteristics in the spin tunnel tests. Force and moment data from the rotary balance tests are recorded in coefficient form and stored on magnetic tapes.

Spin Tunnel Investigation of T-46A Airplane Configuration

At the request of the Air Force, an investigation was conducted in the 20-Foot Vertical Spin Tunnel to determine the spin and recovery characteristics of the T-46A trainer airplane. The investigation consisted of free-spinning tests with a 1/18 dynamically scaled model and rotary balance tests with a 1/6-scale model.

The free-spinning tests showed that with prospin controls, the basic model exhibited a moderately flat, smooth spin at an angle of attack of about 60° and a spin rate of 2.2 to 3.2 seconds per turn. Satisfactory recoveries were attained by rudder and aileron reversal. Spins at the forward and aft center-of-gravity limits showed no degradation of spin or recovery characteristics. Inverted spins were generally smooth at about -55° angle of attack and about 3 seconds per turn. Good recoveries were achieved by rudder reversal.

In the event that the airplane does not recover from a spin, an emergency spin recovery parachute is provided. Tests were conducted to determine the size of this parachute. The recommended emergency spin recovery parachute is 14.4 feet in diameter, has a drag coefficient of 0.5, and is on a 45-foot towline (distance from attachment point to skirt of canopy).

From the rotary balance tests, aerodynamic coefficients for rotational flow conditions were obtained and used to calculate equilibrium spin modes. These calculated modes were generally in

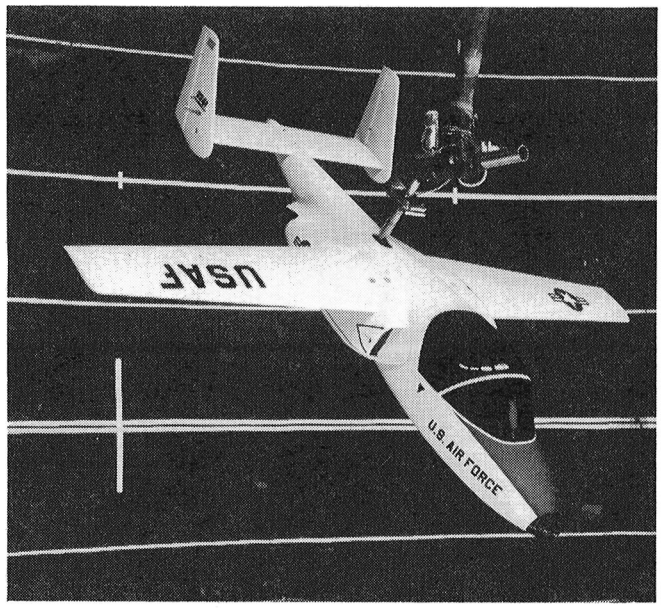

T-46A model on rotary balance.

good agreement with the free-spinning test results. Component buildup tests showed that the wing dominated the rotational aerodynamics of the T-46A at spin angles of attack and the vertical tails were relatively ineffective in this area. A piloted simulation planned by the Air Force will incorporate the rotary balance data to permit simulation of spin characteristics.

James S. Bowman, 2521

7- by 10-Foot High-Speed Tunnel

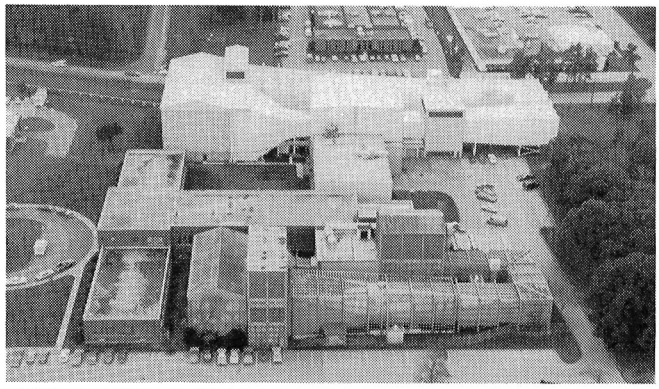

The Langley 7- by 10-Foot High-Speed Tunnel is a closed-circuit single-return continuous-flow atmospheric tunnel with a test section 6.6 feet high, 9.6 feet wide, and 10 feet long. A 14,000-horsepower electric motor drives a series of fan blades to provide subsonic operating speeds from Mach 0.2 to Mach 0.9 and to produce a maximum Reynolds number of 4×10^6 per foot. In addition to static testing of complete and semispan models, the facility is equipped for both steady-state roll and oscillatory stability testing.

Currently the facility is playing an important role in a wide range of basic and applied aerodynamics research, including advanced vortex lift concepts, fuel-conservative aircraft design technology, highly maneuverable aircraft concepts, and the development of improved aerodynamic theories such as the difficult separated-flow and jet interaction effects needed for computer-aided design and analysis.

Forward-Swept Wing

A wind tunnel investigation has been conducted to study the effects of canard deflections, wing leading- and trailing-edge flap deflections, and fuselage strakes on the longitudinal aerodynamic characteristics of a fighter with forward-swept wings. The forward-swept-wing configuration was designed for good transonic maneuver performance with a transonic wing-canard-fuselage code. The wing had a leading-edge sweep of 20.2° forward and an aspect ratio of 3.28. The exposed canard area was 15.6 percent of the wing reference area. The fuselage strakes were designed to produce a stable vortex at high angles of attack. Both the leading- and trailing-edge flaps were tested at deflection angles of 0°, 5°, 10°, and 20°. The configuration was tested with the wing alone, wing plus canard, wing plus strakes, and wing plus canard and strakes. The canard angle of incidence was varied from 10° to -20° in 5° increments. The tests were run at a Mach number of 0.3 with angles of attack from -2° to 22°.

The experimental results showed that lift coefficients as high as 1.8 were generated. The leading- and trailing-edge flaps produced substantial improvements in the drag polars at maneuver conditions. The addition of the canard also produced substantial improvements in maneuver performance. The addition of the strakes to the wing-canard configuration improved performance at the higher angles of attack. The moment increments generated by the canard were sufficient to trim the configuration without the strakes over most of the angle-of-attack range and with the strakes over a somewhat limited angle-of-attack range. For the selected center-of-gravity location, the static margin ($\partial C_m / \partial C_L$) varied from 0.2 to 0.3 for the wing-canard configuration.

Michael J. Mann, 2601

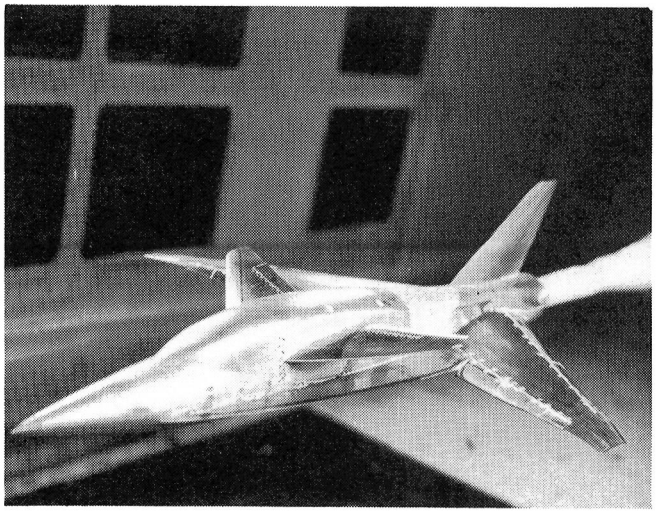

Fighter model with forward-swept wing.

Aerodynamic Effects of Distributed Spanwise Blowing on a Fighter Configuration

In support of a flight test program to be conducted at the Dryden Flight Research Facility in 1984, a series of wind tunnel tests were performed in the 7- by 10-Foot High-Speed Tunnel to investigate the benefits of distributed spanwise blowing on a 1/10-scale F-4C model. Static longitudinal data were obtained for a range of outer-panel nozzle parameters, blowing distributions, leading- and trailing-edge flap deflections, and blowing coefficients at low speed and at up to 24° angle of attack.

With the outer-panel nozzles aligned parallel to and 3° above the wing leading edge, the jets stabilized the leading-edge vortices (using a realistic blowing coefficient) and produced a lift increment approaching 0.3 at 22° angle of attack. Distributed spanwise blowing improved lift performance as an increasing percentage of blowing was shifted from the inboard to the outboard nozzles; however, the reverse was true for longitudinal stability. Leading-edge flaps delayed the favorable effects of spanwise blowing but improved the longitudinal stability. Blowing improved both the performance and the stability of trailing-edge flaps.

Jarrett K. Huffman, 2556

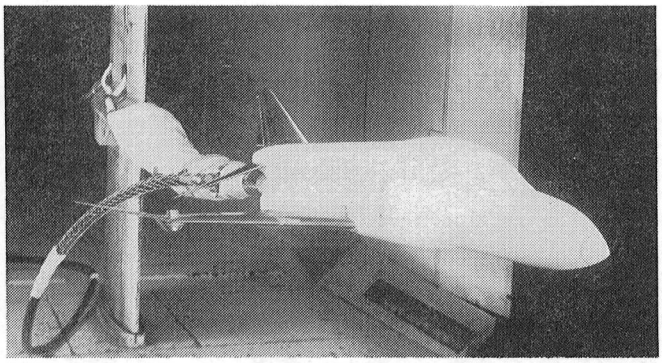

One-tenth-scale F-4C spanwise-blowing model.

Designed Vortex Flaps on 74° Delta for Validation Studies

This test in the 7- by 10-Foot High-Speed Tunnel was carried out primarily to validate a design procedure developed at Langley by which the planform shape of an "optimal" vortex flap may be established to achieve a specific lift coefficient at a particular angle of attack and flap deflection angle. (An "optimal" vortex flap is one in which the upper surface pressure has the suction peak on the flap, and the "knee" in this pressure curve occurs at the hinge line.) Comparisons of measured pressure shapes with expected ones indicated that the leading-edge vortex system (characterized by high-suction pressure peaks) was essentially captured all along the flap. Only a small amount of vortex migration was noted near the aft part of the flap at the design conditions.

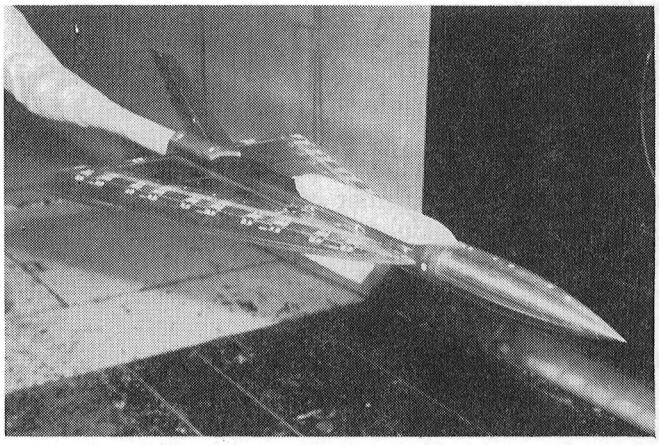

Designed vortex flaps on 74° delta.

Many aspects of this test remain to be analyzed because data were taken with various vortex flap and trailing-edge deflection angles. Furthermore, hinge moments were measured for the vortex flap with the intention of comparing these data with measured and calculated pressure data. This test, with its overall force moment, pressure, and hinge moment data, provides a very good data base with which to compare current and future theoretical methods. It should further serve to help improve the design procedure by suggesting regions of local modification.

Neal Frink, 2601

4- by 7-Meter Tunnel

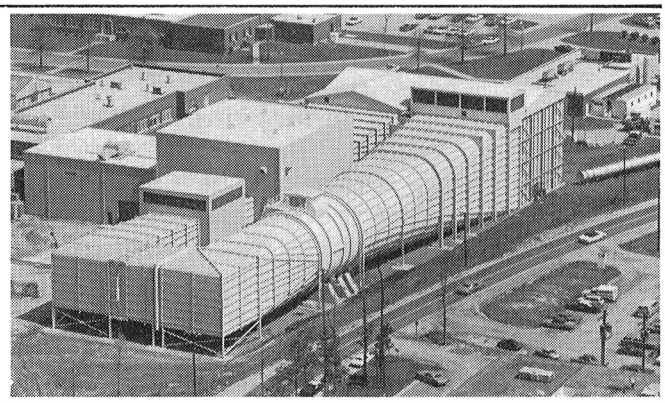

The Langley 4- by 7-Meter Tunnel (formerly V/STOL Tunnel, or Vertical/Short Takeoff and Landing Tunnel) is used for low-speed testing of powered and unpowered models of various fixed- and rotary-wing civil and military aircraft. The tunnel is powered by an 8000-horsepower electrical drive system, which can provide precise tunnel speed control from 0 to 200 knots with the Reynolds number per meter ranging from 0 to 0.64×10^7. The test section is 4.4 meters high, 6.6 meters wide, and approximately 15.2 meters long. The tunnel can be operated as a closed tunnel with slotted walls or as one or more open configurations by removing the side walls and ceiling to allow extra testing capabilities, such as flow visualization and acoustic tests. The tunnel is equipped with a two-component laser velocimeter system. Furthermore, boundary layer suction on the floor at the entrance to the test section and a moving-belt ground board for operation at test section flow velocities up to 70 knots can be installed for ground effect tests.

Small-Scale Rotor Test System

A new small-scale rotor test system was used both in an exploratory test program to measure hover characteristics of three rotors with different blade planforms and in a 4- by 7-Meter Tunnel test of the Army Helicopter Improvement Program (AHIP) helicopter. The AHIP test was conducted to determine stability effects associated with the nonrotating mass-mounted sight. Data from the hover tests indicated that the model was a useful tool for comparison testing of different blade planforms. The wind-on testing of the AHIP configuration showed the rotor test system to be stable and controllable, and the comparatively small size of the rotor (2 meters in diameter) made it possible to perform valuable smoke flow visualization studies of the rotor flow field in the very complex transition regime.

The small-scale rotor test system was designed and developed in-house by members of the Army Structures Laboratory at Langley. The new rotor model was designed specifically to allow rapid, comparatively inexpensive testing of rotors for general aerodynamic research by the Rotorcraft Aerodynamics Office. In addition, the new model allows exploratory performance testing of complete configurations to evaluate the gross effects of rotor-body interference, hovering characteristics, and stability and control, as well as similar investigations of a general nature.

The rotor test system consists of a rotor drive system, rotor blades, and a fuselage. The dynamic system is mounted on a six-component strain gage balance, which is used to measure rotor loads; a second balance mounted parallel to the rotor

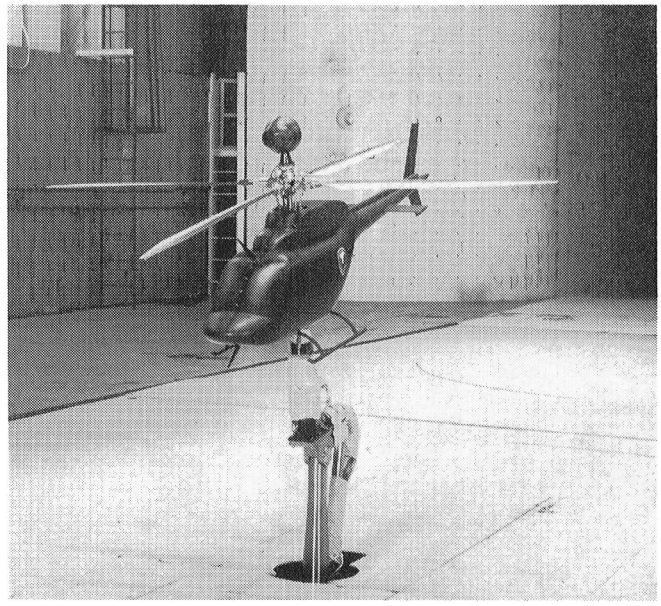

Rotor test system in 4- by 7-Meter Tunnel.

balance is used to measure fuselage loads. The new system is a complement to the larger, more sophisticated General Research Model System (GRMS) used for rotor performance studies. For some applications, such as far-field noise studies and ground effects studies, the new model provides a capability not previously available with the larger GRMS model. The cost of rotor blades for the small-scale system is about 15 to 20 percent of that for aeroelastically scaled blades for the GRMS, and blades for the small-scale system can be fabricated much more quickly.

Art Phelps, 3611

Main Rotor/Tail Rotor Acoustic Investigation

The overall objective of this research effort is to study main rotor/tail rotor interaction noise. The first test phase of three was conducted in July 1983 in the 4- by 7-Meter Tunnel. Acoustic measurements were taken for a series of 9-foot-diameter models (main rotor only) with different twists and various tip shapes (sweep angle, taper, airfoil, and anhedral). The first phase investigated blade-vortex interaction noise as a measure of tip strength and source effectiveness. Preliminary results identified two promising tip configurations to use for the third test. These tips, in addition to the old UH-60 tip, have tentatively been chosen based on their effectiveness in minimizing blade-vortex interaction noise.

The second test phase will investigate the tail rotor installation effects. The test will be conducted at the United Technology Research Center. The third phase will be a test in the 4- by 7-Meter Tunnel in 1985. Emphasis in the program is placed on understanding those factors influencing main rotor and tail rotor noise in frequency ranges which are important to proposed certification metrics.

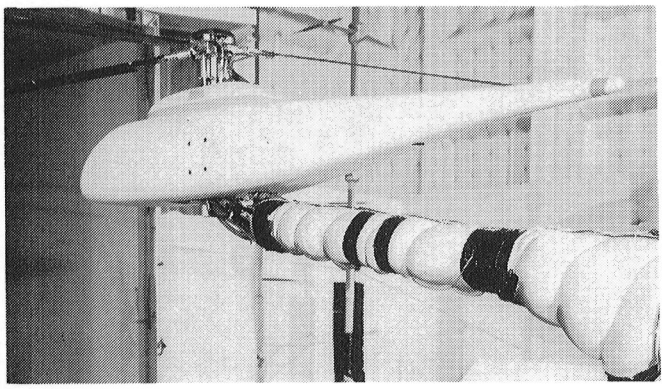

Rotor model mounted in 4- by 7-Meter Tunnel.

Danny Hoad, 3611

Advanced Turboprop Transport

During the late 1970's and early 1980's, NASA and industry researchers explored the use of advanced turboprop engines to improve aircraft fuel economy. These studies identified potential fuel savings of as much as 40 percent over conventional jet aircraft performing the same mission. One of the more promising aircraft configurations used aft-mounted engines to provide cabin noise reduction and an aerodynamically clean wing. However, very little information is available on the effects of aft-mounted turboprop engines on aircraft performance, stability, and control during the low-speed phases of flight (*i.e.*, takeoff, climb, approach, and landing). To obtain this information, NASA modified an existing wind tunnel model to incorporate alternative aft-mounted turboprop engine arrangements. The turboprop engines were simulated using 29-horsepower electric motors housed in the nacelle. The model was designed for testing with either tractor or pusher propellers. Furthermore, gearboxes and propellers were designed for either single-rotation propellers or two rows of propellers turning in opposite directions (counterrotating propellers).

Initial parametric wind tunnel tests were conducted in the 4- by 7-Meter Tunnel in late 1983 to define overall aircraft forces and moments as well as the forces and moments acting on the propeller and nacelle installation. The results of these tests quantified the large normal and side forces produced by the advanced single-rotation propeller/nacelle over a range of angles of attack. The aircraft configuration test results indicated the importance of the forces induced by the propeller and the propeller slipstream on the aircraft stability and control characteristics. Power effects for the aft-mounted counterrotating pusher configuration were caused primarily by propeller forces and moments, whereas the aft-mounted single-rotation tractor configuration was influenced primarily by propeller slipstream-pylon interactions. In addition, valuable information regarding the acoustic characteristics of isolated

propeller-nacelle installations and detailed measurements of the propeller flow fields were obtained.

Paul Coe, 3611

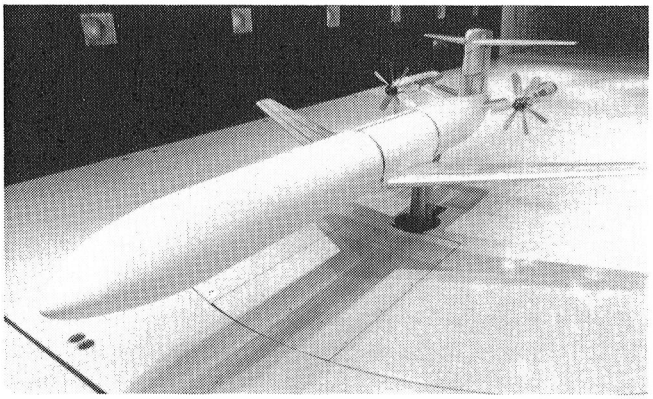

Advanced aircraft configuration with aft-mounted engines.

Transition Measurements on an NLF Airfoil

In October 1983, a wind tunnel investigation of boundary layer transition behavior on a natural-laminar-flow (NLF) airfoil model was conducted in the 4- by 7-Meter Tunnel. The model was an NLF airfoil glove originally designed to fit over a wing section of the NASA T-34C research support airplane for flight research. For the wind tunnel test, the 3-foot-span, 7.67-foot-chord glove was mounted between end walls which were designed to promote two-dimensional flow over the airfoil.

The purpose of the test was twofold. The first purpose was to investigate the particular nature of transition that occurred on this airfoil. The hope was to positively determine whether or not a laminar separation bubble was tripping the flow, and if so, to determine the identifying pressure and hot-wire signal characteristics of a separation bubble. The second purpose of the test was to obtain an exact comparison of different transition-measuring techniques. Four types of transition detection methods were used. These included sublimating chemicals, oil flow, boundary layer pressure rakes, and hot-wire anemometers. The oil flow visualization method positively showed that under certain conditions, transition was caused by a separation bubble. Clearly defined lines marked the chordwise boundaries of the the bubble in the oil. In contrast, the sublimating chemicals produced a line only at the end of the separation bubble and gave no indication of the existence of the bubble. The chemicals mark transitions more clearly, but the oil flow tells more about the nature of the transition. Data from the hot-wire anemometers and pressure rakes positioned exactly within a bubble are being analyzed to determine heat transfer characteristics and velocity distributions which uniquely identify a laminar separation bubble.

The understanding gained by these experiments will improve accuracy in the measurement of boundary layer transition in flight and wind tunnel research. Each of the techniques used works best under particular conditions. Also, the combination of certain measuring techniques gives a much clearer picture of transition than when they are used separately. With improved transition-measuring capabilities, better correlations between theory and experiment can be made and the nature of transition can be better understood during research experiments.

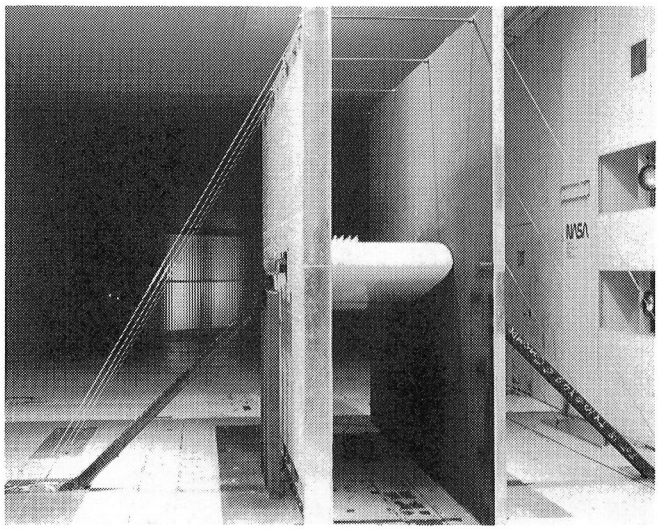

NLF airfoil model tested in 4- by 7-Meter Tunnel.

Lisa Richardson, 3611

Local Blade Surface Dynamic Pressure Measurements on a Model Helicopter

In January 1983, a rotorcraft wind tunnel investigation was conducted in the 4- by 7-Meter Tunnel to evaluate a dynamic measurement technique for local surface pressures on a model scale rotor blade. Because a limited number of slip-ring chan-

nels were available through the rotor shaft, a method was needed to multiplex the signals of many pressure gages while still maintaining a large frequency bandwidth capability. The rotor model used for this investigation was an existing two-blade 1/4-scale model of the UH-1H.

The multiplexing system allows the signal from one gage from each of two strips to be recorded for a time period equal to a multiple of rotor revolutions. The system then automatically steps to another pressure gage and repeats the process. By continually stepping through all pressure gages, it is possible to record practically continuous time-dependent surface pressures.

Results of the program provided confidence in the feasibility of such a system on a rotor model with a much larger number of pressure gages. Improvements to the multiplexing package have been incorporated into the design of the next-generation system.

John Berry, 3611

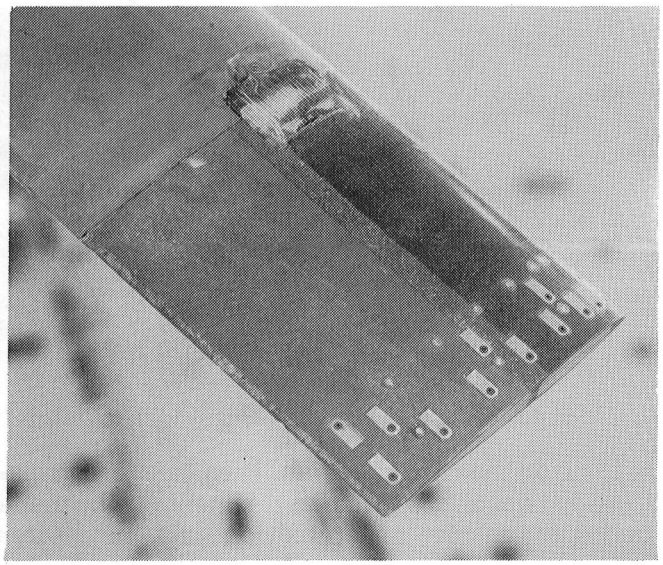

Pressure-instrumented 1/4-scale UH-1H rotor tip.

Advanced Vectoring Exhaust Nozzle Performance on an Advanced Fighter Concept

In order to assess the capabilities of several advanced vectoring exhaust nozzle concepts, a joint wind tunnel test was conducted in the 4- by 7-Meter Tunnel involving NASA, the Grumman Aerospace Corporation, and the U.S. Air Force. The investigation compared the performance of four vectoring nozzle concepts mounted on a model of Grumman's advanced fighter aircraft configuration. The four advanced nozzle concepts tested were selected from a number of proposed concepts. They included an axisymmetric nozzle as the baseline, an asymmetric load-balanced exhaust nozzle (ALBEN), a low-aspect-ratio single-expansion-ramp nozzle (LoAR SERN), and a high-aspect-ratio single-expansion-ramp nozzle (HiAR SERN).

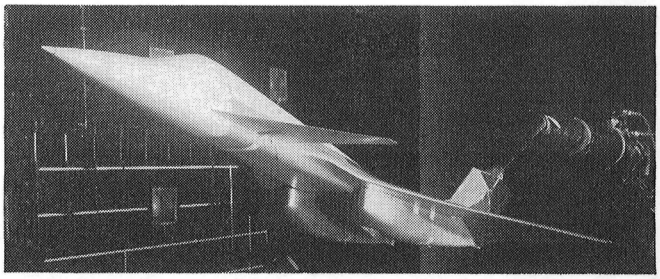

Advanced fighter configuration mounted in 4- by 7-Meter Tunnel.

The results of this test were combined with Grumman's definition of the full-scale aircraft on which the model was based to perform analytical evaluations of each nozzle in a number of flight regimes on the full-scale aircraft. One of the analytical comparisons of the nozzles was made on the basis of takeoff ground roll performance. The results of this comparison indicated that the ALBEN nozzle performed best in the takeoff regime. This was due mainly to its test-demonstrated capability to vector 30° in an afterburning configuration. Takeoff ground roll distances of less than 400 feet were predicted to be possible with this nozzle on a 34,200-pound aircraft with a wing loading of 76 pounds per square foot and a thrust-to-weight ratio of 0.85.

Guy Kemmerly, 3611

Advanced Nozzle Concepts Fighter Nozzle and High-Lift System Investigation

A cooperative wind tunnel investigation was conducted by NASA, McDonnell Douglas Corporation, and the U.S. Air Force to evaluate the STOL performance of an advanced nozzle concepts fighter model. This investigation evaluated the performance of several wing leading-edge high-

lift devices for the landing approach configuration and tested two advanced thrust vectoring nozzles in approach and full thrust reverser modes.

The leading-edge high-lift devices investigated included vortex and Krueger flaps at inboard and outboard locations on the main wing. These were tested on a canard configuration and on an inboard leading-edge glove configuration of the model. Based on the test results, it was determined that the preferred high-lift system for the approach mode had the vortex flaps deflected 45° upward inboard and outboard on the model with the leading-edge glove configuration.

The two multifunction nozzles, one designed by the Pratt & Whitney Group and the other by the General Electric Company, were evaluated in the approach and full thrust reversing modes. Splay doors, which were mounted over the reverser openings and deflected the reversed flow outboard to minimize the reingestion problem, were investigated on the General Electric nozzle. Results showed both nozzles to be acceptable for the approach mode, in which partial thrust vectoring and reversing were simultaneously employed, whereas the General Electric nozzle with splay doors was effective in reducing the reingestion problem in the full thrust reverser mode.

Greg Gatlin, 3611

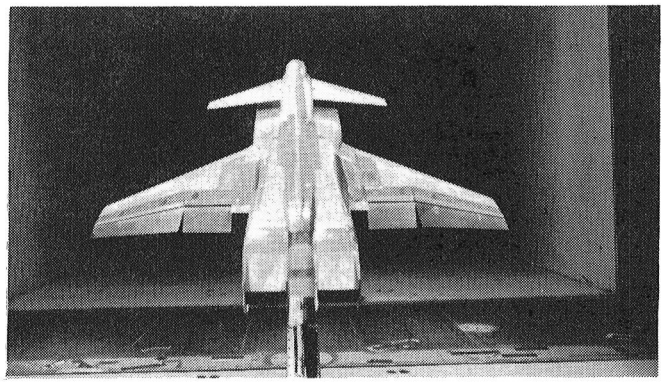

Advanced nozzle concepts fighter model tested in 4- by 7-Meter Tunnel.

Single and Counterrotation Propeller Noise Comparison

Noise measurements of several propeller installations have been made in the Langley 4- by 7-Meter Tunnel. These installations included single (SR) and counterrotating (CR) propellers in strut-mounted pusher and tractor configurations as well as sting-mounted configurations at pitch and yaw. The objective of this research is to provide the technology base for incorporating noise trade-offs into propeller installation design for subsonic aircraft. Experiments will provide a data base from which to infer noise trends for various installations and validate existing analytic noise prediction methods.

The noise measurements were made by microphones which were flush mounted in a moveable carriage. Eleven microphones were aligned perpendicular to the flow direction at about 13° increments from the propeller axis. The microphone carriage itself was stepped in the flow direction in 13 positions at 10° increments covering the range from 60° upstream of the propeller disk plane to 60° downstream. For each propeller installation, 143 noise measurements were made to define the noise radiation pattern.

The results from this study showed that the noise radiated from an unsteadily loaded propeller is highly directional. Knowledge of these patterns may be used to minimize the noise impact of a given propeller installation. The results also showed that for the configurations involving a propeller operating in a wake (CR and SR pusher), the noise increased considerably both in overall level and in harmonic content. In particular, the difference in noise levels radiated in certain directions between a CR and an SR operating at the same thrust level exceeded 15 dB. For an SR, the difference between operation in a pusher mode and operation in a tractor mode exceeded 10 dB.

Patricia J. W. Block, 2645

8-Foot Transonic Pressure Tunnel

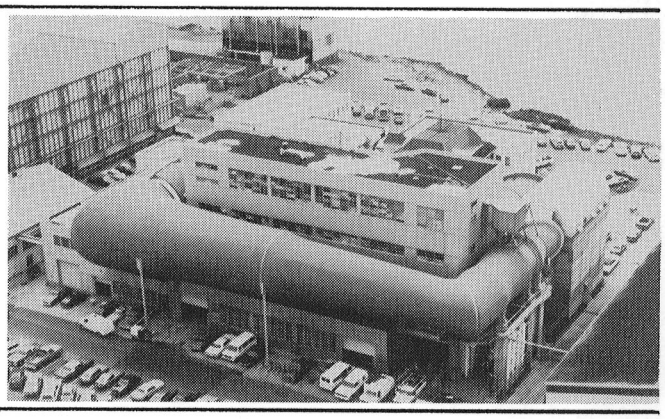

The Langley 8-Foot Transonic Pressure Tunnel is a closed-circuit single-return variable-density continuous-flow wind tunnel. The test section walls are slotted (5 percent porosity) top and bottom, with solid sidewalls fitted with windows for schlieren flow visualization. In 1982 the facility was modified for flow quality improvements and reconfigured for low-drag testing of a large-chord swept laminar-flow-control airfoil at transonic speeds. A honeycomb and screens were permanently installed in the settling chamber to suppress the turbulence level in the test section. A contoured liner was installed on all four walls of the test section to simulate interference-free flow about an infinite yawed wing. This contoured liner produces a contraction ratio of 25:1 and covers existing floor and ceiling slots. An adjustable sonic throat is also located at the end of the test section to block upstream propagation of diffuser noise.

The combination of honeycomb, screens, and choke provides a very low disturbance level in the test region at transonic speeds. Except for the honeycomb and screens, the changes are reversible. In the current configuration, the stagnation pressure can be varied from about 0.25 to 1.25 atmospheres up to a Mach number of less than 0.85 with the transonic slots closed by the liner. The stagnation temperature is controlled by water-cooled fins upstream of the settling chamber. Tunnel air can be dried by a dryer using silica gel desiccant to prevent fogging due to expansion in the high-speed nozzle.

Laminar-Flow-Control Tests

The reduction of drag and hence an increase in vehicle performance has always been one of the primary research goals of aerodynamicists. Large decreases in friction drag can be realized if a laminar boundary layer can be maintained either by passive natural laminar flow (NLF) controlled through geometric shaping or by active laminar flow control (LFC), which usually depends both on shaping and on mass transfer through local surface suction. Langley researchers have defined an experiment with the overall objective of investigating the physical phenomena associated with laminar flow and low-profile drag on advanced swept supercritical airfoils. Furthermore, tests will allow the evaluation and documentation of the combination of suction control laminarization and supercritical airfoil technology at conditions typical of high-performance transports.

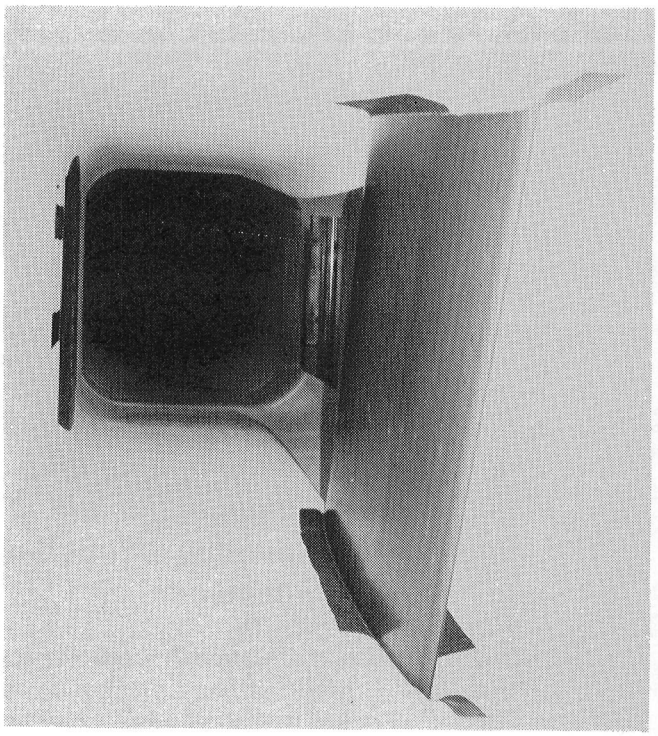

Swept supercritical LFC wing in 8-ft TPT.

8-Foot Transonic Pressure Tunnel

Performance testing with the Laminar Flow Control Experiment installed in the 8-Foot Transonic Pressure Tunnel has been ongoing since September 1982. This research has involved the advanced swept supercritical airfoil, the suction system, and the tunnel liner. Results to date indicate that full-chord laminar flow can be achieved with low drag up to high speeds and high Reynolds numbers. Furthermore, suction laminarization with an extensive supercritical zone has also been obtained at high chord Reynolds numbers. The LFC results indicate performance comparable to that of typical turbulent supercritical airfoils but with significantly lower drag.

W. D. Harvey, 4514

Transonic Dynamics Tunnel

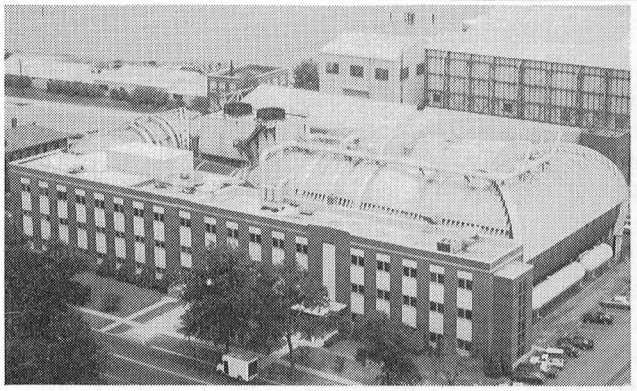

Conversion of the original Langley 19-Foot Pressure Tunnel into the Transonic Dynamics Tunnel (TDT) was begun in the late 1950's to satisfy the need for a large transonic wind tunnel dedicated specifically to work on the dynamics and aeroelastic problems associated with the development of high-speed aircraft. Since the facility became operational in 1960, it has been used almost exclusively to clear new designs for safety from flutter and buffet, to evaluate solutions to aeroelastic problems, and to research aeroelastic phenomena at transonic speeds.

The tunnel is a slotted-throat single-return closed-circuit wind tunnel with a 16-foot-square test section. The stagnation pressure can be varied from slightly above atmospheric to near vacuum, and the Mach number can be varied from 0 to 1.2. Both test section Mach number and density are continuously controllable. The facility can use either air or Freon 12 as the test medium. Freon is usually used because it has several advantages over air as a test medium for dynamically scaled aeroelastic model testing. The tunnel has a Freon reclamation system so that the gas can be purified and reused.

The facility is equipped with many features uniquely suited to dynamic and aeroelasticity testing. These include a computerized data acquisition system especially designed to rapidly process large quantities of dynamic data, a means of rapidly reducing test section Mach number and dynamic pressure to protect models from damage when aeroelastic instabilities occur, a system of oscillating vanes to generate sinusoidal variations in tunnel flow angle for use in gust response studies, and special mount systems which enable simulation of airplane free-flight dynamic motions.

Transonic Body Freedom Flutter on a Forward-Swept-Wing Model

Body freedom flutter is known to be one of the fundamental aeroelastic problems to be avoided on forward-swept-wing (FSW) aircraft. This phenomenon is caused by the adverse coupling of rigid-body pitching and wing-bending motions. Although rare on aft-swept-wing aircraft, this mechanism is generic to FSW configurations due to the tendency of the wing to effectively destiffen (or aeroelastically diverge) with increasing dynamic pressure. A NASA-sponsored model test (with Grumman Aerospace Corporation) was conducted to investigate this phenomenon on a realistic FSW configuration in the flutter-critical transonic-speed regime and to ascertain the ability of existing analytical tools to predict its occurrence. A 0.5-scale aeroelastic model of a FSW airplane was tested in the Transonic Dynamics Tunnel. The model is shown sidewall mounted in the tunnel test section.

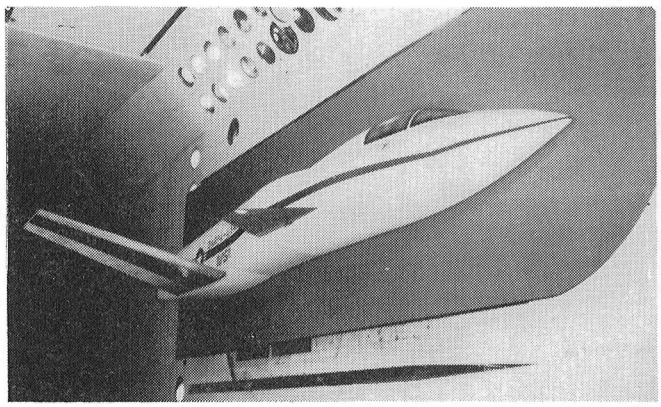

Measured and calculated results for statically stable model configuration.

Measured and calculated results obtained for the statically stable model configuration are shown as functions of Mach number and dynamic pressure. The calculations were performed by Grumman using their SAEL (servo aeroelastic) program, which utilizes double-lattice subsonic aerodynamic theory. As can be seen, the body freedom flutter calculations proved to be considerably higher than the measured data. Additionally, a static divergence instability (square symbol) was predicted using a subcritical response technique applied to data measured below the flutter boundary. By comparison, the flutter actually occurred at about 70 percent of the predicted divergence dynamic pressure.

Rodney H. Ricketts, 2661

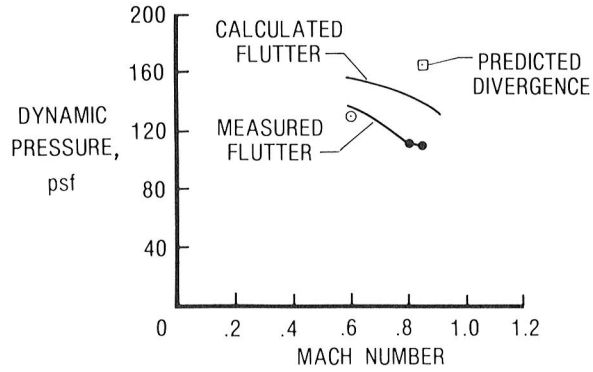

Aeroelastic model of FSW airplane mounted in TDT.

Transonic Flutter Studies of Effects of Winglets Extended to Twin-Engine Transport Type Wing

Previous transonic studies of the effects of winglets on flutter have mostly been limited to wing configuration without engines. This study extended the technology base by providing transonic flutter data on a twin-engine transport type wing with winglet. The specific objectives of this study were to determine experimentally the winglet effect on flutter for different variations in configuration parameters and to correlate these results with strip theory analyses performed by the Boeing Company. The study was a cooperative Boeing/NASA effort. Transonic flutter tests were conducted jointly in the Langley Transonic Dynamics Tunnel using an existing Boeing-built 1/10-size semispan flutter model of a twin-engine transport type wing. The model was equipped with three different wing tips: a nominal wing tip, a tip with a winglet, and a nominally shaped wing tip ballasted to simulate the winglet mass properties. Transonic flutter boundaries were measured with each of the three wing tips on the following configurations: empty fuel, full fuel, and empty fuel with soft-mounted engine nacelle.

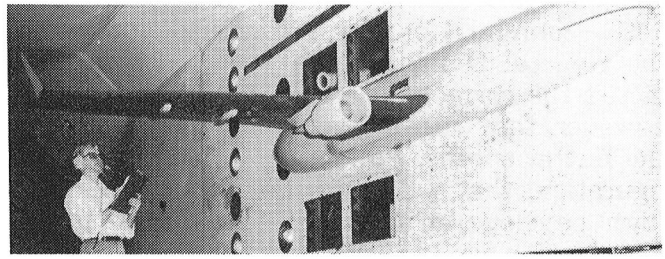

Model mounted in TDT.

As an example of the test results, the winglet effects on the flutter dynamic pressure *(q)* for the empty wing are illustrated. The wing aerodynamic effect (determined by comparing the flutter boundary for the winglet tip with that for the ballasted tip) was much greater than its mass effect and caused a reduction in wing flutter q of about 20 percent near the transonic dip. In general, the Boeing pretest analyses were in good agreement with test results.

Charles L. Ruhlin, 2661

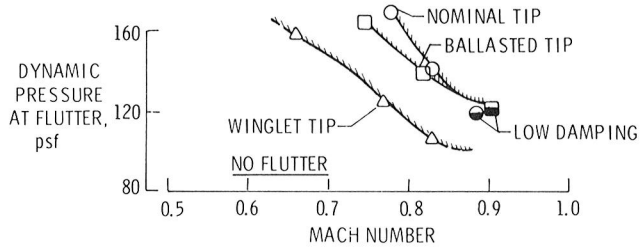

Winglet effects on flutter q *for empty wing.*

Effects of New Fuel Tanks and Nonjettisonable Pylons on F-16 Flutter Characteristics

The objectives of this test in the Langley Transonic Dynamics Tunnel were (1) to verify analyses by General Dynamics Corporation which have shown that carriage of certain external stores

in combination with new 600-gallon fuel tanks may be restricted by flutter, (2) to investigate possible alternative store carriage arrangements, and (3) to investigate the effects of pylon parameters such as stiffness on flutter speeds.

The model was mounted on the two-cable mount system in the TDT and was tested for flutter conditions within the simulated required flight envelope. A total of 32 configurations were tested, sixteen basic configurations and sixteen alternative configurations. Test results indicated that the General Dynamics analyses generally predicted the correct flutter mode and frequency; however, they were not as reliable in predicting the flutter speeds. For the majority of the configurations that had flutter conditions within the flight envelope, an alternative configuration was found which would alleviate the problem. For the other cases, valuable experimental data were obtained which can be used in combination with analysis to develop means of eliminating flutter.

Judith J. Watson, 3596

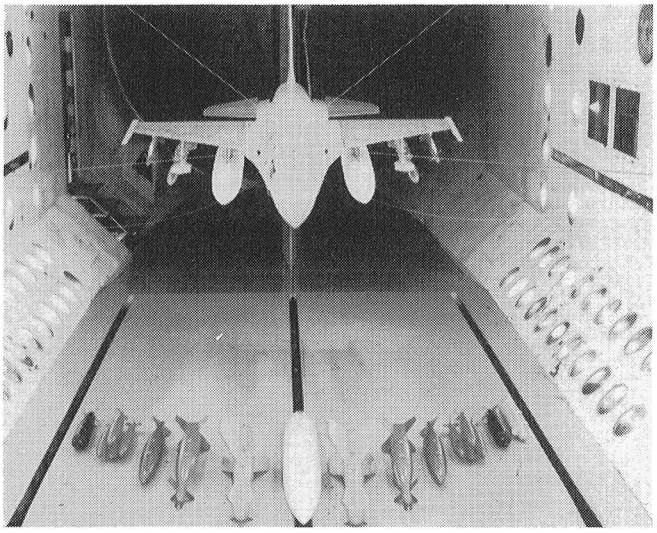

F-16 model and external stores used in flutter tests.

Decoupler Pylon Flight Test Configuration

The decoupler pylon is a Langley patented device for the underwing carriage of stores and passive suppression of wing-store flutter. The concept has been demonstrated in the past with research pylons on several flutter models. Promising results have led to the design and fabrication of flight quality hardware and the implementation of a flight test program using an F-16 airplane. The objective of this wind tunnel study was to evaluate the flutter characteristics of the F-16 with stores mounted on decoupler pylons that incorporated the key features of the flight test hardware.

A 1/4-scale aeroelastic model of the F-16 with the flight test store configuration was tested in the Transonic Dynamics Tunnel. The model is shown on the cable mount system in the TDT. A 1/4-scale decoupler pylon (see insert) was fabricated which incorporated the key features of the flight test hardware, namely the four-bar linkage remote pivot arrangement, a damper, and the tapered-beam spring.

Initially, the flutter boundary was determined with the bombs on standard pylons. Then the bombs were mounted on each wing on decoupler pylons with the scaled friction level. The tests were repeated, and the model was shown to be flutter free to 111 percent above the baseline flutter dynamic pressure. A second study was conducted with the breakout friction varying from no friction to twice the scaled level without any observed degradation in the flutter suppression capabilities of the decoupler pylon.

F. W. Cazier, Jr., 2661

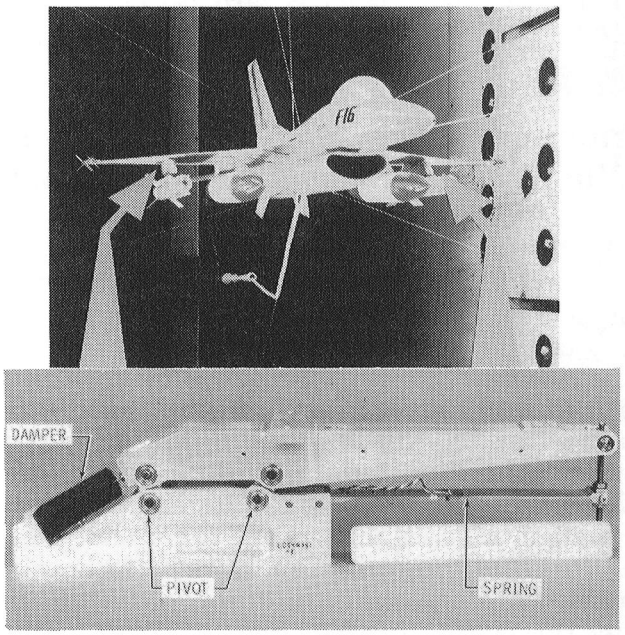

Aeroelastic model with decoupler pylon configuration in TDT.

Galileo Parachute Configuration

The Galileo probe is a space vehicle designed to record atmospheric measurements while decelerating through Jupiter's atmosphere in 1989. A parachute will be used to decelerate this probe. To determine the effectiveness of the parachute system, a drop test of a full-size Galileo probe with parachute was made from a hot air balloon. Upon release of the main parachute, 6 seconds were needed to fully open the chute. This was considerably longer than the 0.5 second required by design. Movies showed that the parachute had become trapped unopened in the viscous wake of the blunt probe body. Therefore, wind tunnel tests were conducted in the Transonic Dynamics Tunnel to define the optimum ratio of riser line length to probe diameter (*X/D*) for a successful deployment of the parachute.

Parachute behavior was investigated for *X/D* of 5.5, 7, 9, and 11 at Mach numbers ranging from 0.6 to 1.1. Preliminary tests were made with the parachute in the deployed mode to determine the best *X/D*. During the final tests, the parachute was actually deployed from a containment bag near the probe to verify this result. The wind tunnel tests were very successful and the results were verified during a subsequent balloon drop test.

Bryce M. Kepley, 2661

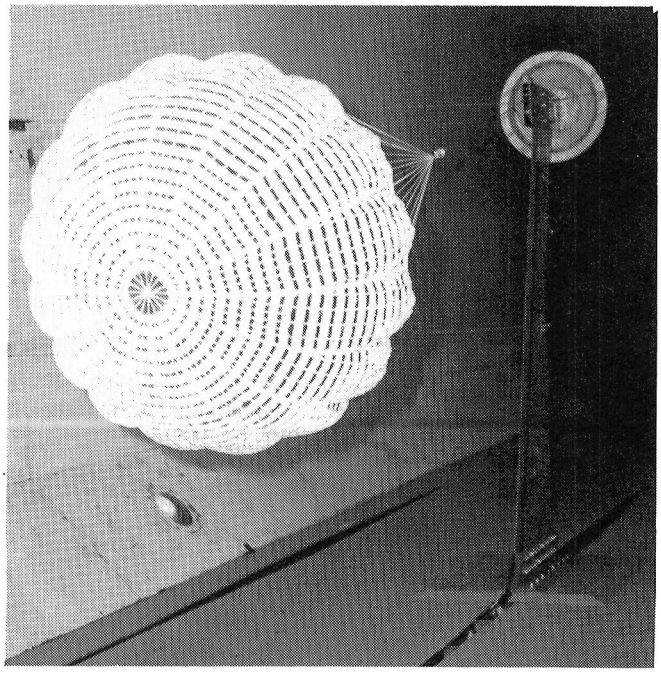

Galileo parachute deployed during test in TDT.

Effects of New AMRAAM Missiles on F-16 Flutter Characteristics

Modern fighter airplanes such as the F-16 carry many types and combinations of external wing-mounted stores, such as bombs, missiles, and fuel tanks. Carriage of these stores changes the dynamic and aerodynamic characteristics of the airplane, which in turn affect the flutter characteristics of the airplane. The objectives of the current test were to study the validity of analyses that have shown that F-16 carriage of the new advanced medium-range air-to-air missiles (AMRAAM), especially in combination with other stores, may be critically restricted by flutter, and to study possible modifications (fixes) that would eliminate these restrictions. A test was conducted in the Transonic Dynamics Tunnel using a 1/4-scale aeroelastic model of the F-16 airplane. The model is shown carrying an AMRAAM missile on an AMRAAM launcher under each wing and an empty AMRAAM launcher on each wing tip.

The experimental results obtained during this test substantiated the need for a flutter fix. Two possible flutter fixes were studied during the test. First, pylon pitch stiffness was greatly reduced, and second, a small amount of mass was added to the nose of each wing tip launcher. Both fixes appear promising.

Moses G. Farmer, 2661

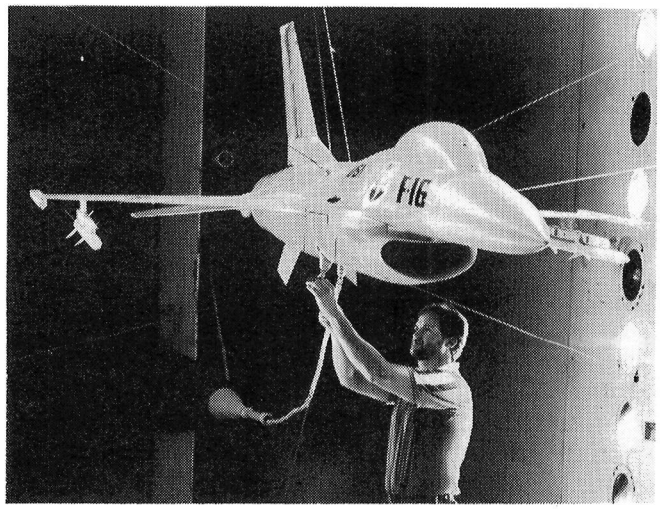

Aeroelastic scale model of F-16 airplane in TDT.

16-Foot Transonic Tunnel

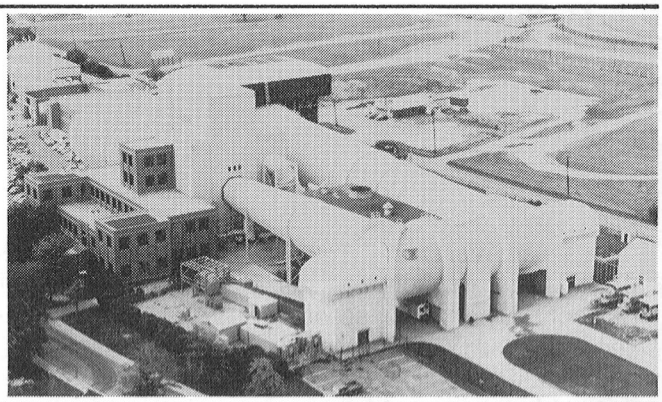

The 16-Foot Transonic Tunnel is a closed-circuit single-return continuous-flow atmospheric tunnel. Speeds up to Mach 1.05 are obtained with the tunnel main-drive fans, and speeds from Mach 1.05 up to Mach 1.30 are obtained with a combination of main-drive and test section plenum suction. The slotted octagonal test section measures 15.5 feet across the flats. The tunnel is equipped with an air exchanger with adjustable intake and exit vanes to provide some temperature control. This facility has a main drive of 60,000 horsepower and a 36,000-horsepower compressor provides test section plenum suction.

This tunnel is used for force, moment, pressure, flow visualization, and propulsion-airframe integration studies. Model mounting consists of sting, sting-strut, and fixed-strut arrangements. Propulsion simulation studies are made utilizing dry, cold, high-pressure air.

B-1B Nozzle Study

A test was conducted in the Langley 16-Foot Transonic Tunnel in support of the U.S. Air Force B-1B program. Test objectives included a determination of propulsion installation drag increments for use in performance calculations, an investigation of the dynamic flow characteristics around the nozzles, and a study of the flow characteristics on the overwing fairing. The test was conducted over a Mach number range from 0.55 to 1.25 at angles of attack from -1.0° to 6.0°. The model was mounted upside down in the tunnel in order to minimize strut interference effects on the propulsion installation components. Modifications made during the test to the overwing fairing resulted in a signifcant increase in cruise performance.

David E. Reubush, 2675

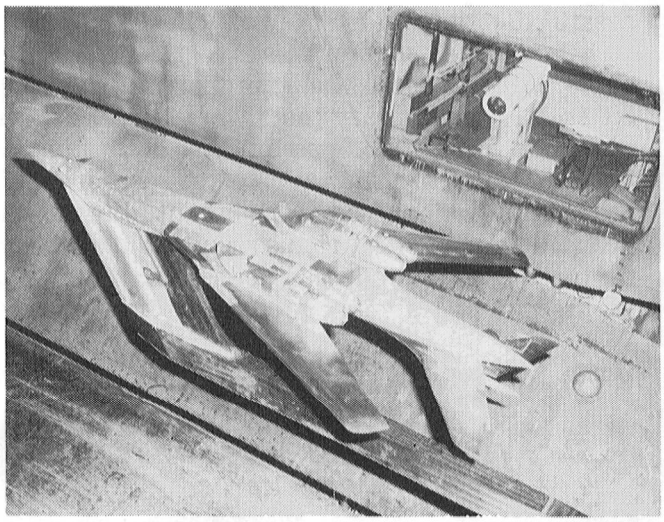

B-1B in 16-Foot Transonic Tunnel.

Laminar-Flow Nacelles

Tests were conducted in the Langley 16-Foot Transonic Tunnel to determine the drag reduction potential of installing laminar-flow nacelles on a high-wing transport configuration. Flow-through nacelles designed to achieve laminar flow over a large portion of the nacelle surface were used. Force and pressure data were obtained at Mach numbers from 0.70 to 0.85 and at angles of attack from -2.5° to 4.0°. Data were obtained with both free and fixed transition. Flow visualization studies were conducted to determine the extent of laminar flow achievable on this concept. Preliminary analysis of the data indicated that

nacelle drag was reduced on the order of 50 percent.

James C. Patterson, 2675

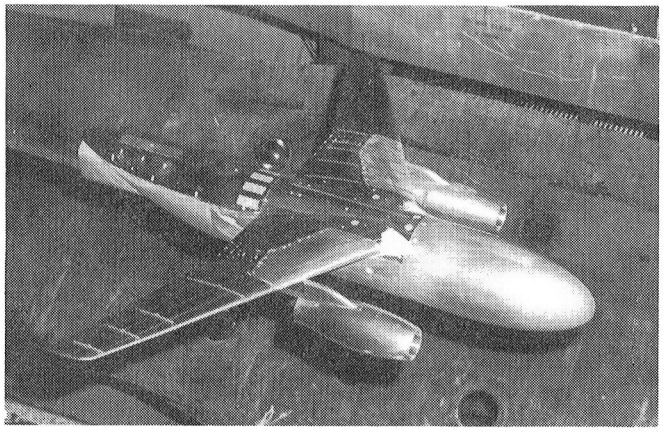

Transonic transport with laminar-flow nacelles.

Thrust Vectoring and Thrust Reversing for Control

A test was conducted in the Langley 16-Foot Transonic Tunnel to study the installation of nonaxisymmetric nozzles on an advanced fighter aircraft. The primary purpose was to evaluate the effects of 2D-CD nozzle installation and to expand the current data base on the use of thrust vectoring and reversing as the primary control. The test was conducted at Mach numbers from 0.60 to 1.2 and at angles of attack from -2.0° to 15°. The nozzle pressure ratio varied from 1.0 (jet-off) to 5.0.

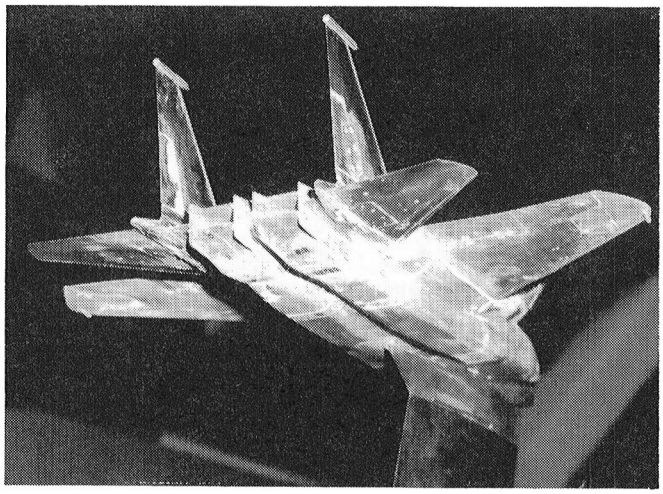

Nonaxisymmetric nozzle installed on fighter aircraft configuration.

Steady-state force and pressure data as well as dynamic pressure data were obtained.

All test objectives were met. The results of the study illustrated that nonaxisymmetric nozzles can be integrated into a twin-engine fighter aircraft such that a significant drag reduction can be obtained. (Drag for a configuration with 2D nozzles was less than drag for same configuration with axisymmetric nozzles.) The data also demonstrated that thrust vectoring and thrust reversing can provide trim and control for fighter aircraft over a significant portion of the aircraft flight envelope.

W. P. Henderson, 2676

Installation Effects of Advanced Turboprop Nacelles on Supercritical Wing

A test was conducted in the Langley 16-Foot Transonic Tunnel to study the effects of the flow field generated by a turboprop on the characteristics of a thick supercritical wing. An unswept, untapered 12.5-percent-thick supercritical wing section was mounted on a bifurcated strut support system. The turboprop nacelle employed SR-2 blades and was studied in both overwing and underwing locations. Extensive static pressure data were obtained on the wing and nacelles at Mach numbers from 0.50 to 0.80 and angles of attack from 0° to 3°. Other variables included in the study were geometric pitch angle and rpm of the propeller configuration. The primary purpose of this study was to acquire the very detailed,

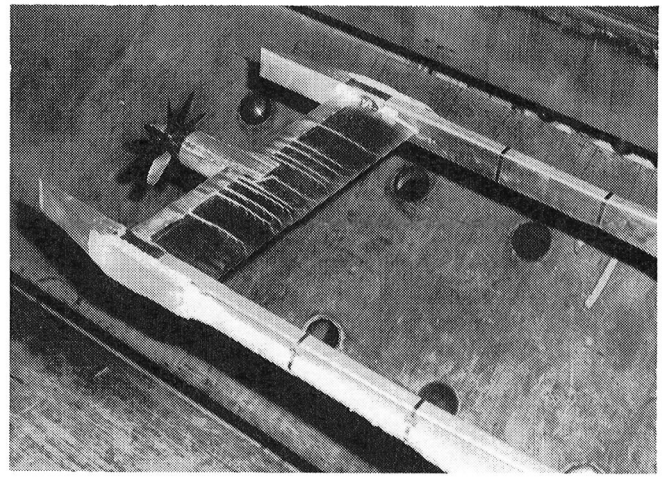

Turboprop model.

high-quality data necessary to verify new computational methods and develop an understanding of the complex flow interactions associated with turboprop-wing integration.

The results of this study illustrated that the propeller slipstream caused an increase in wing lift coefficient throughout the test Mach number range. Large beneficial effects were noted at low speeds ($M < 0.60$) but tended to diminish as the Mach number increased. The data also showed that a large portion of the swirl was recovered by the wing.

W. P. Henderson, 2676

National Transonic Facility

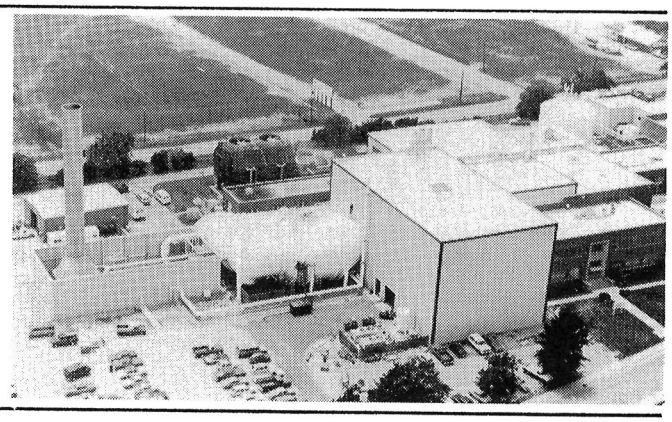

The most difficult aerodynamic regime for aircraft designers to understand is the transonic region, where speeds near Mach 1 (760 mph at sea level) are attained. At these speeds, the flow around an aircraft is distorted by shock waves, and the resulting turbulence decreases the lift and increases the drag in such complex patterns that designers cannot accurately predict the results. To develop a test facility that would allow full-scale testing of aircraft at such speeds would be very costly and would require an enormous power supply.

NASA Langley's approach to this problem was to use nitrogen gas at high pressures and ultralow, cryogenic temperatures to simulate the transonic flow about full-sized aircraft. The principle that allows this simulation is that even if the sizes, speeds, and altitudes of two aircraft are very different, the aerodynamic properties of the flow about them will be identical if the Reynolds number (a parameter describing the flow which is a function of aircraft size and speed as well as of the density and viscosity of the flow) and the Mach number are the same for the two aircraft. By employing ultralow temperatures in a new tunnel, the viscosity of the nitrogen gas can be greatly reduced and Reynolds numbers can be achieved using small models which will be identical to those characteristic of the airflow about full-sized aircraft in the real, more viscous atmosphere.

The new tunnel, the National Transonic Facility (NTF), is a cryogenic fan-driven transonic wind tunnel designed to provide full-scale Reynolds number simulation in the critical flight regions of most current and planned aircraft. It will operate at Mach numbers from 0.2 to 1.2, stagnation pressures from 1 to 9 bars, and stagnation temperatures from 340 to 80 K. The maximum Reynolds number capability will be 120 million at a Mach number of 1.0, based on a reference length of 0.25 meter. Construction of the facility was completed in September 1982, shakedown operations started the following month, and the maximum Reynolds number was obtained in May 1983.

The NTF operating envelope is illustrated. The symbols represent test points covered during shakedown. The facility has been operated in both air and nitrogen modes covering a Mach number range up to 1.17 at pressures up to 8.5 atmospheres and at temperatures down to 100 K. The shakedown effort should be completed by mid-1984 and will be followed by aerodynamic calibration.

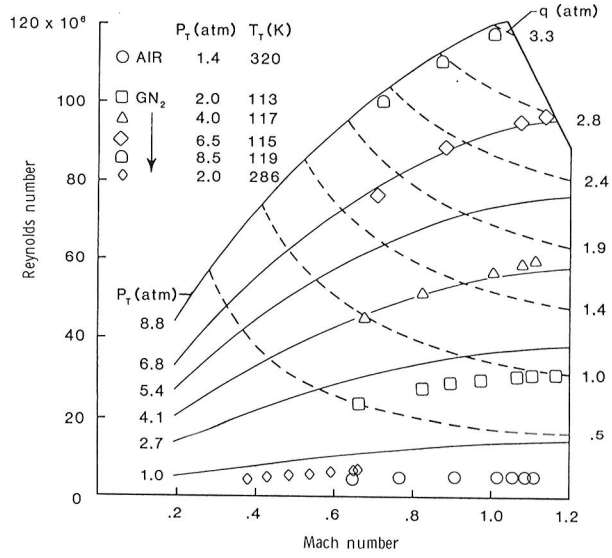

NTF operating envelope.

0.3-Meter Transonic Cryogenic Tunnel

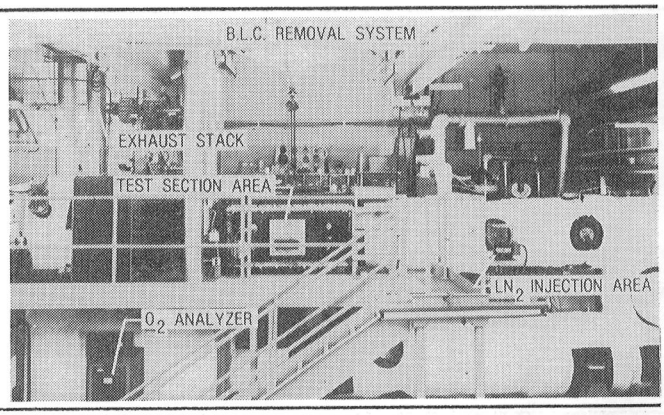

The Langley 0.3-Meter Transonic Cryogenic Tunnel (TCT) is a continuous-flow fan-driven transonic tunnel that uses nitrogen gas as the test medium. It is capable of operating at Mach numbers up to about 0.85, stagnation pressures up to 6 atmospheres, and stagnation temperatures from 340 to about 80 K. At the maximum test condition, a Reynolds number (based on a model chord of 15.24 centimeters) of 50×10^6 can be achieved. In its present configuration, a two-dimensional slotted-wall test section is installed. The test section is 20 centimeters wide and 60 centimeters high and the slotted top and bottom walls have a 5-percent open-area ratio. It is equipped with motorized model support turntables and a traversing wake survey probe, both of which are computer controlled.

This facility was first placed in operation in 1983 as a pilot three-dimensional tunnel to demonstrate the cryogenic wind tunnel concept at transonic speeds. The successful demonstration of this concept in the 0.3-m TCT played a major role in the decision to build the National Transonic Facility. In its present mode of operation, the 0.3-m TCT is used for routine airfoil testing at high Reynolds numbers, as a test bed for components and instrumentation for the NTF, and for advanced cryogenic wind tunnel testing techniques.

Sidewall Boundary Layer Removal Effects on Two Different Chord Airfoil Models

An investigation was carried out on two CAST 10-2 airfoil models with chords of 3 and 6 inches to evaluate the extent of sidewall influence on airfoil tests at transonic Mach numbers. The tests were conducted in the Langley 0.3-Meter Transonic Cryogenic Tunnel two-dimensional test section equipped with an upstream sidewall boundary layer removal system which reduced the boundary layer displacement thickness to about 1 percent of model halfspan from an initial 2 percent without boundary layer removal.

Test results showed that the changes in the location of the shock on the upper surface of the airfoil were about the same for both models with and without sidewall boundary layer removal. Even though large differences were noted in the high-lift characteristics of the two models, the sidewall boundary layer removal had little effect on these differences. These tests also served to validate the boundary layer removal technique and the associated Mach number correction required with upstream boundary layer removal.

C. Johnson, 4380

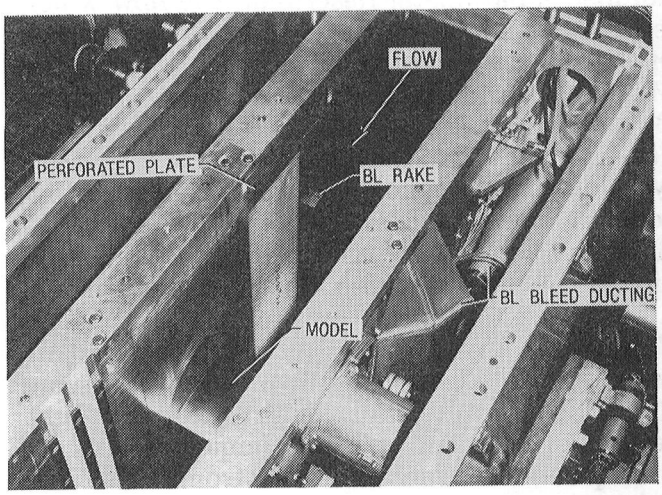

Two-dimensional test section with perforated plates for boundary layer removal.

Reynolds Number Effects on Sting Interference

With the advent of the National Transonic Facility, the need for an understanding of Reynolds number effects on sting support interference has become urgent. The unit Reynolds number range of the Langley 0.3-Meter Transonic Cryogenic Tunnel is substantial; therefore, initial studies into the effects of Reynolds number variation on sting support interference were conducted in this tunnel.

Tests were made in the Langley 0.3-Meter Transonic Cryogenic Tunnel to investigate the effects of Reynolds number at constant Mach number and Mach number at constant Reynolds number on boattail pressure drag for a variety of sting shapes. Experimental data were obtained over a Mach number range from 0.60 to 0.90 and a Reynolds number range (based on body length) from 5.4×10^6 to 74.7×10^6. The boattail pressure drag did not increase over the Mach number range investigated for constant Reynolds numbers. However, at constant Mach number the boattail pressure drag generally continued to be a function of Reynolds number over the Reynolds number range tested. Thus, further work in the area of Reynolds number effects on sting support interference at the higher Reynolds numbers of the NTF is required. The data indicated that as the disturbance produced by the sting on the boattail increased, the boattail pressure drag became less sensitive to Reynolds number. Also, it was shown that the model base pressure became insensitive to Reynolds number change for the higher Reynolds numbers tested, whereas the model base pressure varied linearly with Mach number for a constant Reynolds number.

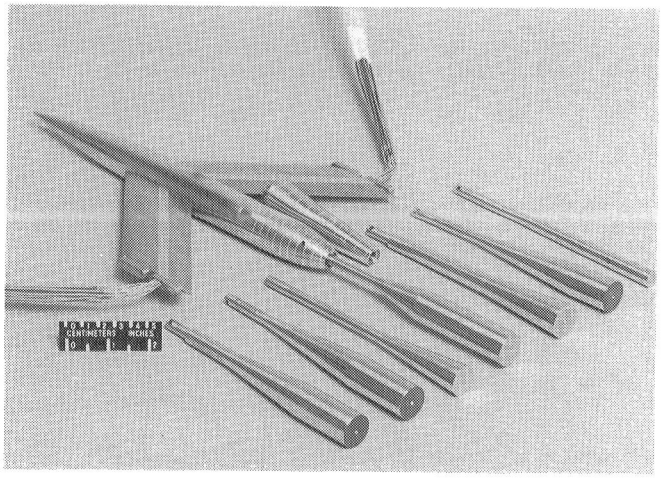

Variety of sting shapes.

B. Gloss, 2601

Detecting the Presence of Liquid Nitrogen Droplets in Cryogenic Tunnels

Cryogenic wind tunnels, including the National Transonic Facility, obtain their high Reynolds number capability by cooling the test gas; the lower the operating temperature, the greater the Reynolds number will be. Consequently, it is desirable to operate cryogenic tunnels as cold as possible to maximize Reynolds number through temperature reduction. The tunnel is cooled or kept cool during data acquisition by continuously injecting liquid nitrogen (LN_2) directly into the tunnel stream. The injected LN_2 is atomized into large numbers of small droplets (about 10^6 per cubic centimeter) which absorb heat from the surrounding gas as they evaporate. If these droplets do not evaporate by the time they are convected around to the test section, they could disrupt the quality of the aerodynamic data being taken. The concern which motivated the research was that at some low-temperature condition in the wind tunnel, the tunnel gas would not be warm enough to evaporate the droplets before they reached the test section.

The test procedure involved mounting a droplet-sizing probe in the 0.3-m TCT through an access flange in its settling chamber. (The number of droplets detected in the settling chamber will be greater than the number reaching the test section since the injection takes place upstream in the diffuser section.) The probe was mounted so that the instrument package, which was enclosed in a box-like structure, remained outside the tunnel, and the long cylindrical portion was inserted into the tunnel through a pressure flange. At the end of the cylindrical portion, light was focused down to a scattering volume in the tunnel flow. Droplets passing through this volume scattered light, which was returned up the cylinder to the instrument package, where the magnitude of the scattered light was related to a droplet size. With the probe installed, the tunnel was operated over a range of pressures, temperatures, and Mach numbers.

It was found that the injection system used in the 0.3-m TCT resulted in nearly complete droplet evaporation, and even at the lowest temperatures tested, concentrations of LN_2 droplets in the settling chamber were on the order of only 1 to 10 per cubic centimeter, which is too small a number to influence the flow in the test section. The same probe and test procedure will be used for a similar experiment in the National Transonic Facility.

B. Hall, 2601

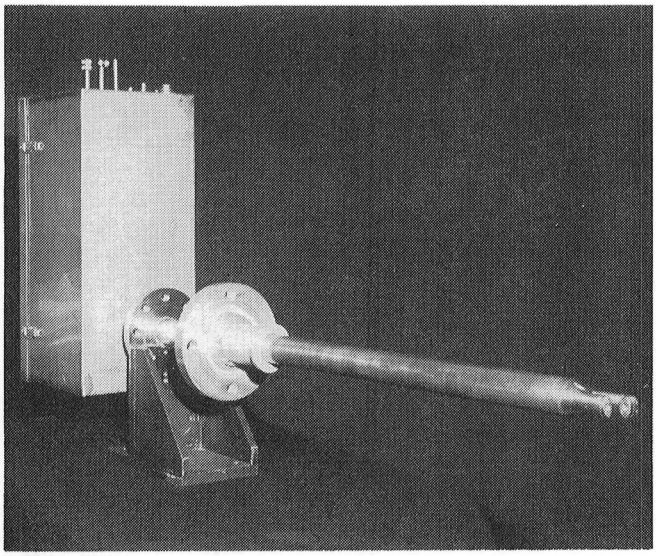

Droplet-sizing probe.

Unitary Plan Wind Tunnel

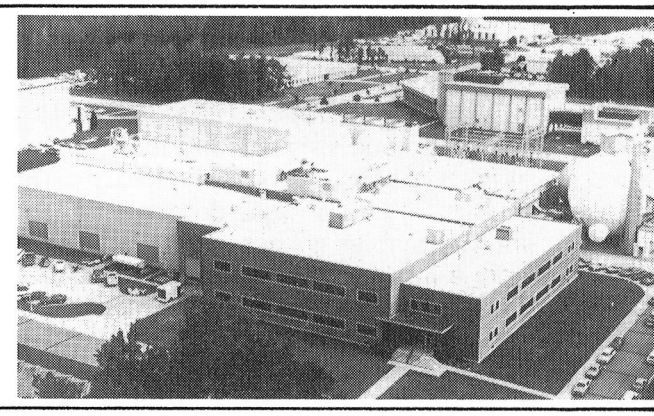

Immediately following World War II, the need for wind tunnel equipment to develop advanced airplanes and missiles was recognized. The military and the National Advisory Committee for Aeronautics (NACA) developed a plan for a series of facilities which was approved by the U.S. Congress in the Unitary Wind Tunnel Plan Act of 1949. This plan included five wind tunnel facilities, three at NACA laboratories and two at the Arnold Engineering Development Center. The Langley Unitary Plan Wind Tunnel was among the three built by NACA. The Unitary Plan Wind Tunnel is a closed-circuit continuous-flow variable-density tunnel with two 4- by 4- by 7-foot test sections. The low-range test section has a design Mach number range of 1.5 to 2.9 and the high-range section varies from 2.3 to 4.6. The tunnel has sliding block type nozzles which allow continuous variation in Mach number while on-line. The maximum Reynolds number per foot varies from 6×10^6 to 11×10^6 depending on Mach number. The tunnel is used for force and moment, pressure distribution, jet effects, dynamic stability, and heat transfer studies. Flow visualization data, which are available in both test sections, include schlieren, oil flow, and vapor screen.

Supersonic Multibody Aerodynamic Research and Technology (SMART)

An experimental and theoretical program has been established to investigate the supersonic aerodynamics of multibody concepts and to define multibody aerodynamic design logic and goals. Previously, an initial wind tunnel test of two axisymmetric bodies set on a rectangular planform was conducted to generate a generic data base and to evaluate existing theoretical methods. (See Langley Test Highlights — 1982, NASA TM-84655, 1983.) Based upon these results, this second multibody wind tunnel model was designed, constructed, and tested.

This second multibody wind tunnel model consisted of a center wing/balance housing system upon which various outboard wing panels and bodies could be attached. Testing was performed at Mach numbers of 1.6, 1.8, 2.0, and 2.16. Longitudinal and lateral-directional aerodynamic force and moment characteristics were measured. Test results from this second multibody wind tunnel model have identified the impact of sidebody shaping on both longitudinal and lateral-directional characteristics. In addition to the various twin-body arrangements tested, a Mach-1.80 three-body concept was designed and tested, using an existing fighter model as a baseline. Results from the three-body fighter model tests indicated that the multibody concept could be applied to fighter type configurations in order to improve the aerodynamics at supersonic speeds.

Richard M. Wood, 3181

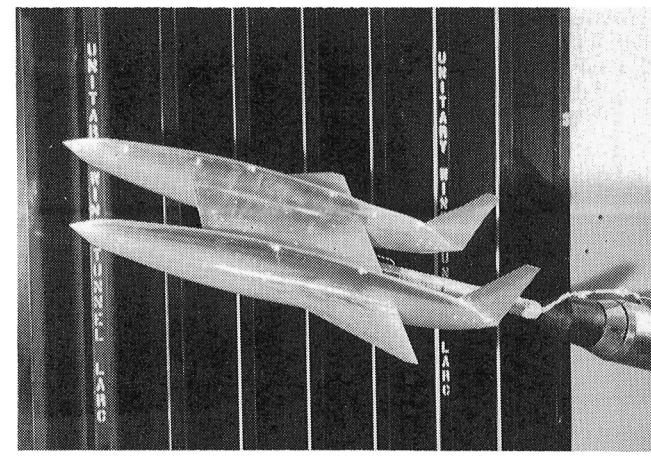

Multibody model in Unitary Plan Wind Tunnel.

Raman Doppler Velocimeter Tests at Supersonic Speeds

Recent developments in the application, measurement, and analysis of stimulated Raman spectroscopy have shown that the velocity of test medium molecules can now be determined from Doppler shift principles without particle seeding. The method employs two lasers to stimulate specific Raman spectrum signals to measurable levels. By combining this velocity-measuring capability with standard Raman techniques for temperature and density measurement, a totally nonintrusive device is available for flow field surveys. The capabilities of a Raman Doppler velocimeter (RDV) are ideally suited for high-speed flows, particularly where shock waves, rapid expansions, strong vortices, and separated-flow regions occur.

Initial tests were conducted in the Langley Unitary Plan Wind Tunnel at Mach numbers from 3.0 to 4.5 to develop and evaluate the RDV system for measuring supersonic flow fields. A continuous and a pulsed laser beam each entered the test section windows at a 65° horizontal inclination to the tunnel centerline. Comparisons of the RDV-measured free-stream Mach number with tunnel calibration values differed by 6 to 8 percent. These differences were due primarily to inaccuracy in the temperature measurement. Differences of only 1 to 6 percent occurred when the tunnel calibration value of static temperature was used. These first attempts to use the RDV in a research wind tunnel produced encouraging results. Future tests are planned to enhance the signal quality through improvements in laser resolution, signal acquisition, and data processing.

Reginald J. Exton, 2791

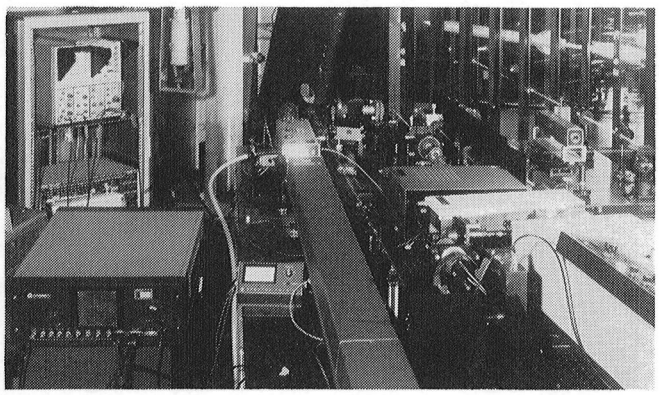

RDV system in Unitary Plan Wind Tunnel.

Flow Visualization Tests of Two Conical Wings

NASA and the Grumman Aerospace Corporation conducted a joint experimental and theoretical research program to develop a supersonic high-lift nonlinear wing design technology. Aerodynamically efficient high lift ($C_L = 0.4$) is achieved by carefully contouring the wing so the upper-surface flow achieves supercritical crossflow conditions and low drag is maintained by avoiding strong crossflow shocks. A full-potential nonlinear flow code was used to design a two-dimensional conical wing with a span section cambered to produce the desired flow conditions at Mach 1.62. Wind tunnel force and pressure tests were initially conducted on models of the cambered wing and a flat wing. Surface pressure measurements indicated that the cambered-wing design goal could be obtained experimentally; however, the cambered wing at off-design conditions and the flat wing at most conditions exhibited various degrees of crossflow shocks and flow separation.

A second wind tunnel test was conducted to collect extensive flow visualization information in the form of oil flow, tuft, and vapor screen photographs. Although past experience indicated that good-quality vapor screen photographs could not be obtained below Mach 1.8, excellent photographs were obtained at Mach 1.6 by systematically varying Reynolds number and total temperature. These flow visualization results correlated well with the previously obtained pressure and force data and provided critical information on the character and development of supercritical crossflow breakdown which was unavailable from only pressure and force data. It

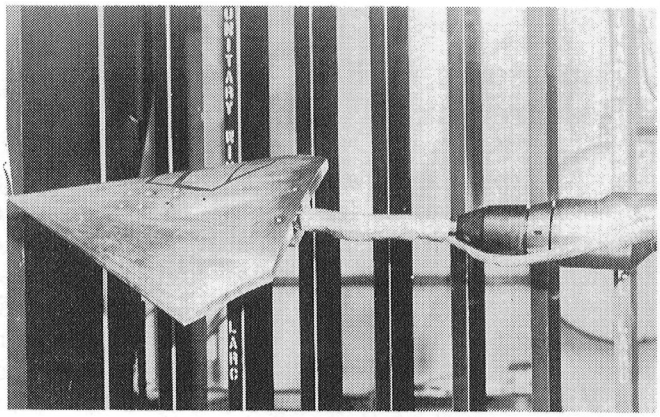

Conical wing in supersonic wind tunnel.

appears that good-quality vapor screen photographs can be obtained at all Mach numbers in the Unitary Plan Wind Tunnel, and a comprehensive study is under way to document the precise flow conditions which provide the optimum vapor screen photographs in the low Mach number range.

Richard M. Wood, 3181

F-16C/AMRAAM Integration Study

One of the primary roles of the the Unitary Plan Wind Tunnel is to support the military in the testing of supersonic aircraft. In keeping with this mission, a 1/15-scale F-16C with various advanced medium-range air-to-air missile (AMRAAM) loadings was tested for the Aeronautical Systems Division, Air Force Systems Command, in the Unitary Plan Wind Tunnel facility. Tests were conducted to determine the effects on drag and stability of adding up to six AMRAAM missiles in various configurations. Horizontal-tail deflections were made to determine aerodynamic trim characteristics. A Reynolds number of 2×10^6 per foot was maintained for all tests at Mach numbers of 1.60, 1.80, and 2.00. The angle of attack was varied from -4° to 20° and the angle of sideslip was varied from -6° to 8°.

These tests were conducted in April 1983 to obtain data to support flight tests. The initial flight test data showed good agreement with the wind tunnel test results. This agreement enabled the number of flights in the planned test program to be reduced significantly. Release of test results is not authorized without prior approval of the Air Force Systems Command F-16 Program Office.

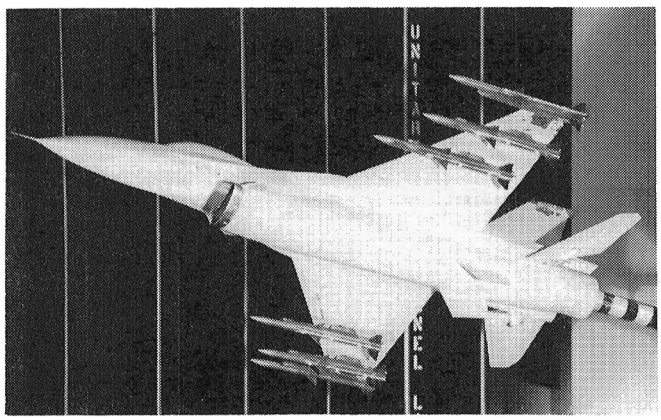

F-16C with six AMRAAM's.

Store Carriage Drag Investigation

A cooperative research program between NASA and the Northrop Corporation was instituted in order to obtain high-accuracy store carriage drag measurements at supersonic speeds. Such data are required for the development of improved prediction methodology. An investigation was conducted in the Langley Unitary Plan Wind Tunnel at Mach numbers from 1.6 to 2.16 on a simplified generic wing-body, as the parent aircraft model, for a range of store shapes and store carriage concepts. The store shapes included circular, elliptical, and rectangular, and the store carriage concepts varied from the conventional pylon-type mount to the more advanced semisubmerged arrangements.

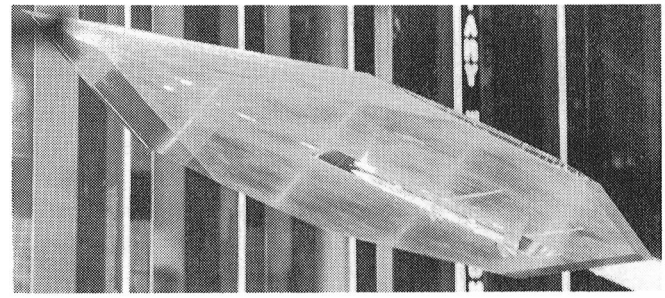

Generic store carriage model with 1/15-scale AMRAAM.

In order to provide improved accuracy force measurements, only the store-carrying section (pallet) of the model was mounted on a sensitive six-component strain gage balance. A small clearance gap was provided around the metric portion of the model, and the flow through the gap was minimized by means of seals made of open-cell foam rubber under the edges of the pallet. The pallet was 3 inches wide by 13 inches long and could accommodate up to nine store models in a three-by-three array. Surface pressures behind and to the side of the pallet could also be measured. A fuselage was simulated on only one surface of the wing, and the metric pallet could be placed on either the fuselage or the wing side of the model.

The metric pallet capability of the model performed well throughout the investigation. Test results indicated that an existing state-of-the-art store drag prediction method (USAF DATCOM/Hoerner) generally overpredicted the drag of tangent and semisubmerged configurations.

William J. Monta, 3181

Advanced Fighter Concepts Utilizing Maneuver Flap Systems

The performance goals of advanced fighter aircraft require that they be capable of high levels of cruise and maneuver efficiency in both the transonic and supersonic speed regimes. The use of wing maneuver flap systems appears to be a means of attaining the desired performance levels over a wide range of cruise and maneuver conditions. Two fighter concepts have been developed to evaluate the performance of wing maneuver flap systems on realistic configurations. One of the concepts has a 60° leading-edge-sweep modified arrow wing, aft-mounted vertical and horizontal tails, and side-mounted inlets. The other concept has a 70°/20° leading-edge-sweep cranked arrow wing, underslung inlet, and provision for either canards or horizontal tails as the primary pitch control surfaces.

Wind tunnel models of the two concepts were tested in the Unitary Plan Wind Tunnel at Mach numbers from 1.6 to 2.2. Forces and moments were measured on the basic configurations and extensive flow visualization studies were conducted using oil flow, vapor screen, and schlieren photographic techniques. Both models included flow-through ducts to simulate engine airflow characteristics, and each model was tested with a variety of duct inlet-to-exit area ratios utilizing a series of exit choke rings and inlet wedges. The models were tested through an angle-of-attack range of -4° to 14° and a yaw range of -6° to 6° with the primary control surfaces set to several deflection angles. In addition, the 70°/20° cranked leading-edge wing was installed on a generic wind tunnel model and tested with leading-edge flaps deflected and undeflected, in and out of the flow field of a canard, at several deflection angles. These tests were conducted at Mach numbers of 1.5, 1.8, and 2.2 to evaluate the force and moment characteristics of various combinations of flap and canard deflections without the influence of inlets or complex fuselage flow fields.

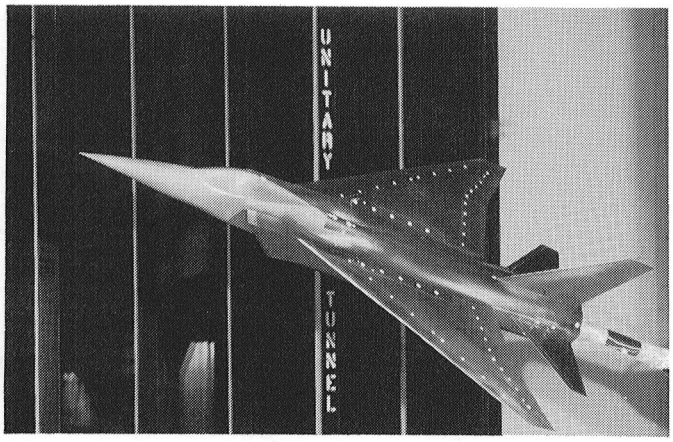

60° modified arrow wing concept.

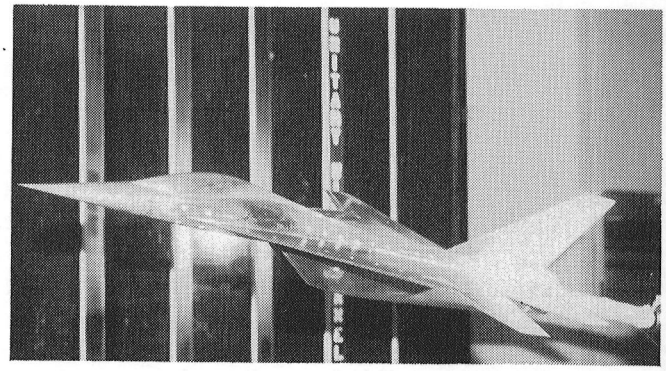

70°/20° cranked arrow wing concept.

Results of the tests accomplished to date on the two fighter concepts have permitted the selection of duct inlet and exit geometries to ensure consistent measurable duct flow. In addition, the lift and pitching moment characteristics of the two concepts were essentially linear over the angle-of-attack range in which maneuver flaps would be utilized. For the generic model, deflection of the inboard leading-edge flaps resulted in improved wing performance regardless of the canard configuration employed. Further tests are planned at transonic and supersonic speeds.

Barrett L. Shrout, 3294

Hypersonic Facilities Complex

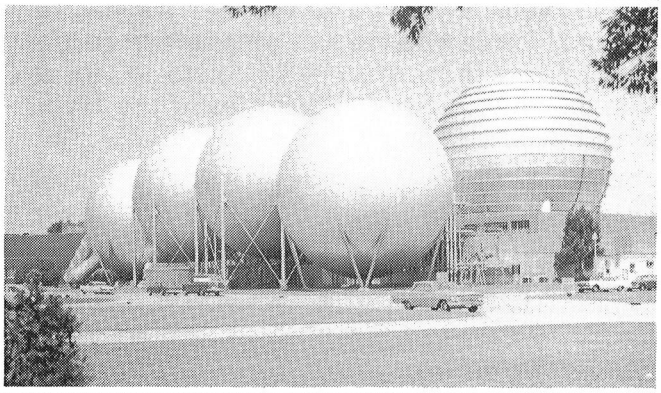

The Hypersonic Facilities Complex consists of several hypersonic wind tunnels located at four Langley sites. They are considered as an entity because as a complex these facilities represent a major unique national resource for wind tunnel testing. The complex currently includes the Hypersonic CF_4 (tetrafluoromethane) Tunnel ($M = 6$), the Mach 6 High Reynolds Number Tunnel, the 20-Inch Mach 6 tunnel, the Mach 8 Variable-Density Tunnel, the Continuous Flow Hypersonic Tunnel ($M = 10$), the Hypersonic Nitrogen Tunnel ($M = 17$), and the Hypersonic Helium Tunnel and its open jet leg ($M = 20$). These facilities are used to study the aerodynamic and aerothermodynamic phenomena associated with the development of space transportation systems, including the current Space Shuttle and future advanced orbital-transfer and launch vehicles; to support the development of advanced military spacecraft capability; to support the development of future planetary entry probes; to support the development of hypersonic missiles and transports; and to perform basic fluid mechanics studies and develop measurement and testing techniques.

This complex of facilities provides an unparalleled capability at a single installation to study the effects of Mach number, Reynolds number, test gas, and viscous interactions on the hypersonic characteristics of aerospace vehicles.

20-INCH M-6 TUNNEL
$M_\infty = 6$ AIR R_∞ 0.7-9.0x10^6

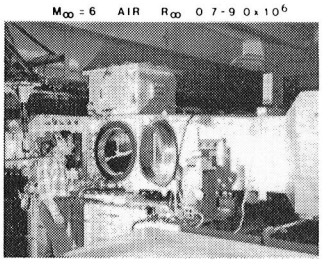

M-8 VAR.-DENS. TUNNEL
$M_\infty = 8$ AIR $R_\infty = 0.1\text{-}10.7 \times 10^6$

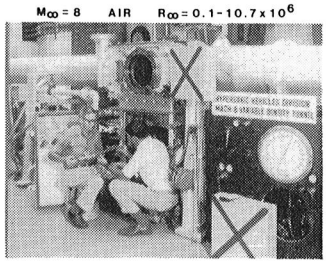

CONTINUOUS FLOW TUNNEL
$M_\infty = 10$ AIR $R_\infty = 0.4\text{-}2.4 \times 10^6$

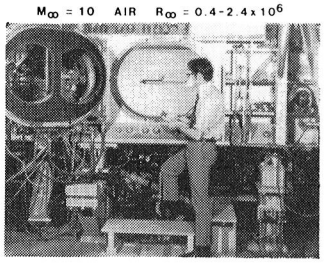

NITROGEN TUNNEL
$M_\infty = 17$ N_2 $R_\infty = 0.35 \times 10^6$

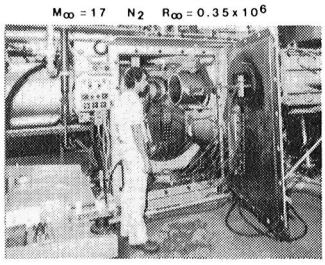

HELIUM TUNNEL
$M_\infty = 19\text{-}21.6$ He $R_\infty = 3.5\text{-}12.5 \times 10^6$

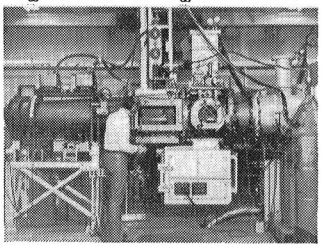

OPEN JET LEG-HE TUNNEL
$M_\infty = 20$ He $R_\infty = 6.0 \times 10^6$

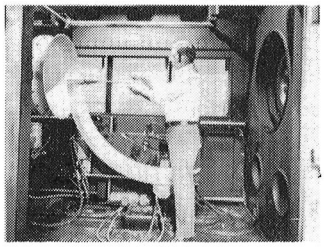

CF_4 TUNNEL
$M_\infty = 6$ CF_4 $R_\infty = 0.25\text{-}0.55 \times 10^6$

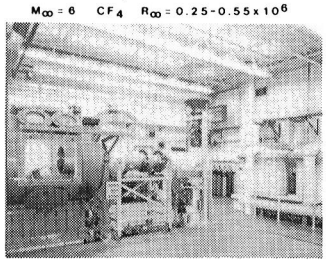

HIGH R_∞ M-6 TUNNEL
$M_\infty = 6$ AIR $R_\infty = 0.8\text{-}42.0 \times 10^6$

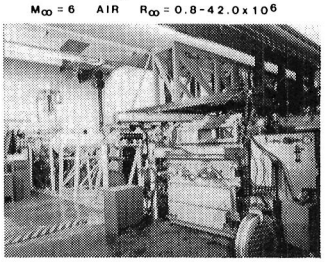

Heating Distributions for Biconics Demonstrate New Application of Thin-Film Gages

A study was initiated at Langley to establish a comprehensive experimental data base for a proposed generic planetary vehicle which is also a candidate moderate-lift-to-drag Earth orbital

transfer vehicle (OTV). This vehicle is a spherically blunted biconic with the fore-cone section bent upward relative to the aft-cone section to provide self trim capability. Several facilities of the Hypersonic Facilities Complex were used in this study.

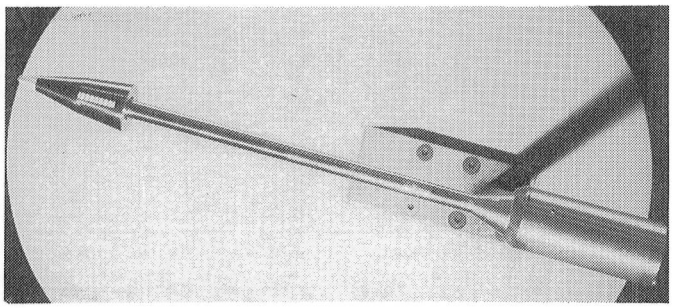

On-axis biconic heat transfer model in Continuous Flow Hypersonic Tunnel.

The most recent tests represent the first demonstration at Langley of the successful use of a large number of thin-film resistance heat transfer gages in a conventional hypersonic wind tunnel, namely the Continuous Flow Hypersonic Tunnel. Although these gages were designed and fabricated for use in the Langley Expansion Tube, which had a run time of only 250 microseconds, they performed flawlessly in the CFHT for run times up to 2½ seconds, four orders of magnitude longer than in the Expansion Tube. This study illustrates that the thin-film gage can provide many advantages over the commonly used transient calorimeter technique, including rapid response time (microseconds), increased sensitivity, and small size, which provides the potential for significant increase in the number of gages.

Using the same spherically blunted 13°/7° biconic models tested previously in the Expansion Tube, heating distributions were measured in the CFHT at Mach 10 in air and over a range of Reynolds number (based on model length) from 0.2 to 0.9 million and angles of attack from 0° to 20°. Although no effect of Reynolds number on laminar windward heating was observed for angles of attack from 0° to 20°, quite the opposite was true along the most leeward ray. The leeward flow separated when the fore-cone angle of attack exceeded about 0.8 times the fore-cone half angle, and an increase in Reynolds number caused the leeward flow to separate at a lower angle of attack. Upon separation, this flow became very complex (characterized by primary and secondary vortices), as revealed by oil flow patterns. When the leeward flow was attached, leeward heating was observed to increase with decreasing Reynolds number. However, once the flow separated, the opposite was true; that is, leeward heating increased with increasing Reynolds number. These results verified the ability of a NASA code which solves the parabolized Navier-Stokes equations to predict windward and leeward heating to within approximately 10 percent over the present range of angle of attack.

Charles G. Miller III, 4328

Heating Distributions for a Shuttle Orbiter Over a Range of Hypersonic Flow Conditions

The experimental hypersonic heat transfer base for the Shuttle orbiter was derived using several models and ideal-air wind tunnels. The present investigation is the first reported study to obtain a consistent set of heat transfer distributions for a single Shuttle orbiter model over ranges of Reynolds number, Mach number, and γ (ratio of specific heats for the test gases). To add to the existing data base, which will serve as the foundation for the next generation of STS vehicles, heating distributions were measured on a 0.006-scale orbiter model in three facilities of the Langley Hypersonic Facilities Complex; namely, the 20-Inch Mach 6 Tunnel, the Continuous Flow Hypersonic Tunnel, and the Hypersonic CF_4 Tunnel. These facilities provided a variation in Mach

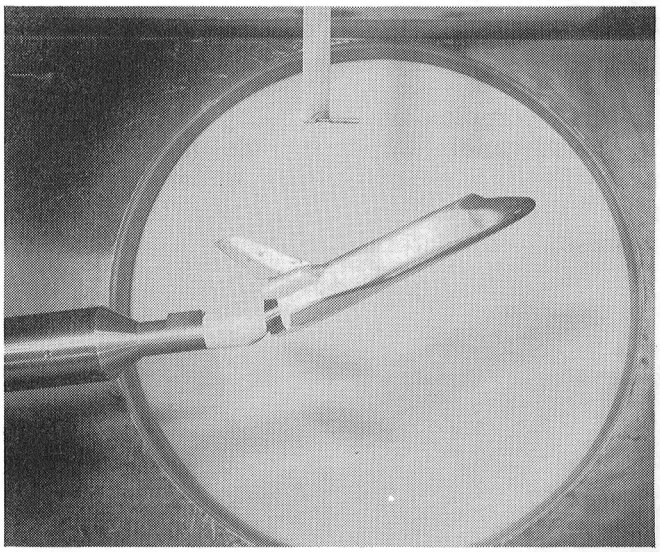

Heat transfer model in 20-Inch Mach 6 Tunnel.

number from 6 to 10 in air, a range of Reynolds number (based on model length) from 0.4×10^6 to 5.4×10^6 at Mach 6 and 0.3×10^6 to 1.4×10^6 at Mach 10, and a variation in γ within the shock layer from 1.13 to 1.4 at Mach 6. This variation in γ is particularly noteworthy because it provides qualitative information on the effect of a decrease in γ within the flow field such as occurs during reentry due to dissociation (*i.e.,* real-gas effects).

To ensure meaningful comparisons between these facilities, especially between air and CF_4, orbiter heating rates were nondimensionalized by the stagnation point heat transfer to a sphere measured in each facility at the same flow conditions as the orbiter. Laminar heating on the windward centerline was found to be independent of Mach number for angles of attack greater than 15°, but increased with decreasing Reynolds number and decreasing γ. The effects of Reynolds number and γ diminished with increasing angle of attack, and for the angle-of-attack range corresponding to the hypersonic portion of the early orbiter flights ($\alpha > 35°$), the effects were quite small. However, as the entry cross range is increased in future flights, resulting in lower angles of attack, these test results indicate that the effects on heating of these two flow quantities, as well as the effect of Mach number, will become significant.

Charles G. Miller III, 4328

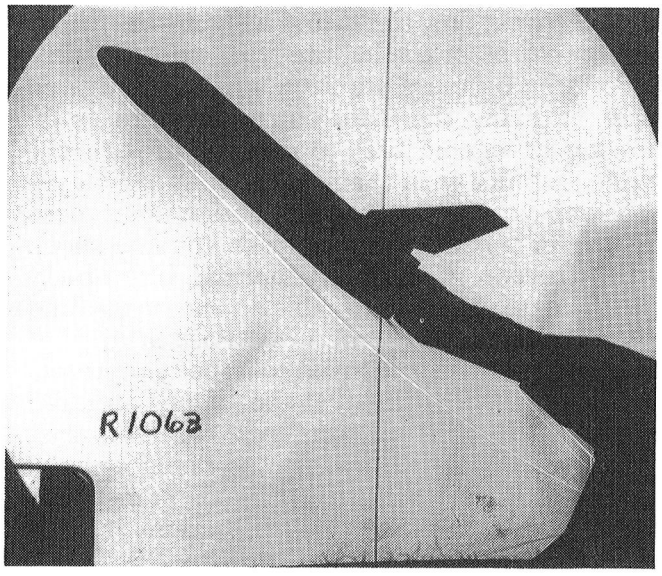

Schlieren photograph of orbiter heat transfer model in Hypersonic CF_4 Tunnel.

Surface Pressure Measurements for an Advanced Winged Entry Vehicle

Although an extensive data base has been developed for the Space Shuttle orbiter over the past decade, advanced entry vehicle concepts differ considerably from the present orbiter in terms of planform, planform loading, and length. In addition, high cross range requirements will necessitate the use of low-angle-of-attack entries. Far aft center-of-gravity locations drive the future designs toward control-configured vehicle concepts. This trend emphasizes the need for accurate flow field definition in the vicinity of deflected control surfaces, areas which are very difficult to predict analytically.

A series of surface pressure measurement tests on a 0.006-scale model of an advanced winged entry vehicle concept were performed at Mach 10 in the Continuous Flow Hypersonic Tunnel.

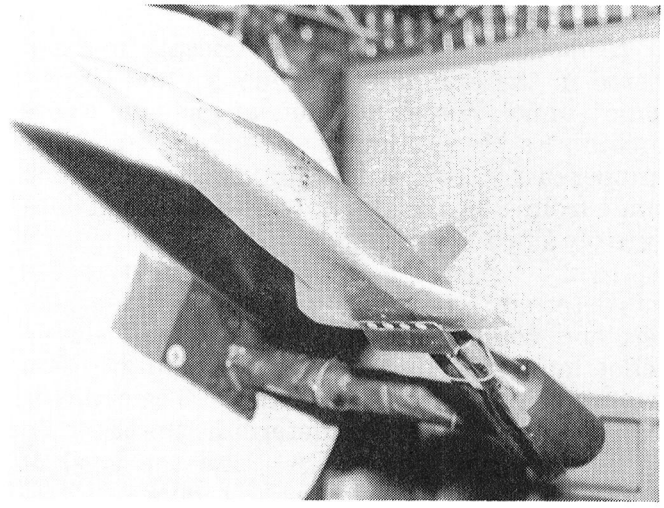

Surface pressure model of advanced winged entry vehicle installed in CFHT.

The objectives of these tests were to obtain experimental pressure distributions to complement the corresponding heating study performed previously, to enhance the data base on this new class of vehicle, and to obtain data that define the critical flow regions for advanced space transportation systems. Data were obtained for angles of attack from 0° to 40°, sideslip angles from -2° to ±5°, Reynolds numbers of 0.5, 1.0, and 2.0 million per foot, and body flap deflections of 0°, 10°, and 20°.

The data obtained in these tests are being used to help determine whether present prediction

techniques will need refinement to handle any flow phenomena which may be unique to the advanced configurations and not evident on the present Shuttle orbiter. Preliminary results indicate that no such unique phenonmena exist on this configuration and that the pressure distributions behave similarly to those on the current Shuttle orbiter.

Kathryn E. Wurster, 3911

Experimental Investigation of a Transatmospheric Vehicle at Mach 10

A transatmospheric vehicle (TAV) is being considered for use as an advanced tactical fighter of the 1990's. Because requirements include global range capability in which the TAV must go into orbit and deorbit to target and landing areas, the TAV must be tested throughout the entire speed regime.

A model of one of the TAV concepts has been tested in the Langley Continuous Flow Hypersonic Tunnel. Force and moment tests were conducted at a Mach number of 10 and a Reynolds number of 2×10^6 per foot for an angle-of-attack range from -5° to ±20°. Lateral-directional data were obtained for an angle-of-sideslip range from -3° to ±3°. Aerodynamic control effectiveness was determined by varying elevator, elevon, rudder, and combinations of elevator and elevon deflections. In addition, a tailless configuration was tested to obtain sideslip effects. The main objective of this test was to determine the trimmed lift-to-drag ratio of the TAV and the level of stability near the maximum *L/D* values.

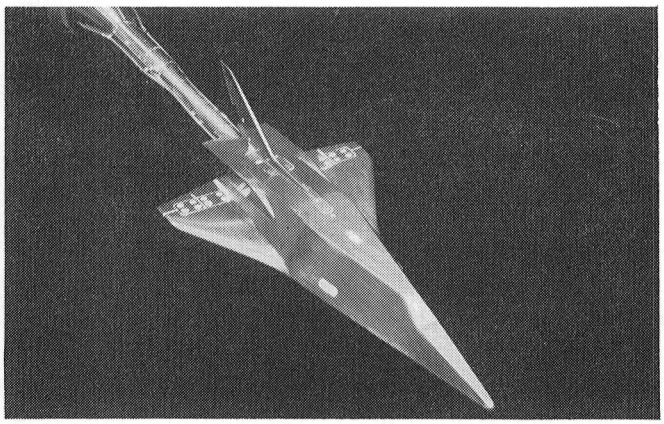

0.015-scale TAV model in Continuous Flow Hypersonic Tunnel.

Results showed a sharp increase in pitching moment coefficient between angles of attack of 5° and 10° and corresponding abrupt decreases in axial-force and normal-force coefficients. Oil flow tests conducted to obtain an explanation for this behavior showed large separation on the wing upper surface at an angle of attack of 5°, even larger separation at 7.5°, and a return to more attached flow at 10°. This corresponded to the pitching-moment, axial-force, and normal-force coefficients measured at those angles of attack. An adequate trim capability was present; however, most configurations were longitudinally unstable at their maximum *L/D* values. The vehicle was also shown to be laterally-directionally unstable, and the rudder was very ineffective. This was verified by the oil flow photographs, which showed that the rudder was shielded from the flow even at low angles of attack. This vehicle will be tested in other Langley tunnels to enlarge the experimental data base and contribute to the understanding of the flow characteristics about this type of vehicle.

Ronald S. McCandless, 2483

Hypersonic Flow Characteristics of Aero-Assisted Orbital Transfer Vehicle

In 1979, the Boeing Company proposed a concept for aero-assisted orbital transfer vehicles (AOTV) which utilized an inflated ballute to produce high drag (low structural weight). Sufficient cooling to protect the ballute from entry heating is produced by mass addition which is provided either by firing the main engine forward or by allowing cryogenic fuel to escape through the engine and mix with the natural boundary layer of the vehicle. Varying the stagnation point mass addition in this manner produces unusual shock wave structures, including normal blunt-body shock shapes, highly unstable shock fronts, and stable double-shock structures. Past studies of this concept at Mach 20 used solid-body representations of the expected shape of the inflated ballute to verify predicted flow fields and drag levels. The problem of how to study flexible-body response to these unusual and sometimes unsteady shock-jet flow field interactions remained a concern.

Goodyear Aerospace Corporation and the Boeing Company fabricated a wind tunnel model

from cotton cord and neoprene rubber to be tested at Mach 20 in the Hypersonic Helium Tunnel to determine how such a structure would respond at wind tunnel conditions. Shock structure and drag levels were quite similar to those experienced by the solid model. Ballute deformation occured for zero or low levels of mass addition, but a fixed shape rather than a divergent oscillation resulted. The flexible forebody did not appear to adversely affect the stability of the flow field, and *vice versa.* This was not a dynamic simulation of a flight article, but a test to produce the necessary data base to analyze and develop flight articles.

William C. Woods, 2483

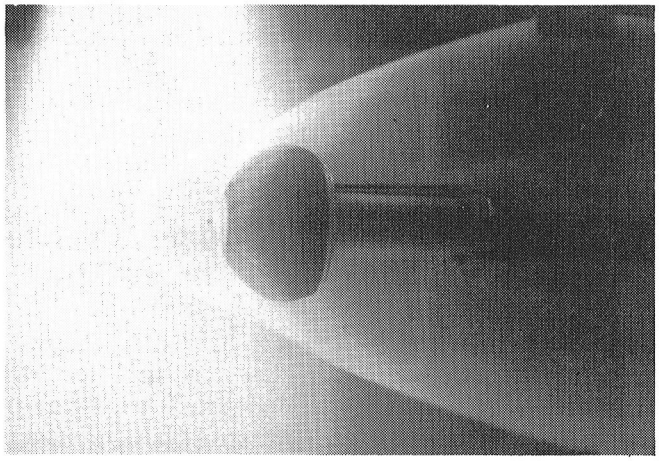

Shock structure on AOTV flexible model in Hypersonic Helium Tunnel.

Space Shuttle Orbiter Side Fuselage Heating Study

Flow reattachment on the Space Shuttle orbiter's side fuselage during entry produces some of the highest heating rates observed on the orbiter's leeward surface. Since current three-dimensional flow field codes are unable to accurately model leeside flow separation and reattachment phenomena, an alternate method of predicting the Shuttle's side fuselage impingement heating was sought. A series of phase change paint and oil flow tests were conducted in the Continuous Flow Hypersonic Tunnel (Mach 10) and the 20-Inch Mach 6 Tunnel to establish a data base of Shuttle side fuselage heating rates and surface flow directions as a prelude to the development of an empirical heating technique for application to the side fuselage reattachment line. These data were obtained at angles of attack from 20° to 40° and Reynolds numbers from 0.59×10^6 to 7.3×10^6.

The side fuselage impingement heating method was derived from a leeward centerline technique developed previously for the Shuttle orbiter. Both methods use the same form of turbulent heating equation, but with appropriate modifications for differences in surface geometry and source of local flow. A new correlation beween changes in local surface flow directions (obtained from oil flow patterns) and variations in heating distribution was developed at Langley and incorporated into these heating equations. Oil flow tests revealed the strake to be the source of impinging flow on the side fuselage. Flow properties along the strake were computed by the Langley HALIS flow field code. Predictions of the side fuselage impingement heating method were demonstrated to be within 10 percent of wind tunnel heating measurements. A preliminary comparison of the technique with entry heating rates obtained at a selected STS-3 trajectory point indicated similar agreement.

An unusual aspect of the Shuttle's side fuselage thermal environment was discovered using the phase change paint technique. Narrow, evenly spaced streaks of locally higher heating rates were observed to originate along the impingement line and extend upward on the side fuselage. This streak heating is believed to be caused by embedded vorticity, which is generated

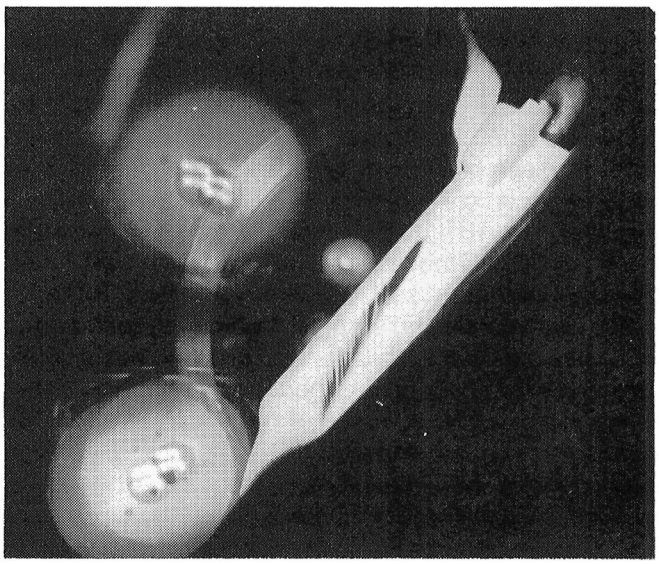

Space Shuttle orbiter side fuselage streak heating pattern.

by flow reattachment. The vortices begin to form at critical values of Mach number and Reynolds number for a given angle of attack. The effect on heating is particularly severe at combinations of high Reynolds numbers and high angle of attack. STS-3 entry heating measurements show that the side fuselage streak heating also occurs in flight, and the associated local temperatures are raised as much as 300°F by this effect. This may pose a potential problem in the design of thermal protection systems for future winged entry vehicles.

Vernon T. Helms III, 3984

Bluntness Effects on Hypersonic Static Stability of 10° Cone

Small-angle cones are of current interest because of their application to maneuvering reentry vehicles. For a generic vehicle of this shape, a major point of concern is the effect of nose ablation and erosion on the hypersonic static stability of the vehicle during reentry. Although a wealth of experimental data exists for cones in general, the effects of small incremental changes in nose bluntness at hypersonic speeds had not been studied previously. A systematic wind tunnel investigation was therefore performed on a series of spherically blunted 10° cones to analyze these effects and their dependence on Mach number and angle of attack. A comparison of computational predictions (using both viscous and inviscid theory) with the experimental data was also included in the study. Although ablation rarely occurs in a symmetric fashion, the results demonstrated the sensitivity of the stability of cones as nose bluntness increases.

Thirteen cones ranging in nose-to-base radius ratio from 0 to 0.5 were tested at angle of attack from -4° to 18° at Mach 10 in the Continuous Flow Hypersonic Tunnel. The cone center of pressure, calculated from the aerodynamic coefficients, is a key parameter in the determination of static stability. Relatively large excursions (8 percent of the pointed cone length) in the center-of-pressure location were observed for small changes in nose bluntness at an angle of attack of 1°. Increases in angle of attack reduced the magnitude of these excursions. Both viscous and inviscid computational predictions compared well with the measured data. Changes in the center-of-pressure location were also noted to be relatively insensitive to viscous effects. However, inviscid pressure calculations at Mach 10 showed large variations in surface pressure distributions, which would account for the large excursions in center-of-pressure location noted at an angle of attack of 1°.

Mark D. Bryan, 2483

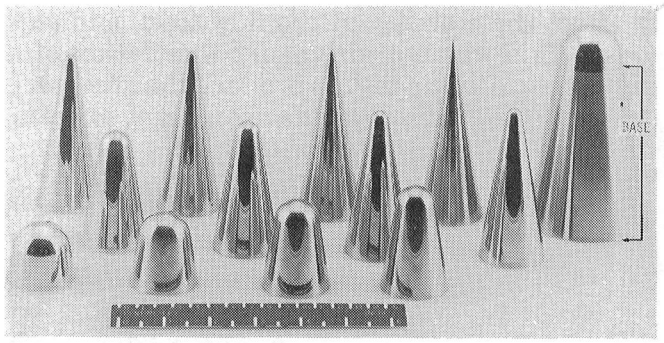

Interchangeable nose tip models.

Aerodynamic Control of Space Shuttle Orbiter With Tip Fin Controllers

Langley Research Center is currently conducting studies to identify the technology requirements that would be necessary to develop a second-generation space transportation system that could replace the Space Shuttle in the post-2000 timeframe. One of the aerodynamic development problems for winged entry vehicles (such as the Space Shuttle) involves obtaining yaw control during entry while the vehicle is transitioning from a high-angle-of-attack low-dynamic-pressure regime to a low-angle-of-attack higher-dynamic-pressure regime. Because a vertical tail is shielded from the flow and is thus ineffective for most of this time, yaw control must be provided by the ailerons and augmented by the reaction control system (a control concept now used on the Space Shuttle). Because of the problems inherent in depending on the aileron as the only source of aerodynamic yaw, and because the vertical tail can only be used at low angles of attack during the last few minutes of flight, alternative designs are being investigated.

One approach proposed at Langley involves removing the vertical tail and adding small tip fin controllers to the wing tips. These controllers are small and are designed to provide only yaw control, not stability. The possible advantages of this

approach include (1) a weight savings when compared to the vertical tail configuration, (2) the possibility of deactivating the reaction control system at low hypersonic speeds (compared to Mach 1 for the Space Shuttle), (3) a reduced dependence on the yawing moment of the aileron, and (4) improved payload handling due to the removal of the vertical tail. Because of these possible advantages, a feasibility study was conducted.

The Space Shuttle was chosen for this feasibility study because of the availability of detailed data and the opportunity to compare the performance of a tip fin controller configuration with that of an operational vehicle. In support of this study, wind tunnel tests were conducted to determine the aerodynamics of the orbiter with tip fin controllers over the speed range from low subsonic to hypersonic. This test was conducted in the 20-Inch Mach 6 Tunnel to complete the Mach number range. The test defined the yaw control authority of the tip fin controllers and the directional stability level of the configuration at Mach 6. These data were used in a simulator to study the flight characteristics of the proposed configuration. The results of the study indicated that the tip fin controllers could provide adequate control for entry with no degradation in vehicle capability.

George M. Ware, 3911

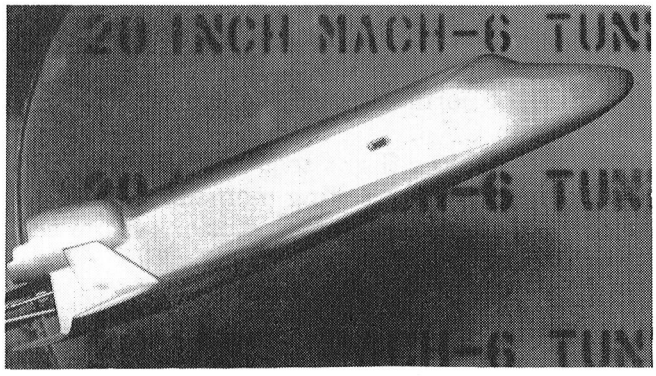

Space Shuttle orbiter with tip fin controllers in 20-Inch Mach 6 Tunnel.

Heating Tests on Circular-Body Advanced Earth-to-Orbit Transport

Studies are continually being conducted at Langley of alternate designs for advanced Earth-to-orbit transports (advanced Shuttles) for both military and civil purposes. In this regard, a single-stage-to-orbit concept having a circular-cross-section body is being investigated because of its inherently low structural weight and simplicity of design. One such vehicle, sized for delivery of a 65,000-pound payload to low Earth orbit, has a body diameter of approximately 33 feet and a length of 197 feet.

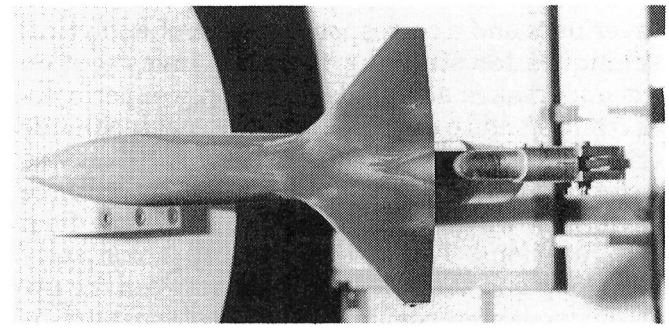

Proposed Earth-to-orbit transport model undergoing phase change paint heating test in CFHT.

Results from a phase change paint heating test of a 0.0055-scale model of this vehicle in the Continuous Flow Hypersonic Tunnel indicated that the heating rate along the bottom centerline was comparable to that of the Shuttle. This suggested that the existing Shuttle thermal protection system could be utilized for this advanced concept. The comparable heating rates for the two vehicles resulted partially because the higher heating rate associated with the greater curvature of the circular under-forebody on the larger advanced concept was offset by the lower heating associated with its lower entry planform loading. Higher heating rates on the wing leading edges were observed near the wing root, where the bow shock and wing shocks interacted. This result was similar to observations made on the Shuttle.

Ian O. MacConochie, 3911

Force Tests on Three Waverider Models at Mach 6

Performance requirements for high-speed missiles have led to renewed interest in waveriders, particularly those derived from conical shapes. Waveriders meet the missile requirements for a slender, flat, volumetrically efficient configuration that offers relatively high lift-to-drag ratios ($3 < L/D < 5$) to achieve ranges

of hundreds of miles at Mach numbers between 4 and 6. Typically, these vehicles are designed to have a lift-producing lower surface and a low-drag, often free-stream-aligned upper surface. The fins or "fences" on the sides of these configurations reduce the cross flow between the lower and upper regions of the configurations at the design flow field conditions (*e.g.*, $M = 6$, $\alpha = 0$).

Because of a lack of experimental data on waveriders and a corresponding lack of analytical techniques for studying them, an investigation was undertaken at Langley to supply experimental results and to develop an analytical technique for studying waverider configurations. A test was performed in the 20-Inch Mach 6 Tunnel on three nonconical waveriders called confined flow field configurations. The models were approximately 2 feet long and the included angle between the upper surface reference line and the bottom surface centerline was 10°. The sides of the three waverider models were inclined 20°, 40°, and 60°. The model shapes were completely defined by analytical geometry so that more accurate comparisons with analysis methods could be made. Parallel efforts were begun to study the configurations with a conservative supersonic full-potential solution. The results of this study will be compared with and validated by the experimental data.

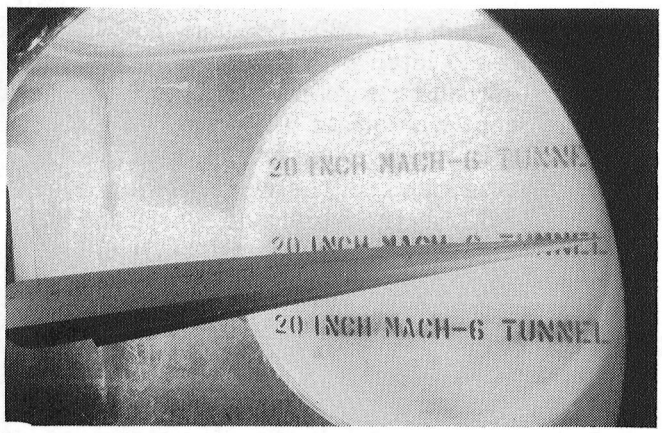

20° waverider in 20-Inch Mach 6 Tunnel.

Force measurements and oil flows were obtained on each of the three confined flow field models. Normal-force, axial-force, and pitching-moment data were taken at Mach 6 for angles of attack from -6° to 6° at zero angle of sideslip. In addition to this, axial-force, normal-force, pitching-moment, and side-force measurements were taken at zero angle of attack with angles of sideslip from -10° to 0°.

Oil flow studies confirmed the zero-cross-flow feature of these configurations at $M = 6$ and $\alpha = 0$. These tests contributed to the data base for high-speed waverider configurations, increased the basic understanding of this class of configuration, and provided the capability for validating the analytical studies.

Kenneth M. Jones, 3294

Experimental Simulation of Hypersonic Flight Aerodynamics

During hypersonic flight of a vehicle through the atmosphere, the gas that passes through the bow shock is subject to what are called real-gas effects. As a result of real-gas effects, the density ratio across the normal portion of the bow shock increases to values two to three times those obtained in conventional, ideal-gas hypersonic air or nitrogen wind tunnels. By testing a model in a wind tunnel that uses a gas (such as CF_4) which can generate high normal-shock density ratios and comparing these results with those obtained from tests conducted in air, a portion of the real-gas effects that occur at higher Mach numbers in flight can be assessed. The Langley Hypersonic CF_4 Tunnel and the Langley 20-Inch Mach 6 Tunnel provide the capability to test a model at the same Mach number and Reynolds number but at two values of normal-shock density ratio (5.2 in air and 12 in CF_4).

Shuttle orbiter flight test results showed a significantly higher pitching moment coefficient (about 0.03) than preflight predictions (from the

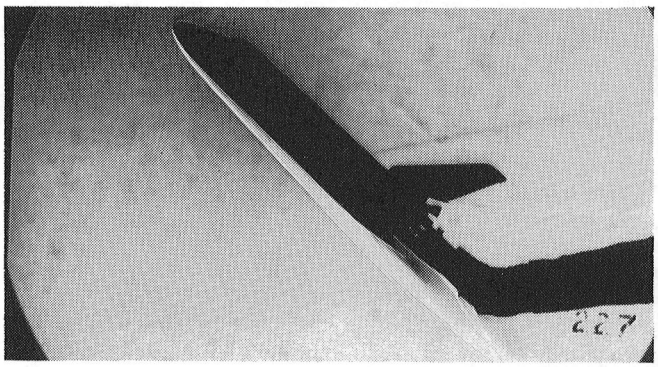

Schlieren photograph of Shuttle orbiter model in CF_4 tunnel at $\alpha = 40°$.

Aerodynamic Design Data Book) in the high hypersonic regime at an angle of attack of 40°. This nose-up pitch difference, which was due mostly to real-gas effects, was matched almost exactly by a comparison of test results in CF_4 and air at Mach 6 on a 0.004-scale orbiter model. Also, direct comparisons between CF_4 results and flight results on the Shuttle orbiter showed that the measured CF_4 pitching-moment coefficient was within 0.01 of the flight value. These results from the CF_4 tunnel show that it can provide meaningful simulation of the increase in density ratio associated with real-gas effects, especially for high angles of attack.

Robert L. Calloway, 2483

8-Foot High-Temperature Tunnel

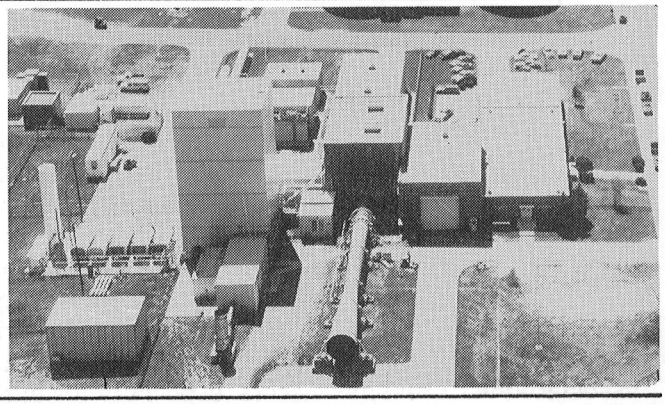

The 8-Foot High-Temperature Tunnel (8-ft HTT) is a blowdown type facility which achieves the required energy level for flight simulation by burning methane in air under pressure and using the resulting combustion products as the test medium with a maximum stagnation temperature near 3800°R. The nozzle is an axisymmetrical conical contoured design with an exit diameter of 8 feet. Model mounting is semispan or sting with insertion after the tunnel is started. A single-stage air ejector is used as a downstream pump to permit low-pressure (high altitude) simulation. The Reynolds number ranges from 0.3×10^6 to 3×10^6 per foot with a nominal Mach number of 7. The run time ranges from 20 to 180 seconds. The tunnel is used for studying detailed thermal-loads flow phenomena as well as for evaluating the performance of high-speed and entry vehicle structural components.

Aerothermal Tests of Metallic TPS

The objective of this research was to determine aerothermal performance, particularly heating, in the gaps between metallic TPS panels. The two 20-panel TPS arrays shown were fabricated for aerothermal tests to evaluate the severity of any heating that might occur in the gaps between panels. The arrays were arranged in a "worst case" orientation with the intersections between panels running parallel to the direction of flow. Tests were conducted with radiant heating only and with aerothermal flow conditions. During the radiant heating tests, the surface was heated at 1900°F and held constant for about 200 seconds. Although the surface temperature remained constant, the temperature at the bottom of the gap gradually increased. During the aerothermal tests, the surface temperature was raised to 1900°F by the radiant heaters and then allowed to decrease between the time the heaters were turned off and the time ($t = 496$ sec) the array was inserted into the aerothermal stream. At this time the surface temperature and the gap temperature both began rising, and the gap temperature greatly exceeded that measured during the radiant-heating-only test. These results indicate that significant gap heating occurs when the array is oriented with panel intersections parallel to the flow.

John L. Shideler, 3423

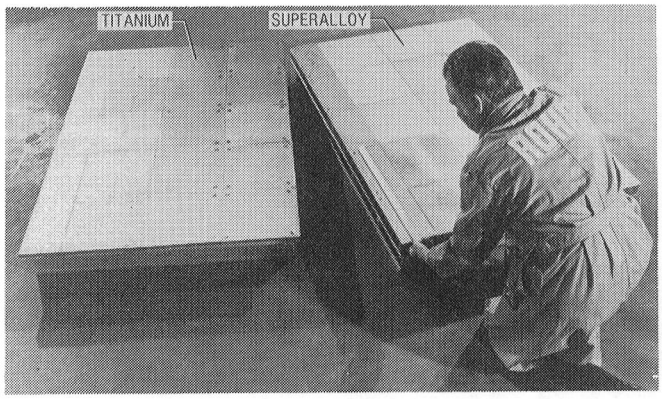

Metallic TPS panel arrays.

Preliminary Evaluation of Bonded Multiwall RSI Tile

The objective of this study was to provide a preliminary evaluation of a titanium multiwall TPS (thermal protection system) bonded to a shortened RSI (reusable surface insulation) tile before the concept could be seriously considered for use on the Shuttle. This was necessary because previous MW (multiwall) development has been for mechanical attachments. The test tiles were

fabricated and tested, and a strain isolation pad (SIP) was bonded between the MW and RSI to accommodate the thermal deformation of the MW. After proof pull flatwise tension tests were conducted to verify acceptable bond joints, the tiles were exposed to heat cycles using a quartz lamp heater to simulate the upper body flap surface temperature history. After the thermal tests, proof pull tests were repeated.

The results of the thermal and proof pull tests were considered successful by both Langley and Johnson Space Center technical personnel. Each specimen was exposed to a 10-psi proof pull and to five ascent thermal cycles with a maximum surface temperature of 1000°F. The maximum bondline temperature for each tile was slightly less than 350°F, which is well within the allowable temperature for the room-temperature vulcanized (RTV) adhesive. The first tile was subjected to an interim proof pull test of 8.2 psi (vacuum chuck separated) and was then exposed to two 1200°F temperature cycles. The maximum bondline temperature was 385°F, which is acceptable. The tile was then subjected to a proof pull of 8.1 psi before the vacuum chuck separated from the tile. The second tile was subjected to a proof pull test which achieved only 6.1 psi because the vacuum chuck damaged the top sheet of the MW. The damage resulted because a thermocouple wire was sandwiched between the MW surface and the vacuum chuck.

John L. Shideler, 3423

Flow Angularity Effects on Tile/Gap Impingement Heating

Previous aerothermal tests on Shuttle type tiles in the Langley 8-ft HTT identified the effects of boundary layer and gap geometry on the impingement heating rate on the tile's forward face at the end of the longitudinal gap aligned with the flow ("T" gap). However, more detailed heating measurements are needed to define the overall tile heating at various flow angles for Shuttle tile certification. The present study extends the previous effort to include the effect of impingement heating on the upstream tile corner due to flow angularity with respect to the longitudinal gap. In addition, the effects of boundary layer state and thickness, Reynolds number, and gap width are being analyzed. In order to obtain the desired detail, a highly instrumented thin-wall metallic tile was tested.

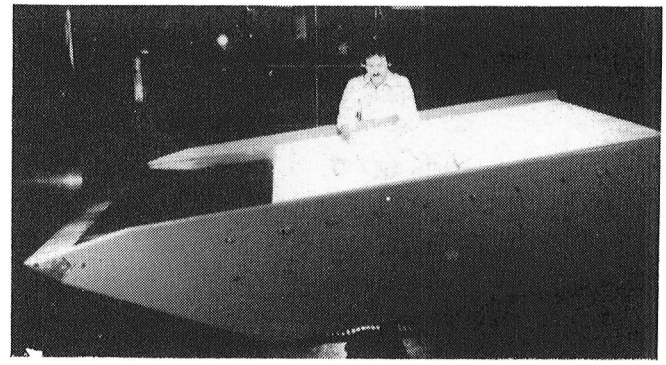

Test apparatus in 8-ft HTT.

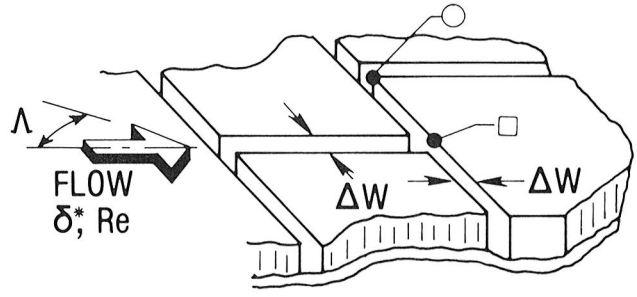

Tile/gap model.

Preliminary results indicating the effects of flow angularity (Λ) effects on the peak impingement heating for a gap width of 0.070 inches for both laminar and turbulent boundary layers are shown. The heating rates ($\dot{q}$) are nondimensionalized to the theoretical flat-plate value ($\dot{q}_{FP}$). For laminar flow, the impingement heating at the upstream corner and at the end of the "T" gap is relatively constant for $\Lambda < 45°$. For $\Lambda > 45°$, the increased heating probably reflects increasing flow in the uninterrupted gap as the gap becomes more closely aligned with the flow. For turbulent flow, the behavior of the heating at the corner is very similar to that of the laminar flow. However, impingement heating at the end of the "T" gap is significantly higher at $\Lambda = 0°$ but reduces with flow angle. Laminar flow over a tile array produces basically two-dimensional gap flow, and for turbulent flow the gap heating is primarily three-dimensional at the "T" junction. Therefore the turbulent boundary layer allows a larger energy transfer into the gaps, which produces the higher impingement heating for flow angles near zero.

These data will allow the effect of flow angularity to be incorporated into an empirical relationship, developed from previous tests, which can accurately predict the effects of gap geometry over a range of boundary layer conditions.

Don E. Avery, 3168

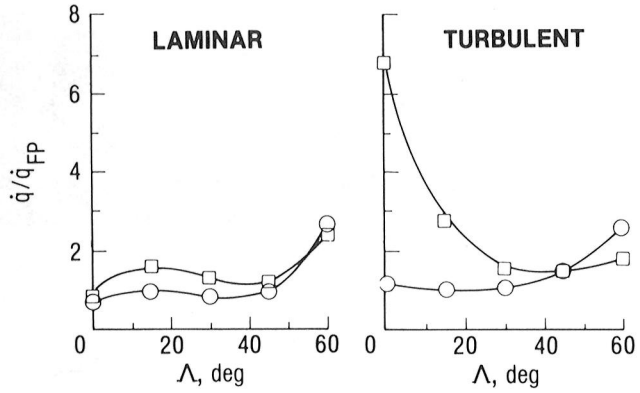

Laminar and turbulent heating.

Method of Measuring Mixing Ratio of Film Cooling Nitrogen to Tunnel Gas

A method for determining cooling gas-air mixing ratios in high-enthalpy flows using cooling nitrogen (N_2) seeded with inert neon (Ne) gas as the tracer and naturally occurring inert argon (Ar) gas in the air as an internal reference for mass spectrometric measurements was developed and demonstrated in the Langley 8-Foot High-Temperature Tunnel. The method involved sampling of the boundary layer flow over the model through either a flush orifice or a surface pitot inlet connected through small-diameter tubing to a quadrupole mass spectrometer, where Ne and Ar at mass units 20 and 40, respectively, were measured and recorded continuously during a tunnel run.

The Ne was a specific quantitative indicator of the cooling N_2; because it did not occur in the tunnel air, it occurred in the boundary layer only by mixing of the cooling N_2 with the tunnel air. Similarly, the Ar was a specific quantitative indicator of the tunnel air because it was not present in the coolant gas and was diluted in the boundary layer by the addition of N_2.

The experimental results were of limited quantitative significance because samples were obtained from only a single point and there were instrument problems affecting the Ne sensitivity. However, these results nevertheless demonstrated the feasibility of the technique, since the measured Ne and Ar displayed the proper change trends with changing conditions in the tunnel tests. The method, when incorporated in future film cooling experiments, will be of much use in directly measuring, analyzing, and interpreting the data.

Beverly W. Lewis, 2466

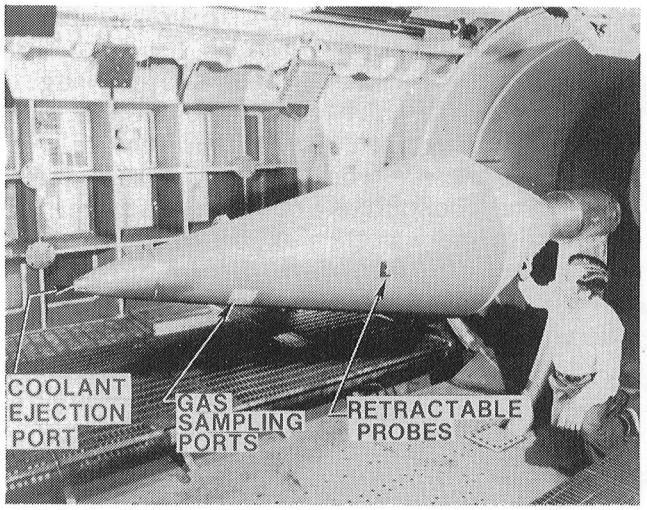

Film cooling test model shown in 8-ft HTT test section.

Aircraft Noise Reduction Laboratory

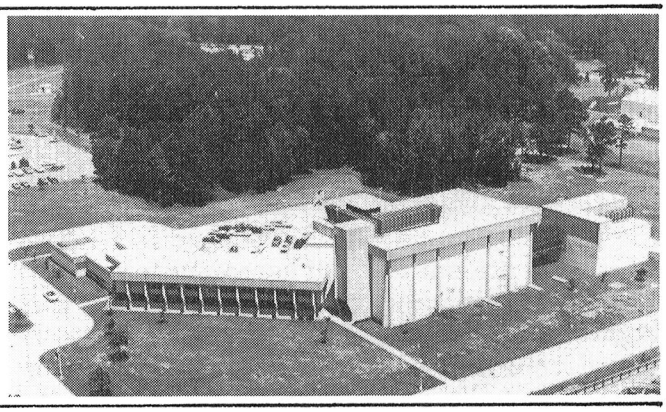

The Langley Aircraft Noise Reduction Laboratory (ANRL) consists of the quiet flow facility, the reverberation chamber, the transmission loss apparatus, the Anechoic Noise Facility, the Jet Noise Laboratory, and the human response to noise laboratories. The quiet flow facility has a test chamber lined with sound-absorbing wedges and is equipped with a low-turbulence low-noise test flow to allow aeroacoustic studies of aircraft components and models. The test flow, which is provided either by horizontal high-pressure or vertical low-pressure air systems, varies in Mach number up to 0.5. In contrast, the Anechoic Noise Facility is equipped with a very high pressure air supply used solely for simulating nozzle exhaust flow.

The transmission loss apparatus has a source room and a receiving room which are joined by a connecting wall. The test panel, such as an aircraft fuselage wall, is mounted in the connecting wall for sound transmission loss studies. The reverberation chamber diffuses the source noise and is used for measuring the total acoustic power spectrum of the test source. The Jet Noise Laboratory has two coannular supersonic jets for studying turbulence evolution in the two interacting shear flows which are typical of high-speed aircraft engines. The human response laboratories consist of the exterior effects room, the interior effects room, and the small anechoic chamber for human response.

Annoyance Prediction Ability of Helicopter Noise Metrics

The objective of this research study was to determine how well the annoyance caused by helicopter noise is predicted by current noise metrics. Two series of tests were conducted by Wyle Laboratories at the University of Loughborough, England, and in the ANRL human response facilities. Human subjects judged the annoyance of recordings of 89 helicopter flyover noises and 30 CTOL (conventional takeoff and landing) flyover noises. The subjective judgments were converted to subjective noise levels on a decibel-like scale and were compared with measured noise levels for each flyover sound using different noise metrics. The prediction errors, (*i.e.*, the differences between the subjective levels and measured noise levels) provided a convenient means of comparing the annoyance prediction ability of the various metrics. A small standard deviation in prediction error indicated a metric which predicted annoyance with good consistency for the wide variety of helicopter and CTOL aircraft noises. Results from both series of tests indicated that the CTOL noise certification metric EPNL was the most consistent metric for both helicopters and CTOL's. Impulsiveness corrections did not improve the prediction ability for the helicopters. When corrected for duration, all metrics predicted the annoyance of CTOL's better than that of helicopters.

Clemans A. Powell, 3561

Annoyance Response to Advanced Turboprop Aircraft Flyover Noise

The purpose of this program is to quantify the community annoyance response to advanced turboprop (ATP) aircraft flyover noise. ATP noise is unique in that the pure-tone harmonic content occurs at frequencies higher than those generated by conventional propeller aircraft.

A computer synthesis system was used to generate 45 realistic time-varying simulations of

ATP aircraft flyover noise in which the harmonic content was systematically varied to represent the factorial combinations of five fundamental frequencies ranging from 67.5 to 292.5 Hz, three frequency envelope shapes representing helical tip Mach numbers of 0.63, 0.73, and 0.78, and three tone-to-broadband-noise ratios of 0, 15, and 30 dB. The range of fundamental frequencies covered both conventional and advanced turboprop aircraft. The simulations were based on takeoff conditions and assumed a single-propeller tractor configuration using the SR-3 blade. Sixty-four subjects judged the annoyance of recordings of the 45 synthesized flyover noises presented at D-weighted sound pressure levels of 70, 80, and 90 dB in a laboratory testing room which simulates the outdoor acoustic environment.

Analyses of annoyance responses and noise measurements showed that frequency envelope shape (helical tip Mach number) did not significantly affect annoyance. However, the interaction of fundamental frequency with tone-to-broadband-noise ratio did have a large and complex effect on annoyance. Other results of the study indicated that the addition of duration corrections to the noise measurement procedures improved prediction ability and that duration-corrected A-weighted sound pressure level predicted annoyance better than any other measurement procedure.

David A. McCurdy, 3561

Excess Noise Generated by a Propeller in a Wake

Since propeller-driven aircraft may offer significant fuel savings over turbofan-powered aircraft, new aircraft concepts are being developed with propellers positioned to optimize performance. One such concept, called a "pusher" configuration, involves mounting the propeller behind the wing or tail surface to maintain clean or undisturbed flow over these surfaces. The noise consequences of this configuration were the subject of a study conducted in the ANRL anechoic flow facility.

In the ANRL vertical jet, an airfoil was placed just upstream of a propeller. The size and position of the airfoil were chosen to be representative of the tail surface of an aft-mounted pusher commuter aircraft. Noise and performance measurements were made at several thrust settings using two different propeller designs. The thickness of the wake going into the propeller was also varied by varying the airfoil angle of attack.

The results from this study show that a propeller operating in a wake produces considerably more noise than a propeller operating in a uniform flow field. The characteristics of this additional noise are that it radiates most strongly upstream and downstream of the propeller disk plane ($\theta = \pm 30°$) and in a direction non-normal to the wake ($\phi = 90°$); it is most apparent at the lower disk thrust loadings; it has a much higher level of higher harmonics; it accounts for as much as a 10 dB increase in the overall sound pressure level; and it does not appear to have a strong dependence on the propeller airfoil section design.

Patricia J. W. Block, 2645

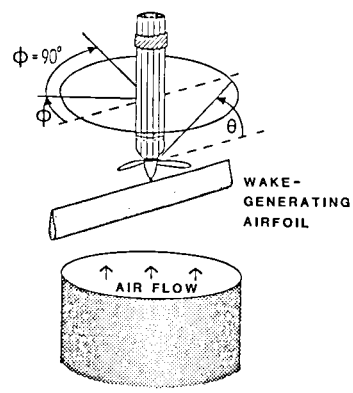

Noise generated by a propeller in a wake.

The Role of Jet Plume Instability in Screech Generation From Supersonic Jet Flows

For shock-containing supersonic jets, a self-sustained aeroacoustic feedback resonance phenomenon can occur which is commonly referred to as "screech". It is thought that screech may be responsible for reported in-flight aircraft structural damage. The present research investigated the role of jet plume instabilities in the generation and maintenance of screech.

The experimental investigation, which was conducted in the Anechoic Noise Facility, consisted of both near-field and far-field noise measurements and flow visualization. Flow

visualizations were phase-locked to the screech so that the dominant mode of jet instability could be determined. Additionally, calculations were performed to determine the evolution of the dominant instability mode found from the experiment.

Intense and stable screech was found to occur in a narrow range of nondimensionalized frequencies. Within this narrow frequency range, the dominant mode of jet instability was found to be helical. Furthermore, the location of the screech source as determined from both near-field measurements and flow visualization agreed well with the calculated amplitude peak of the helical jet instability. These observations strongly suggested that intense screech was produced when a certain helical jet instability was selectively amplified by the jet plume. Regularly spaced shock cells provided the required coupling between the instability in the jet plume and the intense sound it produced. The instability was enhanced by the azimuthal oscillation of the shock cells, which was driven by the upstream propagating helical screech field external to the jet plume.

J. C. Yu, 2619

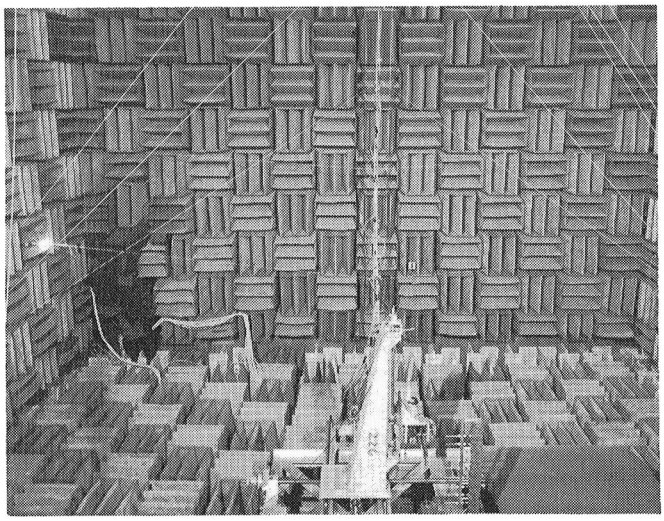

Experimental setup for jet screech investigation in Anechoic Noise Facility.

Analytical Prediction of Aircraft Interior Noise

The objective of this research was to develop and validate a propeller aircraft interior-noise analytical prediction method. The analysis (formulated by Bolt, Beranek, and Newman, Inc., under contract to NASA) was based on the concept of acoustic power flow. The analysis was validated initally by measurements on a simplified model of a fuselage and progressed to models with more realistic structural and interior trim details. The models were exposed to random and tonal convected noise fields, including noise from a model propeller, in the ANRL Quiet Flow Facility.

The current development of the prediction model is illustrated. The cylinder is stiffened with ring frames and stringers and has a floor, thermal-acoustic insulation, and interior trim. One input to the analytical model is the complex pressure loading (amplitude and phase) of the propeller as calculated by the propeller noise prediction module from ANOPP (Aircraft Noise Prediction Program). Additional inputs can include the boundary layer or other sources of noise. The analysis then couples this pressure loading to the dynamic modal response of the shell structure using measured or estimated structural and acoustic loss factors. The analysis accounts for the acoustic radiation of the vibrating structure by using the impedance and the coupling of the structural modes with the interior acoustic modes to determine the sound pressure level for each selected harmonic of the propeller blade passage frequency.

William H. Mayes, 3561

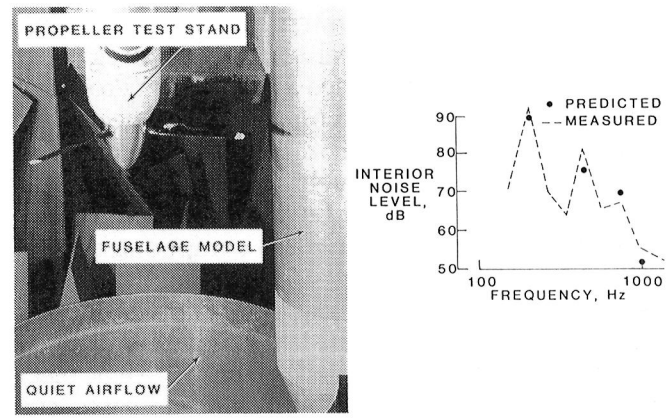

Analytical prediction model (left) and measured and predicted one-third-octave-band interior noise spectra for cylindrical fuselage model with propeller noise source (right).

Avionics Integration Research Laboratory - AIRLAB

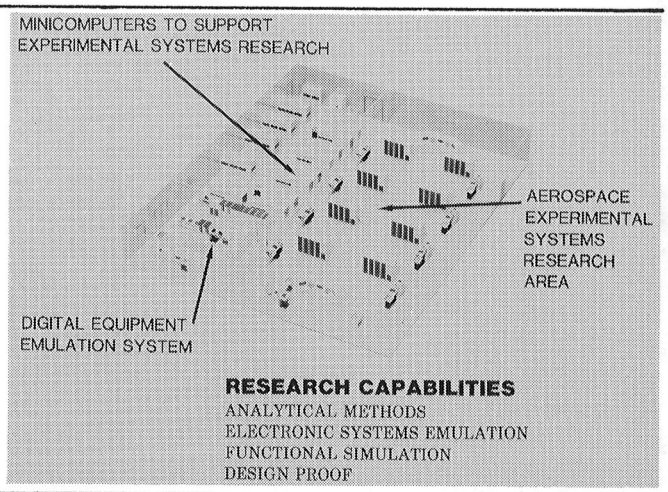

The United States leads the world in the development, design, and production of commercial and military aerospace vehicles. To maintain this leadership role throughout the 1990's and beyond will require the incorporation of the latest advances in digital systems theory and electronics technology into full integrated aerospace electronic systems. Such efforts will entail the discovery, design, and assessment of systems that can dramatically improve performance, lower production and maintenance costs, and at the same time provide a high, measurable level of safety for passengers and flight crews.

AIRLAB has been established at Langley Research Center to address these issues and to serve as a focal point for U.S. government, industry, and university research personnel to identify and develop methods for systematically validating and evaluating highly reliable, fully integrated digital control and guidance systems for aerospace vehicles. The increasing complexity of electronic systems entails multiple processors and dynamic configurations. These developments allow greater operational flexibility in both normal and faulty conditions, thus impacting and compounding the validation process. Whereas a typical reliability requirement for current electronics systems is a probability of failure of less than 10^{-6} at 60 minutes, the requirement for flight-critical electronic controls is for a probability of failure of less than 10^{-9} at 10 hours. Obviously, a new validation process is essential if this significant increase in reliability (four orders of magnitude) is to be achieved and believed.

Validation research in AIRLAB encompasses analytical methods, simulations, and emulations. Analytical studies are conducted to improve the utility and accuracy of advanced reliability models and to evaluate new modeling concepts. Simulation and emulation methods are used to determine latent fault contributions to electronic system reliability and hence aircraft safety. Experimental testing of physical systems is conducted to uncover the latent interface problems for new technologies and to verify analytical methods.

AIRLAB is a 7600-square-foot environmentally controlled structure located in the high-bay area of Building 1220. There are three rooms within the laboratory. The largest room is the experimental systems research area, which is configured into eight research stations and a central control and/or software development station. Each research station is supported by a VAX 11/750 minicomputer system that can be used, for example, to control experiments (fault insertions, performance monitoring, *etc.*) and retrieve, reduce, and display engineering data. A VAX 11/780 minicomputer system supports the central control and/or software development station. The second largest room contains the VAX minicomputers, disk drives, and tape drives supporting the research work stations. The third room contains the Digital Diagnostic Emulator, which is a special minicomputer (Nanodata QM-1A) interconnected to a VAX 11/750. The QM-1A is a nanocodable host computer with a unique emulation algorithm that allows gate logic level emulation of a target computer at a very fast rate. The diagnostic emulator provides the capability to experimentally address design issues of new fault-tolerant computer concepts and reliability issues in the fault behavior of fault-tolerant computers. Also included in AIRLAB are two advanced fault-tolerant computers, SIFT (software-implemented

fault tolerance) and FTMP (fault-tolerant multiprocessor), which are designed to explore fault-tolerant techniques for future flight-critical aerospace applications. These computers, which have been under development by Langley Research Center for years, serve as research test beds for validation studies in AIRLAB.

AIRLAB provides research resources needed by the aerospace electronics research community to address design and validation issues of flight-critical fault-tolerant flight control systems. In this role, AIRLAB functions as a "community center" in which AIRLAB researchers with diverse backgrounds can conduct research with common goals.

Validation Techniques for Fault-Tolerant Computer Systems

Fault-tolerant computer architectures utilize fault-masking and reconfiguration algorithms to ensure correct operation in the presence of failed components. These architectures are essential to the flight-crucial digital control systems of advanced aerodynamic configurations. The SIFT computer system, which is one such architecture, utilizes redundancy management algorithms implemented in software. Experiments have been performed in AIRLAB by NASA personnel to measure the performance of the SIFT operating system. In particular, the system overhead accruing from the fault-masking, reconfiguration, and synchronization subsystems was determined. Alternate algorithms for voting and reconfiguration were investigated and significant improvements were obtained for both the voting and reconfiguration subsystems. The improvement in reconfiguration task execution time is illustrated.

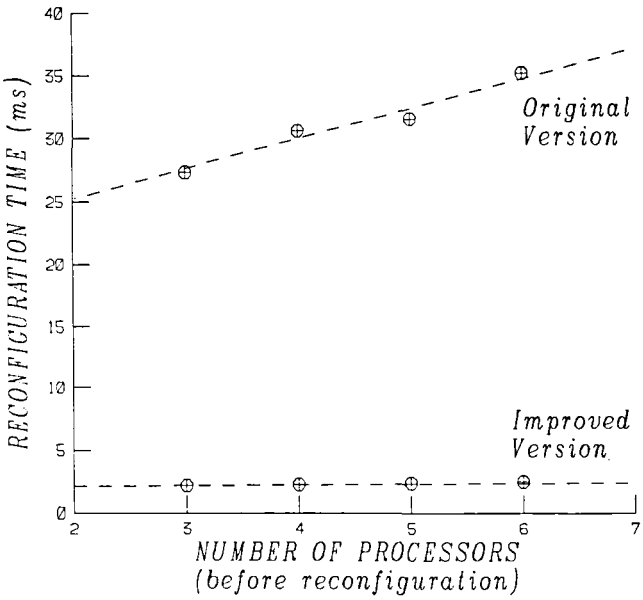

Improvement in reconfiguration task execution time.

Such performance experiments are necessary to assess the reliability of a fault-tolerant architecture. Researchers from the University of Michigan are developing theoretical methods that enable the estimation of the dynamic failure probability; that is, the probability that the computer system will fail to meet a hard deadline of the control system. Results are shown for an analysis of the probability of dynamic failure for reconfigurable and nonreconfigurable n-fold redundant systems with SIFT-like overhead characteristics. Experiments such as this one will be used to estimate the parameters of the theoretical methods developed by the Michigan team.

D. G. Holden, 3681

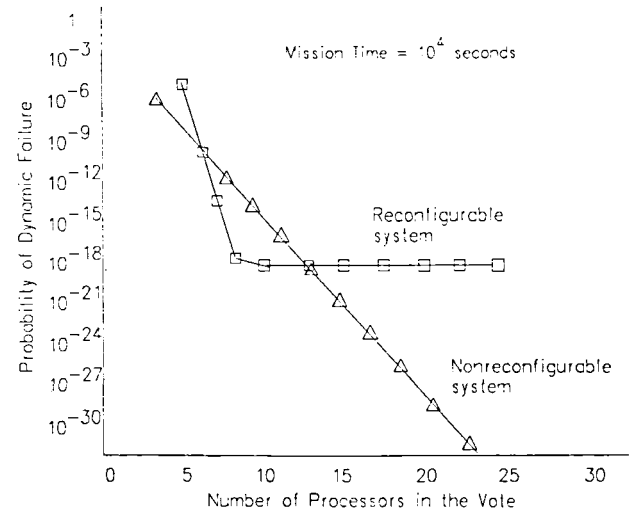

Dynamic failure probabality of n*-redundant systems.*

Reliable Software for Flight-Crucial Systems

A software engineering experiment has been designed and is running in AIRLAB with the objective of acquiring more information on the software failure process. The experiment requires three advanced-skill-level programmers, working

independently and restricted only in time, to design, code, and debug in FORTRAN IV two flight control problems written in English. The programs are tested for acceptance using a predefined set of input data and outputs are compared with predefined correct output. Acceptance test failures are noted, and the program is returned to the programmer for additional debugging.

After all acceptance tests are passed by all programs for a given problem, the programs are exercised simultaneously in simulative testing with inputs having a probability distribution representative of the real application. The program outputs are voted on to determine correct output. Simulative testing continues until a stopping rule (based on failures observed, inputs executed, and interfailure time history) is satisified. Failures observed before the stopping rule is met for the first time are recorded and the program is returned to the programmer for correction, which is also recorded.

Simulative testing is replicated by returning each program to the original version that passed all acceptance tests and then continuing the simulative test process (making the same corrections to a failed program when the error is again observed) until enough observations have been collected to achieve the desired level of statistical accuracy for the experiment.

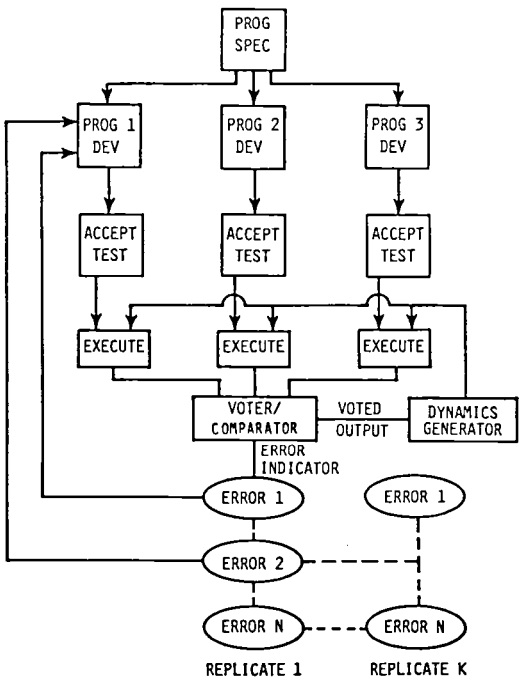

Software error experiment.

A preliminary analysis of initial data, based on over 500,000 simulative tests, indicates that software error rates are not constant. This is contrary to assumptions made by theorists in the development of software reliability models and could impact the usefulness of such models. Much more data are required to verify these initial findings and to acquire more information on the software failure process.

D. G. Holden, 3681

DC-9 Full-Workload Simulator

The DC-9 Full-Workload Simulator consists of a fixed-base McDonnell-Douglas DC-9-30 cockpit, a test console, and electronics cabinets. This cockpit was formerly a DC-8 cockpit, but was recently upgraded to provide the capability for dedicated DC-9 full-workload simulations. Stations are available in the cockpit for a Captain and a First Officer. Flight control responses for elevator, aileron, and rudder are simulated by forces from hydraulic servo systems. Manual throttle control for two engines is provided on the center console. The forward electronics panel of the center console is outfitted with a 9-inch color cathode ray tube (CRT) which can be used to display computer-generated graphic presentations, such as Cockpit Display of Traffic Information (CDTI) or Area Navigation (RNAV). A transparent touchpanel superimposed over the face of the CRT provides a discrete input to the computer when any point on the surface is touched.

Full-workload studies can be performed in this simulator, since the capacity exists to simulate all aircraft instruments, annunciators, switches, and alarms. Three very high frequency (VHF) communication receivers and three VHF navigation receivers are simulated for VOR/ILS (VHF Omnidirectional Range/Instrument Landing System). One ADF (Airborne Direction Finder) radio receiver and three marker beacon receivers are simulated in this cockpit. Anticipated CDTI research applications will include studies on pilot awareness, workload, airborne systems integration, air traffic control procedures, content of CDTI, and aircraft separation. Other studies will use an oculometer to evaluate information transfer rate between instruments and pilots.

Prior to initiating dedicated research in this simulator, it was necessary to evaluate the full-workload aspects of the simulator and to validate the fidelity of the aircraft and subsystem models. In addition, it was necessary to obtain baseline data on airline procedures. Normal approach and departure operations in the Denver area were flown by five pilots from two different airlines. Baseline data on crew procedure, simulator performance, and subsystem modeling were obtained which have been incorporated in the overall simulation. Procedures for simulating Air Traffic Control (ATC) party-line communications were also developed and evaluated.

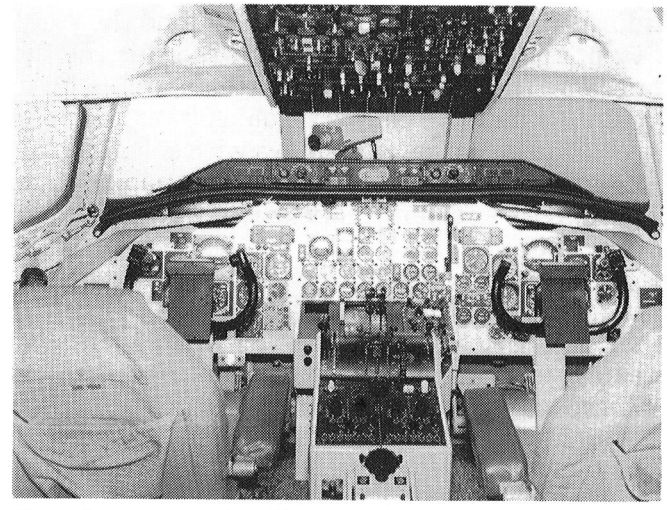

Interior view of DC-9 simulator.

Transport Systems Research Vehicle (TSRV) and TSRV Simulator

The TSRV is a specially equipped Boeing 737 airplane used to conduct flight tests for the Advanced Transport Operating Systems (ATOPS) Program. The airplane is equipped with a special research flight deck located about 20 feet aft of the standard flight deck. An extensive array of electronic equipment and data recording systems is installed throughout the former passenger cabin as part of the experimental research system. The airplane is routinely flown from the research flight deck in all flight regimes using advanced electronic displays and automatic control systems that are all-digital and can be reprogrammed for research purposes. Two safety pilots in the front flight deck are responsible for all phases of flight safety and most traffic clearances. Two research pilots usually fly the airplane from the aft cockpit during test periods. In order to extend the viability of the TSRV as a research tool for the next decade, the experimental systems are being updated to improve computational power and speed, replace monochrome displays with color displays, improve the data acquisition capability, and enhance system flexibility for advanced operations.

The goal of the ATOPS Program is to provide transport aircraft and flight management technology that will improve the efficiency and safety of flight operations in the National Airspace System (NAS). Specific program objectives are to develop aircraft systems concepts and companion procedures permitting more efficient operations in the NAS, to promote the integration of improved airborne capabilities within the evolving NAS to achieve more efficient operations, and to improve aircraft capability to cope with external factors such as wake vortex, adverse weather, and airspace restrictions (including noise).

The TSRV simulator is also being modified to duplicate the upgraded aft flight deck located in the TSRV Boeing 737. This simulator provides the means for ground-based simulation in support of the ATOPS research program. It allows

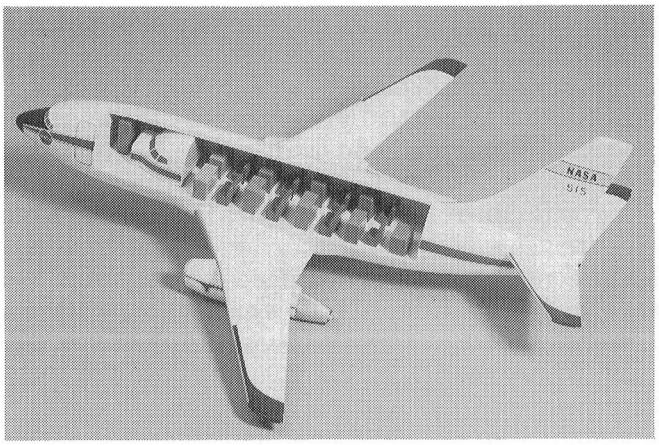

TSRV cutaway showing research cockpit and experimental system equipment.

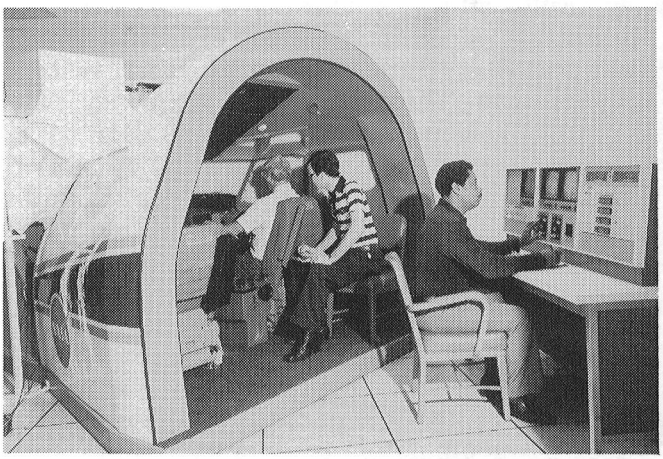

Exterior view of TSRV simulator.

thorough evaluation of proposed concepts in such areas as guidance and control algorithms, new display techniques, operational procedures, and man-machine interface. Promising simulation research results later become the subject of actual flight test research.

Advanced Airborne Energy Management

A feasibility study of the use of an on-board vertical trajectory optimization program is being conducted in the TSRV simulator. The optimization algorithm uses a calculus of variations technique on an energy state model to minimize a cost function throughout the trajectory. The cost function incorporates both the cost of fuel and the cost of time. The program can generate near-optimal trajectories for both fixed and free time-of-arrival problems. The program also has the capability of incorporating speed limit constraints, such as the ATC imposed 250-knot speed limit below 10,000 feet, and the capability of constraining the cruise altitude.

The study is being conducted in an effort to determine the flight crew interface requirements for real-time operational use of the trajectory optimization program. Various display formats will be tested to determine the benefits of specific guidance information for flying and changing the optimal trajectories. Also to be determined is the sensitivity of the optimal trajectory to mismodeling of the airplane's aerodynamic and thrust characteristics and to variations in the atmospheric parameters. From the atmospheric sensitivity information, a strategy for inflight recomputation of the vertical profile can be formulated.

In 1983, the optimization program was incorporated into the TSRV real-time simulation. The program was implemented to run in the slow loop of the simulation computation cycle. Additional pages were added to the pilots Navigation Control/Display Unit (NCDU) to enable the flight crew to initiate trajectory computations, interface with the optimization program, and edit the various program parameters, such as the cruise altitude or the cost variables. Upon completion of the profile computation, the trajectory is stored in the guidance buffer. From the guidance buffer, the data can be used to drive the autopilot or the pitch reference line on the pilot's primary flight display. Later experiments will study the use of these data to drive advanced pictorial display concepts.

Dan D. Vicroy, 3621

Joint FAA/NASA Runway Friction Program

The FAA and NASA have participated for many years in a cooperative effort to measure runway surface friction and to correlate various friction-measuring ground vehicles. The need for timely and accurate assessment of runway friction characteristics under adverse weather conditions and the necessity of identifying the severity of potentially hazardous conditions to airport/aircraft operators are recognized priorities of these efforts. With the recent development of new-technology ground-friction-measuring vehicles, further testing involving the instrumented TSRV Boeing 737 aircraft has been conducted at NASA Wallops Flight Facility and the FAA Technical Center airport. In addition to determining the degree of correlation between the ground vehicle and aircraft friction measurements, the current program effort is also intended to further evaluate a NASA-developed tire friction theory and to obtain a better assessment of aircraft reverse-thrust performance. Future testing, which will include use of an FAA Boeing 727 aircraft, will be conducted to collect friction data on a variety of runway surfaces during periods of precipitation as well as in snow and ice-covered conditions.

Test results show a wide variation in tire friction coefficient values (from 0.2 to 1.2) with speed measured during TSRV 737 aircraft and ground vehicle tests. The dissimilarity in these friction-speed gradient curves is due to differences in test

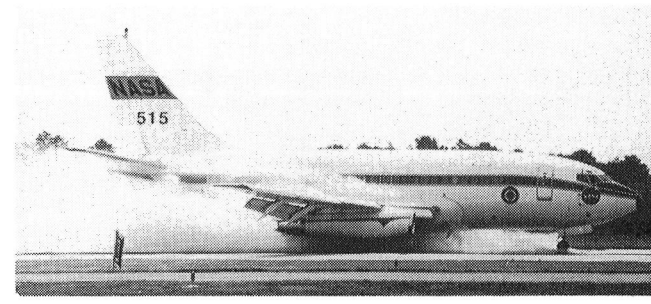

TSRV Boeing 737 showing plume of spray generated by maximum braking on flooded runway test section.

tire characteristics and mode of braking. The data and similar friction-speed gradient data obtained on seven other runway test surfaces will be analyzed to define the degree of correlation between the ground vehicle and aircraft friction measurements. During this effort, the validity of a NASA-developed tire friction prediction theory will also be evaluated.

James R. Hall, 2435

Crew Station Systems Research Laboratory (CSSRL)

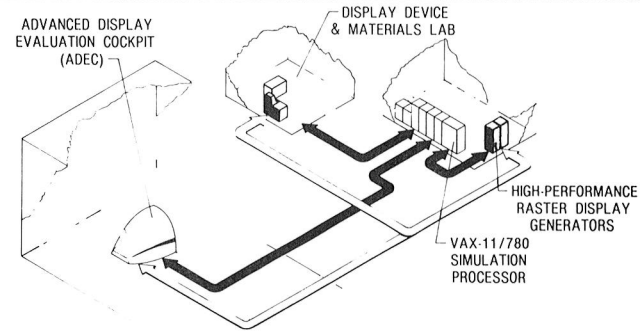

The trend in modern civil cockpits has been to replace electromechanical instruments with electronic control and display devices. The NASA Crew Station Electronics Technology R&T Base program is at the forefront of this trend with research and development activities in the areas of advanced display media, display generation techniques, integrated control panels and keyboards, and cockpit systems integration. The experimental devices being developed have unique drive, interface, and systems integration requirements (as opposed to noncockpit electronics) as well as unique testing facility requirements. In order to provide for candidate device research in a near-real operational electronic and lighting environment in a timely and effective manner, the Crew Station Systems Research Laboratory (CSSRL) is being implemented. This laboratory will provide a unique civil capability to conduct display materials, device, and photometric characteristics research; establish combined display and graphics generation systems performance; determine synergistic features of integrated systems; and establish a data base on cockpit display systems which utilize emissive and reflective devices that are markedly different from their electromechanical counterparts and may be "washed out" by high ambient light or have poor viewability in darkness.

Major existing elements of the CSSRL are the Advanced Display Evaluation Cockpit (ADEC), which is a reconfigurable research cab, a simulation host processor, high-performance raster display generators to drive cockpit displays, and a Display Device and Materials Lab. An FY 85 construction of facilities project will add a variable lighting system for the ADEC, providing the capability of intensities from darkness up to 10,000 footcandles with diffuse through direct sunlight conditions.

Raster Display Scan Standards Compared in Advanced Cockpit

Raster scan cockpit displays have traditionally used the interlaced scan standard for technical and economic reasons. Interlacing is a technique adopted by the television industry in which one frame unit of information is divided into two fields, each of which contains one-half the total number of lines and follows an alternate scan path to produce an interleaved pattern. Because the fields of a frame are rarely identical, interlaced displays show some flicker or scintillation effects at the overall frame rate. Technological advances in raster scan display generators and CRT monitors now make it feasible to generate and display noninterlaced displays.

Experiments with primary flight displays using a variety of scan standards have been conducted in the Advanced Display Evaluation Cockpit (ADEC) of the CSSRL. The CRT monitors in the ADEC can display formats of 512

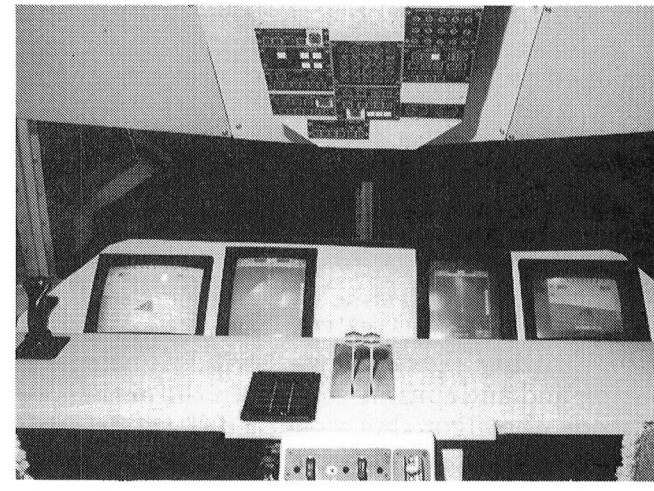

ADEC with dual primary flight displays.

× 512 resolution at 30 Hz interlaced, 40 Hz interlaced, and 60 Hz noninterlaced. The photograph shows both sets of primary displays at the same resolution with noninterlaced on the left and interlaced on the right. The goal of these experiments has been to determine a raster scan standard for cockpit displays which minimizes most forms of flicker while maintaining display resolution. Results have shown that large-area flicker decreases markedly at 40 Hz interlaced compared to 30 Hz interlaced. Scintillation effects still present at 40 Hz interlaced disappear at 60 Hz noninterlaced. The conclusion is that a 60-Hz (or higher) noninterlaced scan standard is best for primary cockpit displays. These research findings should also enhance companion research facilities, such as the Advanced Concepts Simulator.

Jack J. Hatfield, 2171

Real-Time Line Smoothing Achieved for All-Raster Flight Displays

Raster scan electronic display systems, as opposed to stroke display systems, have many potential advantages for flight applications. They permit efficient shading of large areas and generally achieve photographic-like clarity for the pictorial integration of flight information. Further, they use half the power of stroke display devices. Current raster systems, however, show near-horizontal and near-vertical lines as a series of straight line segments (stairsteps). This effect, known as aliasing, is objectionable to pilots.

A real-time vector-drawing algorithm was developed utilizing an all-raster programmable display generator (PDG) in conjunction with a high-resolution color CRT display. The vector-drawing algorithm was incorporated in a real-time applications program which generated an advanced primary flight display. The display was evaluated within the Advanced Display Evaluation Cockpit (ADEC) simulator, which permitted the experimenter to "fly" the aircraft while the vector-drawing algorithm was switched between aliasing and antialiasing modes. In the antialiasing mode, the algorithm smoothed the stairstepping by filtering the high spatial frequency content and shading adjacent picture elements gently toward the background color. Thus, each vector was broadened and made bolder. Experimental results indicated a marked improvement of line quality using the algorithm (see insets) with only a slight loss in execution speed and no degradation in the dynamic quality of the display.

Jack J. Hatfield, 2171

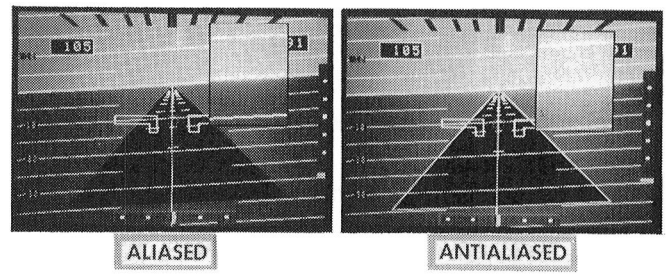

Capability of real-time smoothing of rolled symbology.

General Aviation Simulator

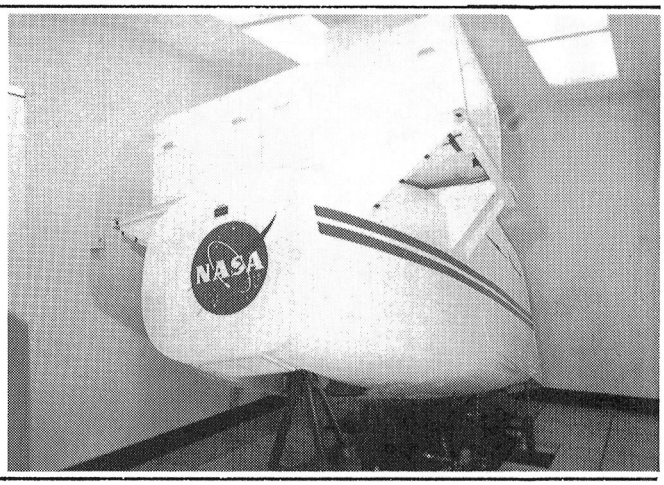

The General Aviation Simulator (GAS) consists of a general-aviation aircraft cockpit mounted on a three-degree-of-freedom motion platform. The cockpit is a reproduction of a twin-engine propeller-driven general-aviation aircraft with a full complement of instruments, controls, and switches, including radio navigation equipment. Programmable control force feel is provided by a "through-the-panel" two-axis controller that can be removed and replaced with a two-axis side-stick controller mountable in the pilot's left-hand, center, or right-hand position. A variable-force-feel system is also provided for the rudder pedals. The pilot's instrument panel can be configured with various combinations of cathode ray tube (CRT) displays and conventional instruments to represent aircraft such as the Cessna 172, Cherokee 180, and Cessna 402B. A collimated-image visual system provides a 60°-field-of-view out-the-window color display. The visual system can accept inputs from a model board system, computer-generated graphics, and a target aircraft/horizon scene. The simulator is flown in real time using a CDC Cyber 175 computer to simulate aircraft dynamics. Research applications of the GAS include the evaluation of systems for approach/landing displays, single-pilot IFR studies, stall/spin inhibiting techniques, and gust alleviation systems.

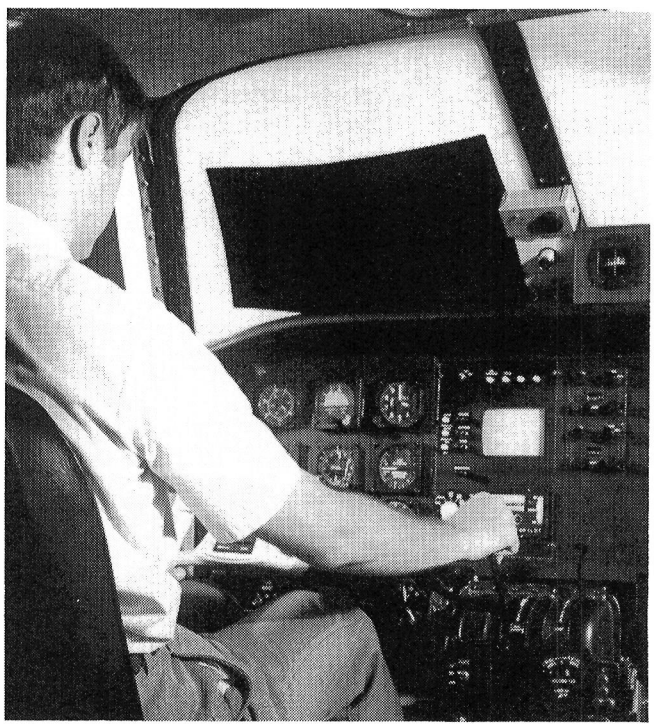

Interior view of General Aviation Simulator.

Light Twin Engine-Out Study

A study was conducted on the General Aviation Simulator to investigate the flight dynamics and piloting problems associated with an engine failure on light twin-engine general-aviation aircraft. A simulation math model representative of current light twins was implemented on the GAS and critical flight conditions were assessed.

The study revealed that the extremely high pilot workload following an engine failure is very conducive to potentially fatal pilot blunders. The high workload results from the large control forces required to counter the engine-out asymmetries and from the urgency of cleaning up the airplane (reducing the drag) because of the characteristically low single-engine climb performance. A simple automatic engine-out trim system designed to reduce pilot workload is being investigated. The system automatically relieves the large control

forces and makes it easier for the pilot to maximize the marginal single-engine climb performance.

Eric Stewart, 2184

Engine-out study conducted in Langley GAS.

Pilot Interface Study of Pictorial Display Formats

The conduct of single-pilot instrument flight rules (SPIFR) operations is a demanding human operator task requiring a combination of manual control skills, the assimilation of information from a variety of sources, and the ability to prioritize a myriad of information in a rapid and efficient manner. Research on the human operator interface of the multitude of tasks that the pilot must perform in the aircraft cockpit is a principal effort of the NASA Langley SPIFR program.

A recent study performed in the General Aviation Simulator and in three NASA aircraft evaluated the man-machine interface of certain combinations of controls and displays in the cockpit. The simulator study examined the usefulness of an advanced pictorial display concept, the "follow-me" box display, which could not be implemented on any of the three aircraft. This display was compared and evaluated in combination with the basic Horizontal Situation Indicator (HSI) and Course Deviation Indicator (CDI) displays currently found in many general-aviation aircraft. The workload rating indicated that the "follow-me" box greatly enhanced the HSI and/or CDI compared to the conventional Attitude Direction Indicator (ADI) in combination with the HSI and/or CDI. In general, these results showed that the "follow-me" box appears to be a good first step in overcoming the primary deficiencies of conventional ADI's and flight directors.

Hugh P. Bergeron, 3917

Pictorial Display System Evaluation

The General Aviation Simulator has been used to evaluate an advanced cathode-ray-tube display system. The simulator modeled a Cessna 402 aircraft in sufficient detail that realistic flight tasks could be performed. The simulator also modeled the navigation system as it actually exists in southeastern Virginia. The flight task involved en route segments between VOR/DME (Very High Frequency Omnidirectional Range/Distance Measuring Equipment) navigation stations and landing approaches using an Instrument Landing System.

The display system consisted of a three-dimensional-box "forward-looking" display and a moving-map "downward-looking" display. The "forward-looking" box display presented high-sensitivity vertical and lateral position information. The "downward-looking" map display presented low-sensitivity horizontal (lateral and

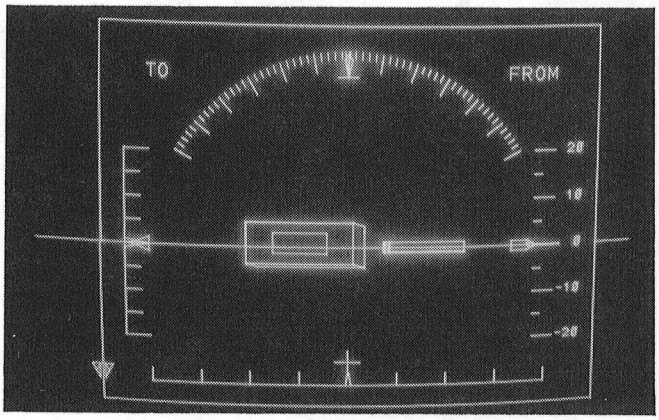

"Forward-looking" box display.

fore-and-aft) information. The simulator also included controls for operating the display system.

This display system was evaluated in tasks conducted in thunderstorm weather conditions. In addition, unexpected flight plan changes were presented to the pilot during the tests. Six instrument-rated subjects executed these flight tasks.

The results showed that when this display system was used, the difficult task was performed successfully each time it was tried. No pilot blunders were noted in any of the tests. The results emphasized that the map display allowed the pilot to maintain large-scale position awareness and the box display allowed precise positioning of the aircraft so that a successful landing approach with a decision height of 50 feet could be performed, even in thunderstorm conditions.

James J. Adams, 3917

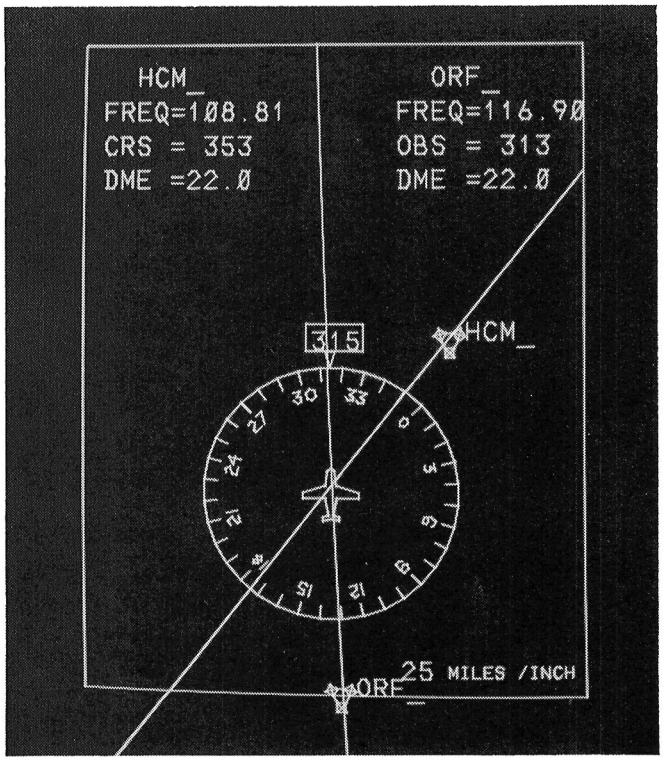

Moving-map display.

Mission Oriented Terminal Area Simulation (MOTAS)

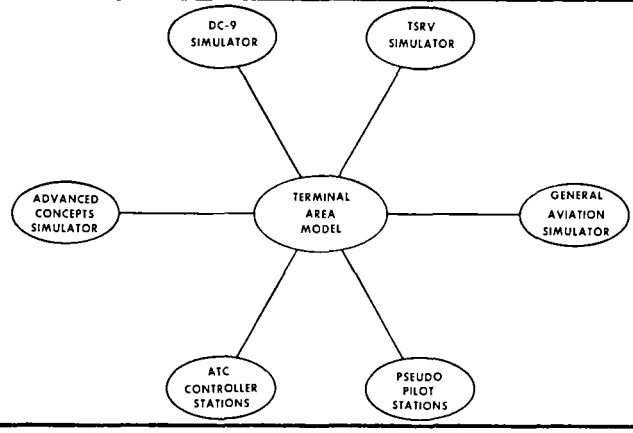

The Mission Oriented Terminal Area Simulation (MOTAS) Facility is an advanced simulation capability that provides an environment in which flight management and flight operations research studies can be conducted with a high degree of realism. This facility provides a flexible and comprehensive simulation of the airborne, ground-based, and communications aspects of the airport terminal area environment. The major elements of the MOTAS facility are an airport terminal area environment model, several aircraft models and simulator cockpits, four pseudo pilot stations, four air traffic controller stations, and a realistic air-ground communications network. The airport terminal area environment model represents today's Denver Stapleton International Airport and surrounding area using either a computer-generated automated metering and spacing system of control or a present-day vectoring system of control with air traffic controllers. In addition, the model simulates various radar systems, navigation aids, wind conditions, and so forth.

The MOTAS facility combines the use of several cockpit simulators and pseudo pilot stations for flying aircraft in the airport terminal area. The MOTAS facility is presently operational with the Transport Systems Research Vehicle (TSRV) Simulator and is ready to conduct research studies. Provisions are being made to integrate the General Aviation Simulator and the DC-9 Full-Workload Simulator during CY 84 and to integrate the Advanced Concepts Simulator after it becomes operational as a stand-alone simulator. These cockpit simulators will allow full crews to fly realistic missions in the airport terminal area. The remaining aircraft flying in the airport terminal area are flown through the use of the pseudo pilot stations. The operators of these stations can control five to eight aircraft at a time, inputting commands to change airspeed, altitude, direction, and so forth. The final major components of the facility are the air traffic controller stations, which are presently configured to display and control the two arrival sectors, the final approach sector, and the tower and/or departure sectors.

Because of its flexibility in reconfiguring according to research requirements, the MOTAS facility can support a variety of flight vehicle and/or air traffic control system research studies that would not be possible in the real world due to safety, economy, and repeatability considerations.

Differential Maneuvering Simulator

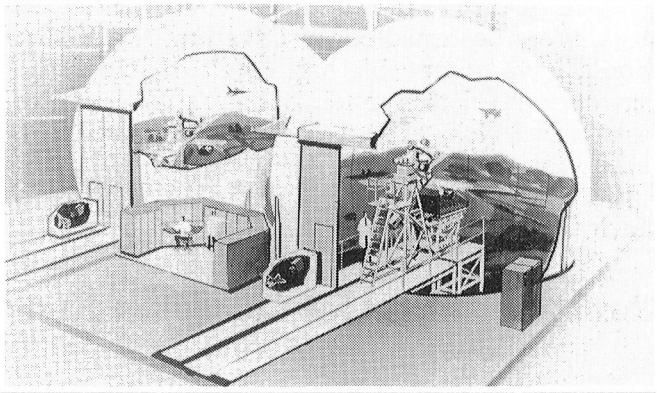

The Langley Differential Maneuvering Simulator (DMS) provides a means of simulating two piloted aircraft operating in a differential mode with a realistic cockpit environment and a wide-angle external visual scene for each of the two pilots. The system consists of two identical fixed-base cockpits and projection systems, each based in a 12.2-meter-diameter (40 foot) projection sphere. Each projection system consists of a sky-Earth projector to provide a horizon reference and a system for target image generation and projection. The internal sky-Earth scene provides reference in all three rotational degrees of freedom in a manner that allows unrestricted aircraft motions. The sky-Earth scene has no translational motion. The internal visual scene also provides continuous rotational and bounded (300 to 45,000 feet) translational reference to a second (target) vehicle in six degrees of freedom. The target image presented to each pilot represents the aircraft being flown by the other pilot in this dual simulator. Each cockpit provides essential instruments and displays along with a wide-angle head-up display. Kinesthetic cues in the form of a g-suit pressurization system, helmet loader system, g-seat system, cockpit buffet, and programmable control forces are provided to each pilot consistent with his aircraft's motions. Research applications include studies of high-angle-of-attack spin susceptibility, evaluation of evasive maneuvers for various aircraft, and evaluations of the effect of parameter changes on the performance of several baseline aircraft.

X-29A High-Angle-of-Attack Simulation Study

The X-29A program is sponsored by the Defense Advanced Research Projects Agency and is administered by the Air Force. In addition to testing the advantages of forward-swept-wing design, the program will also examine a broad range of advanced aircraft technologies. These include extremely strong, lightweight, nonmetallic graphite epoxy composites; a triple-channel-redundancy highly reliable digital fly-by-wire system; a forward all-flying canard with less supersonic trim drag than the usual horizontal tail; and a variable-camber-wing trailing edge that adjusts its shape to match flying conditions.

As part of a broad research program to study the high-angle-of-attack flight characteristics of the forward-swept-wing demonstrator (X-29A), a piloted simulation is being conducted on the DMS to assess pilot-in-the-loop maneuvering characteristics and to define the high-angle-of-attack flight control laws needed for such an airplane design. The piloted simulation is being conducted in parallel with the contractor's efforts to define the airplane's flight control system, and these simulation results are helping to define the systems that will fly on the airplane. Both NASA and contractor test pilots are participating in the study. NASA will begin flight tests of the X-29A in 1985.

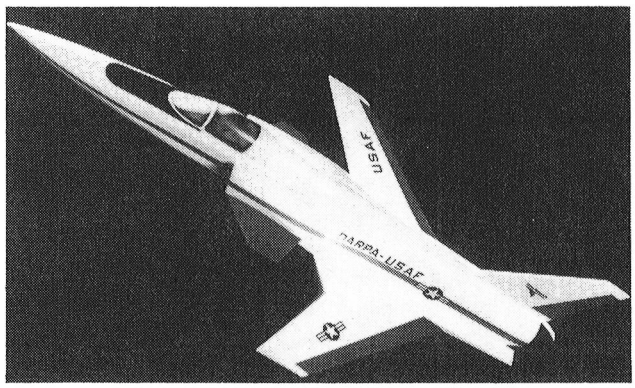

X-29A forward-swept-wing demonstrator.

The results to date indicate that with an appropriately designed control system, the X-29A should have acceptable high-angle-of-attack flying characteristics and a desirable level of resistance to loss of control during high-angle-of-attack maneuvering.

Mark Croom, 2184

Thrust Vectoring for Control at High Angles of Attack

The increased low-speed control provided by thrust vectoring promises the potential of dramatic improvements in high-angle-of-attack agility and departure/spin resistance over what is currently possible with conventional aerodynamic controls. To investigate this concept, a study was conducted on the Differential Maneuvering Simulator using a math model of an advance fighter configuration incorporating thrust vectoring for pitch and yaw control. The objectives were to determine the levels of vectoring required, to investigate the enhanced levels of maneuverability and agility provided by the vectoring controls, to study high-angle-of-attack flight dynamics problems associated with this enhanced capability, and to assess control law and pilot interface requirements.

The results suggest that, as expected, the increased control provided by thrust vectoring allows significant enhancement of low-speed, high-angle-of-attack controllability and maneuverability. However, fairly stringent control law requirements must be met to maximize the benefits obtained from this concept.

Marilyn Ogburn, 2184

Visual/Motion Simulator

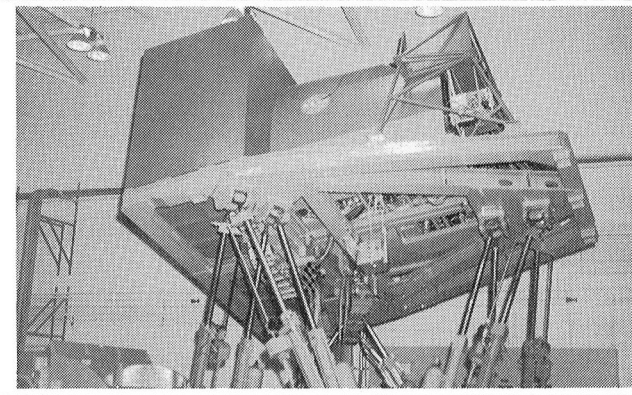

The Visual/Motion Simulator (VMS) is a general-purpose simulator consisting of a two-man cockpit mounted on a six-degree-of-freedom synergistic motion base. A collimated visual display provides a 60° out-the-window color display for both left and right seats. The visual display can accept inputs from several sources of image generation. A programmable hydraulic-control loading system is provided for column, wheel, and rudder in the left seat. A second programmable hydraulic-control loading system for the right seat provides roll and pitch controls for either a fighter-type control stick or a helicopter cyclic controller. Right-side rudder control is an extension of the left-side rudder control system. A friction-type collective control is provided for both the left and the right seats.

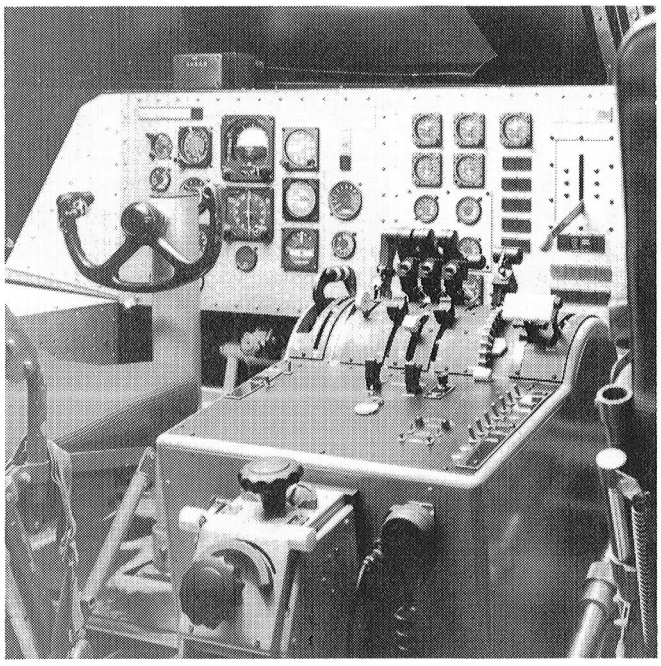

Interior view of VMS.

A realistic center control stand was installed in 1983 which, in addition to providing transport type control features, provides auto-throttle capability for both the forward and reverse thrust modes. Motion cues are provided in the simulator by the relative extension or retraction of the six hydraulic actuators of the motion base. Washout techniques are used to return the motion base to the neutral point once the onset motion cues have been commanded. In addition, a g-seat is provided which can be interchanged between the left and right seats to augment the motion cues from the base.

Research applications have included studies for transport, fighter, and helicopter aircraft. These studies addressed problems associated with wake vortices, high-speed turnoffs, microwave landing systems, energy management, multi-bodied transports, and maneuvering stability flight characteristics. Numerous simulation technology studies have also been conducted to evaluate the generation and usefulness of motion cues.

Simulator Validity/Cue Fidelity

During the summer and fall of 1983, a three-part experiment (involving in-flight, simulator, and analytic modeling) was performed to compare actual flight performance to simulator performance under various cueing configurations. This provided an important opportunity to produce meaningful results in terms of simulator validity/cueing fidelity issues. The attention of the simulation community was drawn to this study because it was uniquely designed to address these issues.

Five test pilots (two NASA pilots, two Navy pilots, and one Grumman pilot) first performed

the simulator tracking experiment at Langley Research Center using the VMS and the Differential Maneuvering Simulator. They then immediately performed the F-14 tracking flights at Dryden Research Facility, followed by a repeat performance at Langley Research Center of the simulator experiment. Because of the different attributes of the VMS and DMS (the VMS is a moving-base simulator with a narrow field of view, whereas the DMS is a fixed-base simulator with a side field of view and helmet loader), both simulators were used during the experiment, thus providing a larger set of simulator cue fidelity parameters for the study. Since the simulator data and flight data were obtained for the performance of the same pilots flying the same task, the potential opportunity for meaningful results in terms of simulator validity/cue fidelity was enormous, particularly in light of the existence of the analytic modeling capability as a pre-test and post-test tool.

This facility model is designed in a manner that allows representation of the various levels of cueing fidelity up to and including the true fidelity of actual flight. As such, it has the potential to be a most useful tool for providing definitive data on the parametric relationships between man-vehicle performance and simulator cueing fidelity parameters. Therefore, Langley's effort will provide meaningful results and a more systematic approach toward the analysis of simulator validity/cue fidelity issues.

Burnell T. McKissick, 3621

Active Controls for Increased Energy Efficiency

By applying the relaxed static stability (RSS) concept and utilizing an active-control stability augmentation system, an airplane can be designed with reduced aerodynamic trim drag due to a farther aft center-of-gravity balance. Consequently, there is a need to develop criteria to ensure satisfactory handling qualities and guarantee safety of flight for these advanced transport designs.

Piloted simulator investigations have been conducted utilizing the Visual Motion Simulator and a math model of a derivative Lockheed L-1011 transport. The first phase of the study was devoted to the evaluation of a simple, "near-term" stability augmentation system suitable for application to aircraft operating with "low" levels of negative static margin, and the second phase evaluated a more advanced complex system designed for application to future transport concepts requiring operation at "high" levels of negative static margin to achieve optimum performance. The simulation results indicated that a transport aircraft with the "near-term" system operative would have satisfactory or safe flying qualities for negative static margins up to 3 percent, and these results were subsequently verified through flight tests. The advanced augmentation system produced satisfactory flying qualities at negative static margins as high as 20 percent. With the application of the RSS concept and the utilization of active-control augmentation, the fuel efficiency of future transports may be improved by 2 to 20 percent, which is a significant cost reduction in terms of today's airline economics.

William D. Grantham, 4681

60-Foot Space Simulator

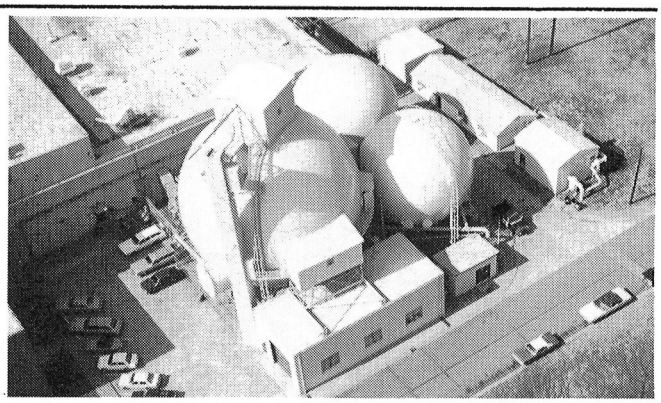

This 60-foot-diameter sphere, which is constructed of carbon steel, can simulate an altitude of 320,000 feet (2×10^{-4} mm Hg). This vacuum level is attainable in 7 hours with a three-stage pumping system. The sphere is accessible through a personnel door, a 12-foot diameter specimen door, and a 4-foot maintenance door at the top. A 2-ton hoist located at the top enhances specimen handling inside the sphere. Sight ports are located both at the top and at the equator. Two closed-circuit television cameras, a video cassette recorder, and an oscillograph are available. Firing circuitry and a programmer are available for the use of pyrotechnics, and a system of flood lights is installed in the sphere to facilitate high-speed photography. The sphere is primarily utilized for dynamic testing of aerospace components and models at near-space environment.

The evacuated sphere can also be utilized as a constant-flow vacuum source, as it was for the LEFT (leading edge flight test) Program, to accurately simulate the temperature, altitude, moisture, and pressures experienced in flight for accurate calibration of the systems associated with the three LEFT flight chambers.

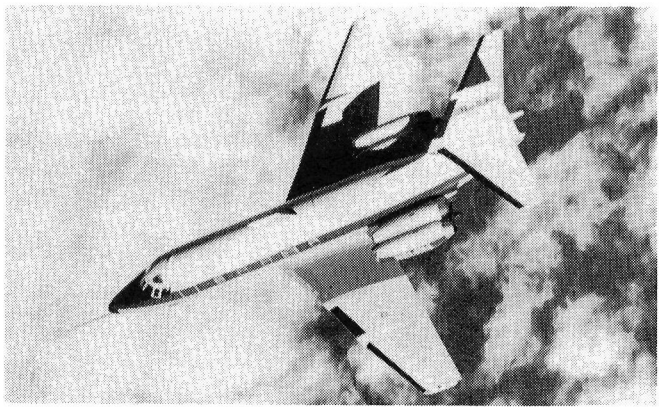

LEFT aircraft.

GEOSAT-A Satellite Tests

Two separate tests were conducted in collaboration with the Johns Hopkins University Applied Physics Laboratory on the GEOSAT-A satellite. The first was to demonstrate the performance of the yo-yo despin system and the partial deployment of the solar panels. It also verified that there was no interference between the antenna, mounted on the solar panels, and the despin system. The second test was a solar-array full-deployment test. The purpose of this test was to demonstrate the performance of the deployment system and to fine tune the energy damping system. Facility instrumentation, high-speed photography, pyrotechnics, and the facility video system were used to complete eight successful runs.

Eugene L. Kelsey, 4621

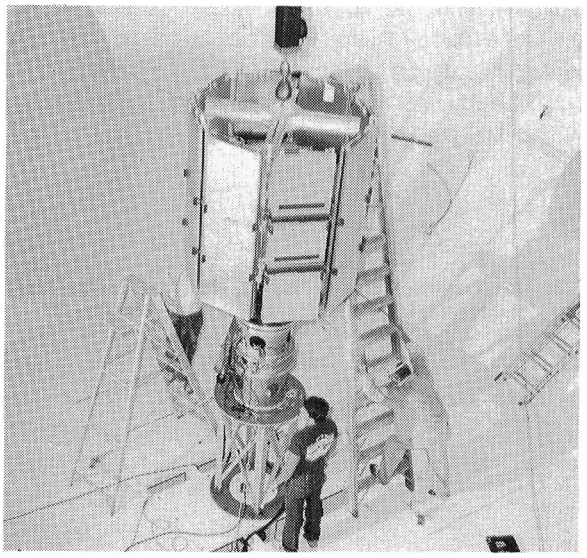

GEOSAT-A in 60-foot Space Simulator.

Vehicle Antenna Test Facility

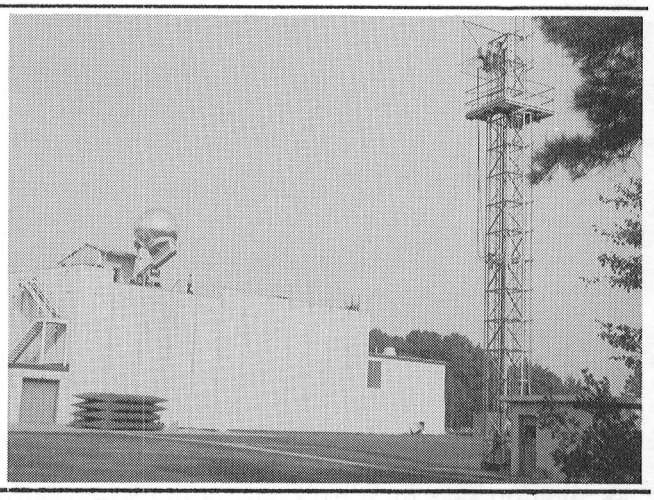

The Vehicle Antenna Test Facility (VATF) is a research facility used to obtain data for new antenna designs and antenna systems and to provide antenna performance data in support of various research programs. The VATF consists of two indoor radio frequency (RF) anechoic test chambers and an outdoor antenna range system. The anechoic chambers, which are RF-shielded, provide simulated free-space conditions for measurements from 100 MHz to greater than 40 GHz. The anechoic chambers, shaped like pyramidal horns to avoid specular reflections of the walls, are over 100 feet long and have test area cross sections approximately 30 by 30 feet.

Antennas and aircraft models measuring up to 10 feet can be evaluated in the facility. A spherical near-field (SNF) measurement capability was added to the low-frequency chamber. This permits automatic measurement of electrically large antennas (*i.e.*, diameters up to 100 wavelengths) up to at least 18 GHz. The near-field data can then be transformed by the SNF system software to obtain the desired far-field data.

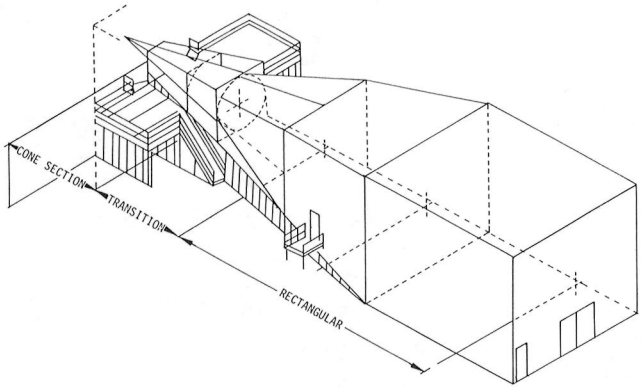

Low-frequency-chamber outline.

Measured data stored on disc or magnetic tape can be processed to provide antenna directivity, polar or rectangular plots of the radiation patterns, and three-dimensional, contour, or false-color volumetric plots of the antenna's radiation characteristics.

The outdoor antenna range system is available for use when the antenna or test model size or frequency precludes the use of the anechoic chambers. The outdoor range consists of two remote transmitting towers that are spaced 150 and 350 feet from the test positioner mounted on the VATF roof. The VATF has several electronic laboratories with the extensive measurement capability needed to support the design of unique antennas for aircraft and missiles prior to their evaluation in the antenna chambers or on the outdoor antenna range system.

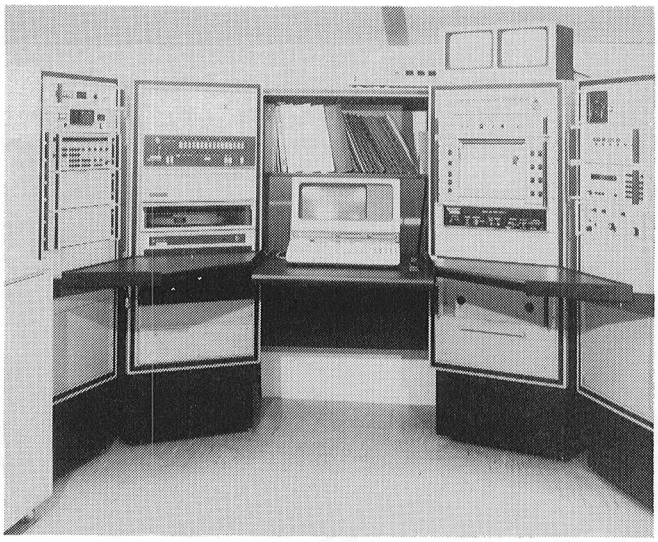

Chamber control console.

Space Station Antenna Technology

Generic antenna designs were evaluated at several locations on a 1/16-scale model of an initial baseline Space Station design. The tests were conducted in the VATF and the objectives were to determine the severity of the antenna blockage problem caused by the various modules and to provide a data base for the development and verification of analytical techniques required for predicting the antenna performance for more advanced Space Station configurations. The scale model tests were conducted at 35 GHz, simulating a full-scale Space Station frequency of 2.2 GHz.

The results of these tests indicate that the antenna blockage can be very severe for some antenna locations; therefore, the antenna designs and locations must be optimized in order to provide the required antenna performance for the many Space Station communications and tracking links that will be needed.

Melvin C. Gilreath, 3631

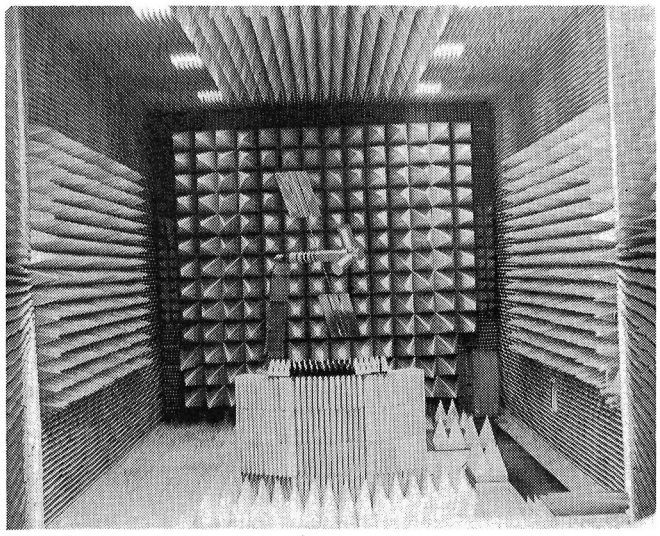

Space Station scale model in VATF.

Large Space Antenna Research

Several 35-GHz scale model reflector antennas were designed and constructed at Langley to provide the capability to experimentally investigate some of the potential problem areas associated with constructing large antennas for space applications and to provide a data base for the development and verification of analytical techniques for predicting the RF performance of large antennas. Tests were conducted in the VATF with these scale models to determine the effect of reflector surface pillowing.

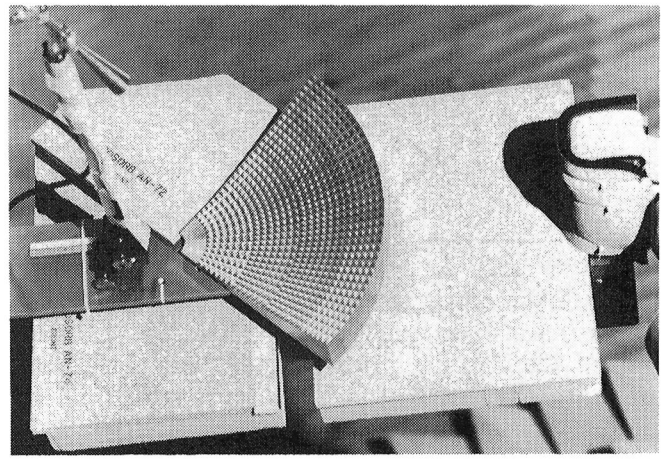

Scale model reflector antenna.

The results of these tests indicated that surface pillowing produced grating lobes (*i.e.*, undesirable side lobes) in the radiation pattern. The analysis technique used to predict the radiation patterns for perfect reflectors with no surface pillowing was modified to model the surface pillowing, and the calculated results exhibited the same grating lobe effect as the measured data. This verified analysis technique was then used to predict the radiation patterns for a large 15-meter quad-aperture antenna with surface pillowing which may result from the mesh construction. These results had the same grating lobe contamination of the radiation pattern.

Thomas G. Campbell, 3631

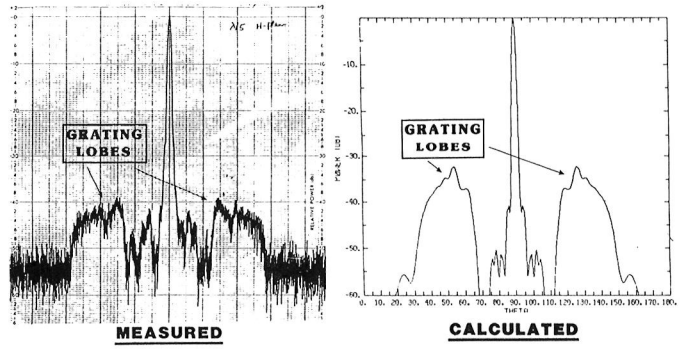

Subscale model verification of pillowed reflector surface.

Impact Dynamics Research Facility

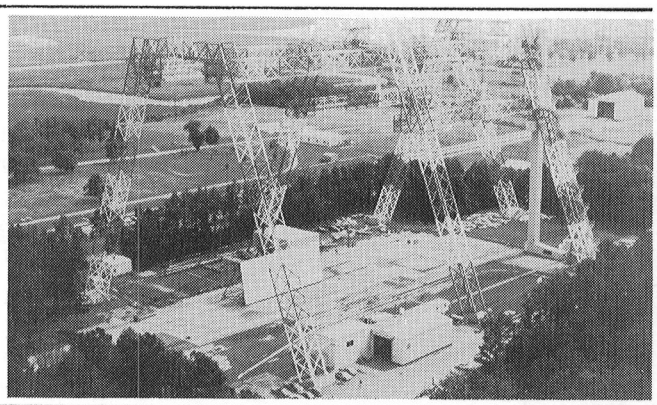

This facility, which was originally used by the astronauts during the Apollo Program for simulating lunar landings, has been modified to simulate crashes of full-scale aircraft under controlled conditions. Simulation is accomplished by swinging the aircraft by cables, pendulum-style, into the concrete impact runway from an A-frame structure approximately 400 feet long and 230 feet high. The impact runway can be modified to simulate other ground crash environments, such as packed dirt with trees. The impact runway has been modified in the past by using soil to meet a specific test requirement. The aircraft is suspended by swing cables from two pivot points 217 feet off the ground. It is then pulled back along an arc to a predetermined height by a pullback cable from a movable bridge on top of the A-frame, released from the pullback cable, and allowed to swing, pendulum-style, into the ground. An instant before impact, the swing cables are separated from the aircraft by pyrotechnics. The length of the swing cables regulates the aircraft impact angle from 0° (level) to approximately 60°. Impact velocity can be varied up to approximately 65 mph (governed by the pullback height) and to 90 mph with rocket assist. Variations of aircraft pitch, roll, and yaw can be obtained by changes in the aircraft suspension harness attached to the swing cables. Onboard instrumentation data are obtained through an umbilical cable attached to the top of the A-frame. Data are transmitted by hard wire to the control room at the base of the A-frame. Photographic data are obtained by ground cameras and cameras mounted on top of the A-frame. Maximum allowable weight of the aircraft is 30,000 pounds.

Vertical Drop Test of Boeing 707 Fuselage Section

The objectives of the transport section drop test were to determine structural, seat, and occupant response to vertical crash loads in preparation for a full-scale crash test of a remotely piloted transport aircraft planned for July 1984 and to obtain data to corroborate the DYCAST computer program being developed for crash analysis of aircraft structures.

Various fuselage sections from Boeing 707 transport aircraft were acquired for dynamic drop testing. The first section tested was located just forward of the wing. The 12-foot-long section, weighing approximately 5000 pounds when loaded with seats, anthropomorphic dummies, and instrumentation, was suspended in the Vertical Test

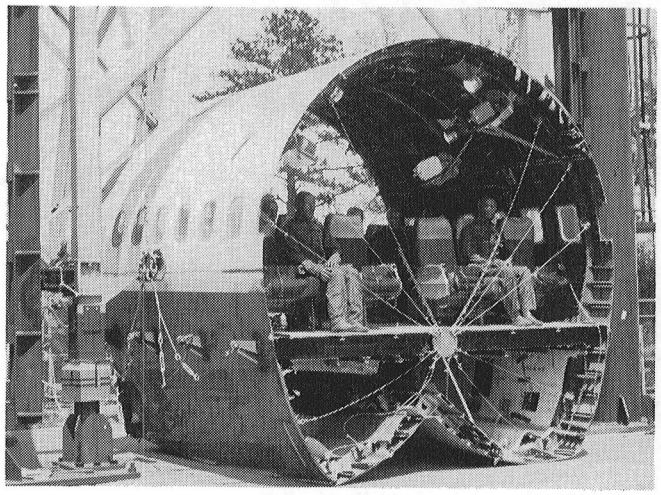

Boeing 707 fuselage section.

Apparatus at the Impact Dynamics Research Facility and dropped to obtain a vertical impact velocity of 20 feet per second.

Post-test inspection showed that the fuselage beneath the floor collapsed inward approximately 2 feet. Bending failures occurred along the centerline of the baggage compartment floor and on both sides of the fuselage about 4 feet below the floor. No apparent damage occurred to the upper fuselage, floor, or seats during the test. Crushing of the fuselage structure in the baggage area resulted in lower normal (perpendicular) accelerations at the floor level. Normal pelvic accelerations ranged from 6.5 to 8 g's.

M. Susan Williams, 2701

General-Aviation Crash Data Playing Major Role in Accident Assessment and Test Criteria Development

In a recently concluded program, Langley conducted 32 controlled, full-scale crash tests of general-aviation airplanes and generated a substantial data base on crash behavior. The objectives of this program were to determine the dynamic response of the airplane structure, seats, and occupants during a crash and to determine the effect of flight parameters at impact on loads and structural damage. A simplified analysis of the complicated crash scenario was developed based on impulse-momentum relationships.

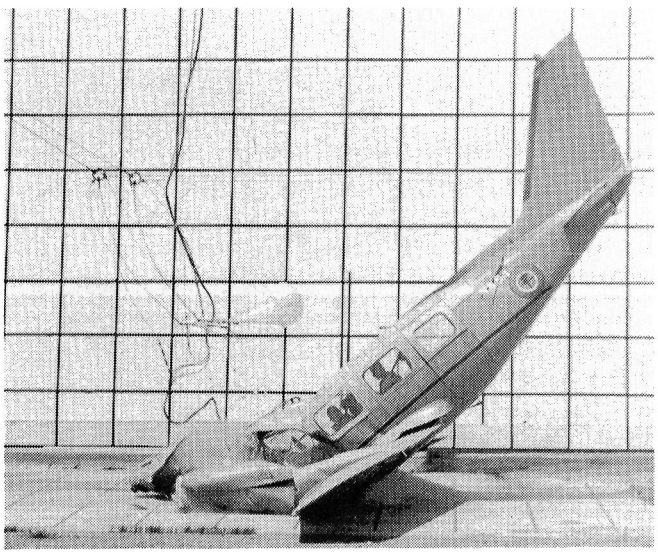

Setup for crash test of general-aviation aircraft.

A typical comparison between this analysis and full-scale crash test data is shown. The solid line represents the analysis, based on the assumption that the acceleration time pulse is triangular in shape. The symbols represent experimental data and include the general-aviation tests, two transport tests, and fighter tests. Clustering of the experimental data about the line confirms that the triangular shape is representative of crash pulses. The National Transportation Safety Board has undertaken a special program of crash investigation to establish a range of accident scenarios for which design for passenger survivability is feasible. A crash assessment analysis methodology stemming from the Langley method is being developed in which the full-scale test data are used to validate the analysis.

Huey D. Carden, 3795

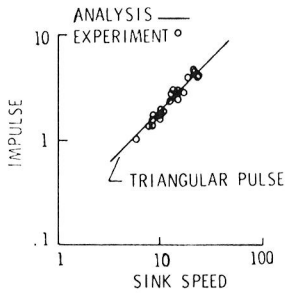

Impulse definition.

Flight Research Facility

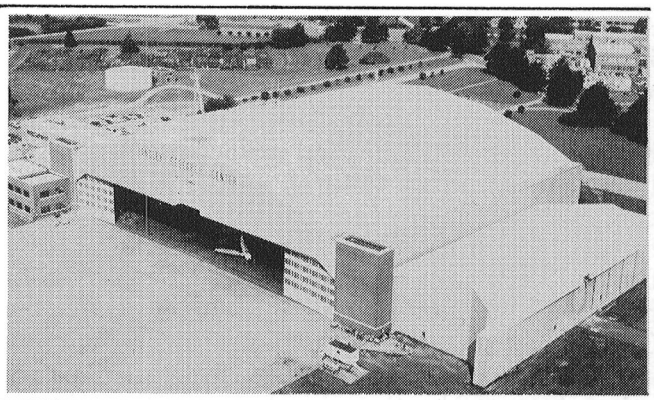

The truss-supported roof of the huge hangar of the Flight Research Facility provides a clear floor space with nearly 300 feet in each direction (over 87,000 square feet).

Door dimensions will allow entry of a Boeing 747. Features such as floor air and electrical power services, radiant floor heating to eliminate corrosion-causing moisture, a modern deluge fire suppression system, energy-saving lighting, modern maintenance spaces, and entry doors and taxiways on either side of the building make this structure equal or superior to any hangar in the country. Extensive and modern maintenance equipment makes it possible to repair aircraft ranging in sophistication from modern metal and composite airliners, fighters, and helicopters to fabric-covered light airplanes. Surrounding the hangar are ramp areas with a load-bearing capacity sufficient to handle the largest wide-body jet now flying. The high-power turnup area can also handle a wide variety of aircraft.

The present array of research and research support aircraft includes an airliner, military fighters, trainers, experimental one-of-a-kind designs, helicopters, and single-engine and multiengine light airplanes. This variety enables research to be carried out over a wide range of flight conditions, from hover to Mach 2 and from the surface to 60,000 feet. Research pilot currency in this wide spectrum of aircraft is important in doing credible in-flight experiments as well as in flight simulator assessments. A variety of research can be conducted in such areas as terminal traffic flow, Microwave Landing System (MLS) approach optimization, airfoil properties, single-pilot IFR, engine noise, turbulence research, natural laminar flow, winglet studies, stall/spin, and severe storm hazards.

One of the support helicopters is used to drop unpowered remotely controlled models of high-performance airplanes to study high-angle-of-attack control characteristics. The drop model test site is located at Plum Tree Island, near Langley Research Center.

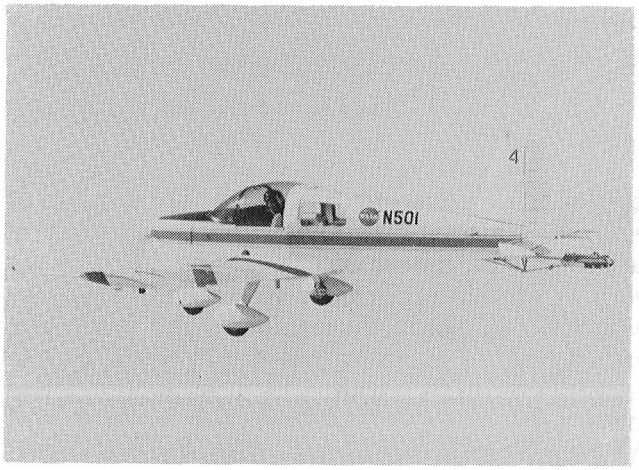

NASA 501, modified American Aviation AA-1 Yankee.

NASA 519, modified Piper PA-28RT-200 Arrow.

NASA 504, modified Beech C-23 Sundowner.

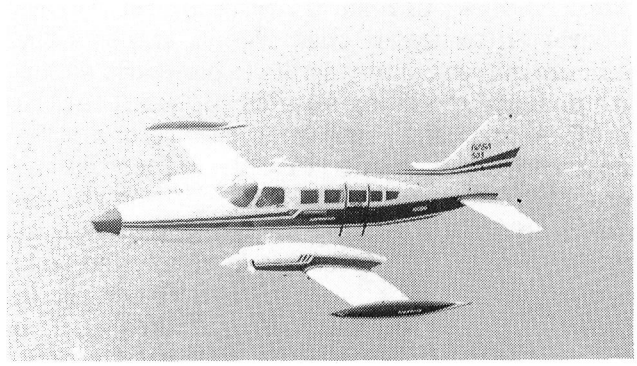

NASA 503, Cessna C-402.

NASA 515, Boeing 737-100.

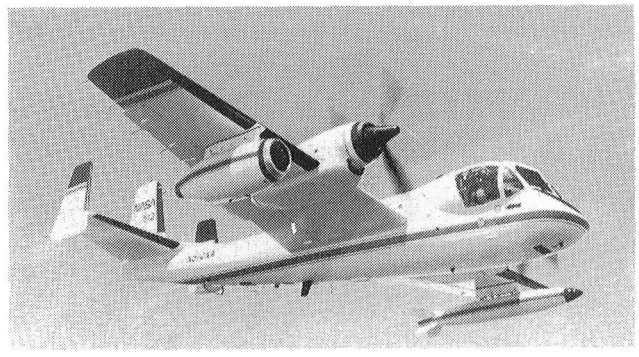

NASA 512, OV-1B Mohawk.

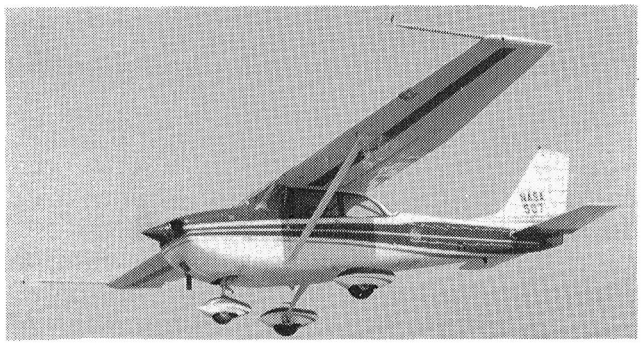

NASA 507, Cessna C-172.

NASA 816, F-106B.

Storm Hazards Program—1983 Results

The NASA Storm Hazards Program continued operations in 1983 with the F-106B receiving 214 direct lightning strikes. This brought the official total to 390 hits in the 4 years of thunderstorm flying. One flight resulted in 40 direct strikes to the aircraft. Changes for 1983 included the removal of paint from *all* external metal surfaces to reduce the burn-through possibility, the addition of 10 more channels of recorders at a 10-nanosecond time resolution for a total of 12 channels, improved operational control of the aircraft through addition of aircraft ground track to the color weather radar displays on the ground, and uplink of the complete weather map and track display to the aircraft for display on its weather radar. Additional changes include forward-looking color movie and aft-looking still cameras to show lightning patterns during the strikes.

Results obtained in 1983 confirm the earlier experience of higher strike rates at colder temperatures aloft as well as the indications that the presence of the aircraft triggers the direct

strikes. Analysis of results from the first 3 years of operation indicates that 15,000 amps is the maximum current in any strike experienced so far. Mathematical modeling studies suggest that the aircraft shape, size, and material strongly influence the voltages and currents induced in the aircraft by these direct strikes. Based on the experience to date in getting almost 400 strikes at altitudes above 20,000 feet, it is concluded that a suitably hardened all-metal airplane can readily survive high-altitude lightning strikes with no significant effects on the aircraft or its systems. The generalization of these results to composite aircraft with low-voltage digital systems via mathematical models is the next research task.

Norman L. Crabill, 3274

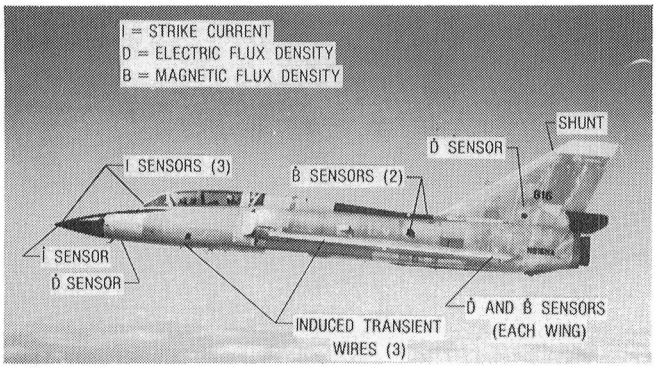

Location of electromagnetic sensors on F-106B.

Investigation of Antispin Control Laws

A drop model test program has been conducted to determine the effectiveness of the antispin portion of the control laws for the F-16XL airplane. The tests were performed with an 18-percent dynamically scaled model. Spins were initiated by attempting intentional spins with the normal control laws deactivated. Recoveries from the spins were effected by reactivation of the spin prevention control laws. During the recovery attempts, the pilot maintained his control inputs to try to force the spins to continue.

Two spin modes were obtained with the test vehicle, one oscillatory and the other smooth. These spin modes correlated well with those predicted from 20-Foot Vertical Spin Tunnel tests of the F-16XL configuration. Activation of the automatic spin prevention features of the control system produced excellent recoveries; about one turn occurred before recovery after the initiation of recovery control action. These automatic spin prevention control laws are derived from earlier research done at Langley and are currently in use on both the F-16A and F-16XL airplanes.

C. Libbey, 2244

F-16XL drop model.

T-34C Natural-Laminar-Flow Glove

The Beechcraft T-34C airplane is a single-engine turboprop training airplane which has been modified by NASA for research on viscous drag reduction. An airfoil glove installed on the left wing of the airplane used a new NASA natural-laminar-flow (NLF) airfoil design designated NLF(1)-0215F. The 200-knot speed capability of the airplane provided a chord Reynolds number of up to 18 million on the 7.67-foot-chord glove. The glove, which had a span of 3 feet, was fitted with endplates to minimize three-dimensional flow field effects on the airfoil.

Using the glove, researchers at Langley validated the extent of laminar flow predicted by both analysis and wind tunnel tests for the new airfoil. In addition, the glove provided a test surface for the development of laminar boundary layer measurement methods in the flight environment. Four different transition measurement methods were used on the glove, including hot films, sublimating chemicals, boundary layer rakes, and oil flow. Correlations between the

various techniques provided an improved understanding of transition phenomena in the flight environment, thus increasing the accuracy of theoretical-experimental correlations.

Research was also conducted on manufacturing tolerances for steps and gaps in laminar flow using the glove. This research led to a means of increasing allowable step heights in laminar boundary layers by more that 50 percent. This technology may provide a practical means for installing leading-edge high-lift or icing protection equipment on laminar-flow wings. In summary, the NLF glove on the T-34C airplane has provided Langley researchers with an important laminar boundary layer research facility in the flight environment.

Bruce Holmes, 3611

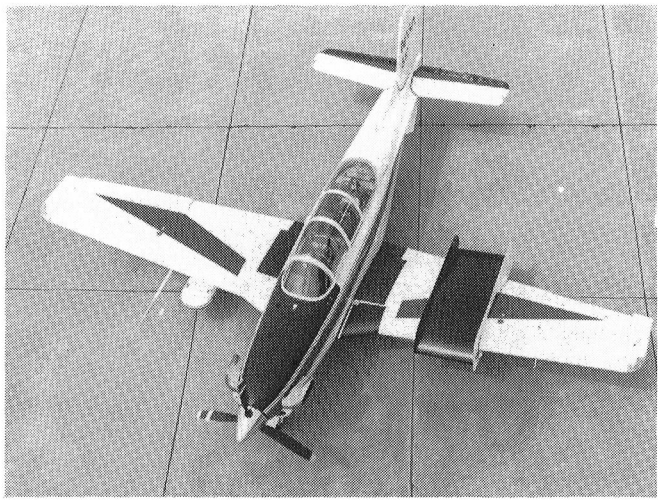

Airfoil glove on T-34C.

General-Aviation Stall/Spin Research

Langley Research Center is currently conducting research to improve the stall/spin characteristics of light general-aviation airplanes. Much of this effort has focused on the influence of wing aerodynamics on the stall and departure characteristics of these airplanes. Wind tunnel and flight tests have identified a wing leading-edge modification that significantly improves stall/spin behavior by increasing the stall angle of attack of the outer wing panels and delaying autorotative tendencies to higher angles of attack. This modification consists of a drooped leading edge added to the outboard wing panels, with a sharp discontinuity at the inboard end of the added droop.

This wing modification has been flown on three research airplanes, an American Aviation AA-1 Yankee, a Beech C-23 Sundowner, and a Piper PA-28RT-200. Prior to modification, each airplane would readily enter a spin; after modification, each airplane was highly spin resistant. Spin entry was obtained only through use of maximum power in conjunction with aggravated control inputs and/or abused airplane loading. Comments by industry and FAA pilots following evaluation flights in the modified PA-28RT-200 were favorable and pointed out a need to establish agreement among those building and certifying airplanes as to what constitutes good departure/spin-resistant characteristics and how such airplanes would be certified.

H. P. Stough, 2064

Piper PA-28RT-200 with spin-resistant modification.

Single-Pilot IFR Control/Display Trade-Off Study

Advanced avionics technologies have the potential to improve cockpit automation, increase aircraft utility, and reduce pilot workload. These benefits will be realized, however, only if the interface with the pilot is well developed. A control/display trade-off study was performed as a

step in developing criteria for pilot interfaces to advanced controls and displays. The study was performed under contract to Systems Technology, Inc., and Milco International, Inc.

The control/display trade-off study consisted of a limited flight test program and a piloted simulation study to extend the analytical data base. The flight tests were flown in three of Langley's small twin-engine airplanes. Each airplane was equipped with different levels of control and display complexities, ranging from simple general-aviation avionics to the Digital Advanced Avionics System (DAAS), which included a moving-map CRT display and extensive avionics integration. The test flights consisted of realistic high-workload instrument flight scenarios flown by professional research pilots.

The flight tests showed that as control/display complexity increased, the workload associated with mental orientation decreased and the system operation workload increased. An optimum level of control/display complexity exists for reducing pilot workload. By improving the pilot/cockpit interface, however, this optimum complexity level could be increased and pilot workload further reduced.

David A. Hinton, 3917

Pilot Interaction With Advanced Integrated Avionics Systems

Digital integrated avionics systems offer numerous advantages over conventional separate analog installations. The additional functions and information requirements of these advanced systems, however, can increase the complexity of operation for the pilot. A study was conducted to determine the benefits and potential disadvantages of a representative integrated digital avionics system from the pilot's viewpoint. The study was flown in the Langley Cessna C-402 airplane equipped with an experimental Digital Advanced Avionics System (DAAS). The DAAS implements numerous functions, including electronic moving-map navigation display, automatic navigation radio tuning, and autopilot/flight director. The study was conducted in the context of general-aviation single-pilot instrument flight operations and was flown by three professional research pilots.

Areas were identified in which further improvements are needed in the pilot-machine interface with this type of system. The present data entry methods tend to produce high pilot workload when entering or modifying flight plan data. This high workload, combined with the large amounts of data handled by the DAAS and the interaction of numerous DAAS functions, tends to increase the frequency of operational errors compared to more conventional avionics installations. Additional research will be needed to develop concepts for improving the pilot-machine interface with advanced integrated avionics systems while retaining the benefits of those systems.

David A. Hinton, 3917

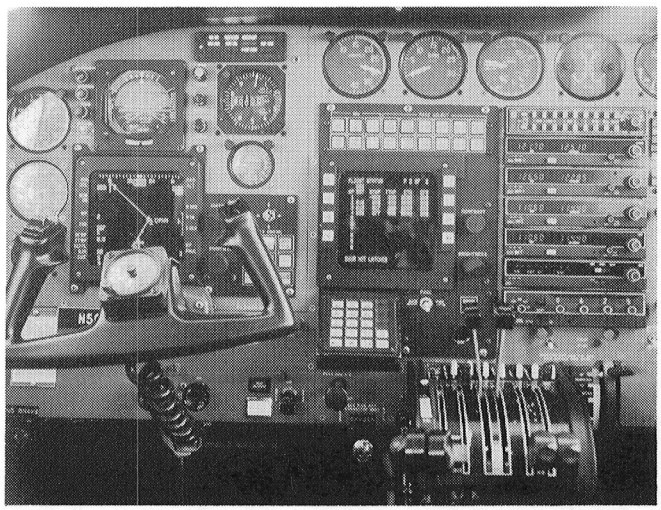

Digital Advanced Avionics System.

1. Report No.	2. Government Accession No.	3. Recipient's Catalog No.
NASA TM-85806		

4. Title and Subtitle	5. Report Date
LANGLEY AERONAUTICS AND SPACE TEST HIGHLIGHTS — 1983	June 1984
	6. Performing Organization Code
7. Author(s)	8. Performing Organization Report No.
	10. Work Unit No.
9. Performing Organization Name and Address NASA Langley Research Center Hampton, VA 23665	11. Contract or Grant No.
	13. Type of Report and Period Covered Technical Memorandum
12. Sponsoring Agency Name and Address National Aeronautics and Space Administration Washington, DC 20546	14. Sponsoring Agency Code

15. Supplementary Notes

16. Abstract

The role of the Langley Research Center is to perform basic and applied research necessary for the advancement of aeronautics and space flight, to generate new and advanced concepts for the accomplishment of related national goals, and to provide research advice, technological support, and assistance to other NASA installations, other government agencies, and industry. This report highlights some of the significant tests which were performed during calendar year 1983 in Langley test facilities, a number of which are unique in the world. The report illustrates both the broad range of the research and technology activities at the Langley Research Center and the contributions of this work toward maintaining United States leadership in aeronautics and space research. Other highlights of Langley research and technology for 1983 are described in "Research and Technology—1983 Annual Report of the Langley Research Center." Further information about both reports is available from the Office of the Chief Scientist, Mail Stop 103, Langley Research Center, Hampton, Virginia 23665 (804-865-3316).

17. Key Words (Suggested by Author(s))	18. Distribution Statement
Research and technology Tests Facilities Wind tunnels Models	Unclassified - Unlimited Subject Category 99

19. Security Classif. (of this report)	20. Security Classif. (of this page)	21. No. of Pages	22. Price*
Unclassified	Unclassified	79	A05

* For sale by the National Technical Information Service, Springfield, Virginia 22161 NASA-Langley, 1984